UNIVERSIDADE FEDERAL DO CEARÁ
CENTRO DE TECNOLOGIA
PROGRAMA DE PÓS-GRADUAÇÃO EM ENGENHARIA CIVIL: ESTRUTURAS E CONSTRUÇÃO CIVIL

AMANDA MOREIRA LIMA MACHADO

THERMAL ANALYSIS OF MASSIVE CONCRETE FOUNDATIONS AT EARLY AGES

FORTALEZA
2024

AMANDA MOREIRA LIMA MACHADO

THERMAL ANALYSIS OF MASSIVE CONCRETE FOUNDATIONS AT EARLY AGES

M.Sc. Thesis presented to the Post-Graduate Program in Structures and Civil Construction, as a partial fulfillment of the requirements for the Master's degree in Civil Engineering at Federal University of Ceará.

Area within the Graduate Program: Civil Construction

Advisor: Lucas Feitosa de Albuquerque Lima Babadopulos, Ph.D.

Co-advisor: Antônio Eduardo Bezerra Cabral, Ph.D.

FORTALEZA

2024

Dados Internacionais de Catalogação na Publicação
Universidade Federal do Ceará
Sistema de Bibliotecas
Gerada automaticamente pelo módulo Catalog, mediante os dados fornecidos pelo(a) autor(a)

M129t Machado, Amanda Moreira Lima.

Thermal analysis of massive concrete foundations at early ages / Amanda Moreira Lima Machado. – 2024.159 f. : il. color.

Dissertação (mestrado) – Universidade Federal do Ceará, Centro de Tecnologia, Programa de Pós-Graduação em Engenharia Civil: Estruturas e Construção Civil, Fortaleza, 2022.

Orientação: Prof. Dr. Lucas Feitosa de Albuquerque Lima Babadopulos.
Coorientação: Prof. Dr. Antônio Eduardo Bezerra Cabral.

1. Thermal analysis. 2. Mass concrete. 3. Finite element simulation. 4. Delayed ettringite formation. 5.Thermal cracking. I. Título.

CDD 624.1

AMANDA MOREIRA LIMA MACHADO

THERMAL ANALYSIS OF MASSIVE CONCRETE FOUNDATIONS AT EARLY AGES

M.Sc. Thesis presented to the Post-Graduate Program in Structures and Civil Construction, as a partial fulfillment of the requirements for the Master's degree in Civil Engineering at Federal University of Ceará.

Area within the Graduate Program: Civil Construction

Advisor: Lucas Feitosa de Albuquerque Lima Babadopulos, Ph.D.

Co-advisor: Antônio Eduardo Bezerra Cabral, Ph.D.

Approved in: 30 / 11 / 2022.

COMMITTEE

_____

Prof. Lucas Feitosa de Albuquerque Lima Babadopulos, Ph.D. (Advisor)
Federal University of Ceará

_____

Prof. Antônio Eduardo Bezerra Cabral, Ph.D. (Co-advisor)
Federal University of Ceará

_____

Prof. Esequiel Fernandes Teixeira Mesquita, Ph.D.
Federal University of Ceará

_____

Prof. Saber Imanzadeh, Ph.D.
INSA Rouen Normandie (Antenne du Havre)

To my mother Monica and my husband Flavius for all their unconditional love and support during my academic journey.

ACKNOWLEDGEMENTS

The following paragraphs were written in Portuguese and English for the complete understanding concerning the eternal gratitude I do have to everyone that took part to this achievement.

Gratidão é a palavra ideal para eu descrever tudo o que foi vivido durante os anos do mestrado. Apesar dos diversos obstáculos encontrados ao longo do caminho, hoje, ao fim desta jornada, consigo ver este período como uma ponte, a qual me levou para vários desafios, surpresas e realizações quando consegui atravessá-la. A travessia não foi fácil, mas Deus sempre esteve ao meu lado. Agradeço a Ele por tudo o que me foi dado e, principalmente, por colocar pessoas tão especiais na minha vida neste tempo.

Agradeço à minha mãe, Mônica, por todo o amor dedicado a mim desde o meu primeiro respirar. Mãe, sem a senhora, eu não teria chegado até aqui. Muito obrigada por todos os ensinamentos e por toda a sua dedicação para eu conseguir atingir meus objetivos. Sei que esses últimos anos não foram fáceis para você, mas toda a sua força me enche de orgulho. Você é minha inspiração para seguir em frente sempre. Agradeço também às minhas tias, aos meus tios e à minha irmã por se fazerem presentes nos momentos difíceis do seu tratamento que eu não pude estar.

Ao meu marido, Flavius, agradeço por ser meu porto seguro e por sempre trazer leveza aos momentos mais turbulentos, você foi peça fundamental para a conclusão deste trabalho. Obrigada por sonhar comigo, por todo incentivo, amor e por toda paciência ao longo desses anos.

Ao meu sogro, Flávio, à minha sogra, Elane, e à minha cunhada, Flaviane, agradeço pelos nossos almoços de domingo que sempre foram muito especiais e uma pausa para descansar a mente do trabalho. Obrigada por todos os ensinamentos e por trazerem calmaria para minha vida.

De maneira bem especial, quero agradecer ao meu orientador Prof. Lucas Babadopulos e ao meu coorientador Prof. Eduardo Cabral por tudo que me ensinaram e por todas as suas contribuições e os seus conselhos durante esses anos. Sou muito grata por contar com dois professores admiráveis no desenvolvimento deste trabalho. Muito obrigada pelo tema escolhido e por terem feito eu me apaixonar mais pelo estudo do concreto.

Ao Prof. Esequiel Mesquita, participante da banca, agradeço o aceite e interesse em se fazer presente neste momento.

I would like to thank Prof. Saber Imanzadeh for accepting to participate in the advisory board of this work. Furthermore, I am grateful for all your receptiveness when I visited INSA-Rouen in Le Havre during my academic mobility in France. It was a memorable moment for me.

To professors Tulio Honorio and Farid Bendoudjema, thank you for accepting me at the Ecole Normale Supérieure Paris-Saclay for my academic mobility during my master's degree. My gratitude is immense for all your receptiveness and for all your teachings, which were so many, during my stay at ENS. No doubt, it was one of the best experiences I have ever had.

To Erik Steen Pedersen, from Contech Analysis, I thank you for providing the license of the b4cast software and for all the available support during the development of this work.

Às construtoras das fundações de concreto massa analisadas neste trabalho, agradeço pelo fornecimento das informações e por todas as contribuições e todo apoio, que foram imprescindíveis ao desenvolvimento desta pesquisa.

Ao Grupo de Pesquisa em Reologia dos Materiais (ReoM), agradeço pelo companheirismo, compartilhamento de materiais, reuniões semanais e apoio sempre que precisei.

Agradeço aos meus companheiros de mestrado, que foram um presente de Deus na minha vida, Amanda Fontenele, Camila, Laury, Wyo, Estevão, Éden, Marcelo, Matheus e Kayque pela convivência, amizade, trocas de experiências e, principalmente, pelo incentivo de nos mantermos firmes nesta caminhada. Vocês foram um ponto de apoio importantíssimo durante esses anos.

Agradeço ao meu grupo de amigas Josi, Kébia, Mayara e Patrícia por estarem sempre ao meu lado e por toda a paciência que tiveram comigo durante meus dias de ansiedade com o desenvolvimento deste trabalho.

Aos profissionais técnicos e administrativos, agradeço por todo suporte ao sanar dúvidas e pelo auxílio na realização das atividades em laboratório.

À CAPES, pelo apoio financeiro com o fornecimento da bolsa de auxílio.

À Funcap, pelo financiamento da mobilidade acadêmica realizada.

Por fim, agradeço a todos que contribuíram, direta ou indiretamente, para esta formação pessoal e profissional.

Muito obrigada!

"Doors of opportunity do not just pop up in our lives; we actually build them with much work throughout the way according to our purposes to open them at the most appropriate moment."

(BABADOPULOS, 2022)

ABSTRACT

The power generation from wind has been showing high rates of production growth, especially in the Northeast region of Brazil. To produce this type of energy, it is necessary to build tall towers that are supported on bulky concrete foundations. In addition, the increasing verticalization of urban centers in concentrated areas is intertwined with the need for measures to ensure the structural stability of tall buildings, such as the use of mass concrete foundation blocks. For the construction of these types of structures, measures are needed both to optimize the concreting process, which involves previous planning and experience of the labor involved, and to avoid the appearance of pathological manifestations, such as cracks and delayed ettringite formation, due to the changes in the thermomechanical behavior of these concrete structures caused by the exothermic reactions of cement hydration. Thus, this dissertation aimed to evaluate the thermal behavior of mass concrete structures by performing computational predictions in two software (Ansys and b4cast) and applying a case study in the field. The influence of some input parameter variation on the results obtained and the reliability of the prediction models were verified. The analysis showed that the main difference identified between the results obtained in the two software was concerning the time to reach the internal temperature peaks. In general, the b4cast software presented higher temperature results than Ansys and was closer to the field measurements. The influence caused by the variation of the specific heat of concrete was the most significant among the parameters evaluated, causing a closer approximation of the predictive models with the measured data, especially about the values of maximum temperatures. Finally, the case study was fundamental to implement, in the field, the casting plan developed for the structure and to identify the main challenges, improvements, and care during the process of prediction, casting, and monitoring of mass concrete structures.

Keywords: thermal analysis; mass concrete; finite element simulation; delayed ettringite formation; thermal cracking.

RESUMO

A geração de energia elétrica a partir dos ventos vem mostrando elevadas taxas de crescimento de produção especialmente na região Nordeste brasileira. Para gerar este tipo de energia, é necessário construir torres altas que são apoiadas sobre fundações de volumosas de concreto. Além disso, a crescente verticalização dos centros urbanos em áreas concentradas está entrelaçada com a necessidade de medidas para garantir a estabilidade estrutural dos edifícios altos, como o uso de blocos de fundação de concreto massa. Para a construção desses tipos de estrutura, necessitam-se de medidas tanto para otimizar o processo de concretagem, o que envolve planejamento prévio e experiência da mão de obra envolvida, quanto para evitar o surgimento de manifestações patológicas, como fissuras e formação de etringita tardia, devido às alterações do comportamento termomecânico dessas estruturas de concreto causadas pelas reações exotérmicas de hidratação do cimento. Desse modo, esta dissertação teve o objetivo de avaliar o comportamento térmico de estruturas de concreto massa através da realização de previsões computacionais em dois softwares (Ansys e b4cast) e da aplicação de estudo de caso em campo. A influência da variação de parâmetros de entrada nos resultados obtidos e a confiabilidade dos modelos de previsão foram verificadas. As análises realizadas mostraram que a principal diferença identificada entre os resultados obtidos nos dois software foi em relação ao tempo para atingir os picos de temperaturas internas. De modo geral, o software b4cast apresentou resultados de temperaturas superiores aos do Ansys e mais próximos das medições de campo. A influência causada pela variação do calor específico do concreto foi a mais significativa entre os parâmetros avaliados, provocando uma maior aproximação dos modelos preditivos com os dados medidos, principalmente em relação aos valores das temperaturas máximas. Por fim, o estudo de caso realizado, foi fundamental para implementar, em campo, o plano de concretagem desenvolvido para a estrutura e para identificar os principais desafios, melhorias e cuidados durante o processo de previsão, concretagem e monitoramento de estruturas de concreto massa.

Palavras-chave: análise térmica; concreto massa; elementos finitos; fundações de torres eólicas; formação de etringita tardia; fissuração térmica.

LIST OF FIGURES

LIST OF TABLES

LIST OF ABBREVIATIONS AND ACRONYMS

ABEEÓLICA	Associação Brasileira de Energia Eólica (Brazilian Wind Energy Association)
ABNT	Associação Brasileira de Normas Técnicas (Technical Standards Brazilian Association)
ACI	American Concrete Institute
ASTM	American Society for Testing and Materials
DEF	Delayed Ettringite Formation
EEF	Early Ettringite Formation
FEM	Finite Element Method
GWEC	Global Wind Energy Concil
LMCC	Laboratório de Materiais de Construção Civil da Universidade Federal do Ceará (Laboratory of Building Materials of the Federal University of Ceará)
NBR	Norma Brasileira Regulamentada (Brazilian Standard)
UFC	Universidade Federal do Ceará (Federal University of Ceará)
WWEA	World Wind Energy Association

LIST OF SYMBOLS

c	Specific heat
k	Thermal conductivity
ºC	Degree Celsius
K	Kelvin
m	Meter
J	Joule
g	Gram
G	Giga
W	Watt
h²	Thermal diffusivity
γ	Density
h	Hour
Δ	Variation
w/c	Water / cement ratio
ΔT	Temperature gradient
q_n	Rate of heat flow
h_c	Convective heat transfer coefficient

TABLE OF CONTENTS

1 INTRODUCTION

1.1 Contextualization

Social and economic development influences the technological progress of the construction industry. The concern to achieve high performance and to build taller and slender structures has been growing over the years, resulting in the need for more robust foundations to receive the structural loads (GAMBALE, 2017). Thus, the use of bulky concrete structures is notorious in several civil engineering fields, such as the building and structure construction and infrastructure sectors, highlighting the energy industry, with the construction of dams and wind farms.

These elements can be classified as mass concrete structures, which differ from other types of concrete elements due to their thermal behavior (generation and dissipation of heat) (ACI 207.1R, 2006). In mass concrete, it is necessary to control the rise of heat generated by the hydration reaction of cement, which is a result of exothermal reactions, to avoid the appearance of cracks (ACI 207.1R, 2006). According to Sfikas, Ingham and Baber (2017), some examples of such structures are foundation blocks and rafts, dam structures, nuclear containment structures, buried piles, wind tower foundations, armor (breakwater) units, precast structures for tunnels and bridges, retaining walls, among others (FIGURE 1).

Concrete structures, when exposed to ambient temperature and humidity, can suffer thermal contraction (deformation associated with cooling) and shrinkage by drying (deformation associated with moisture loss) (TANG; HUANG; HE, 2021). Commonly, in massive structures (with a thickness – smallest dimension – higher than or equal to 1 m), the thermal shrinkage stands out, being more concerning than the volumetric expansion generated by the hydration heat of cement due to the resulting tensile stresses (MEHTA; MONTEIRO, 2014). According to the referred authors, to reduce the risk of cracking, the concrete should have low elastic modulus, high creep, and high tensile strength.

Figure 1 - Examples of massive concrete structures: (a) ground slabs; (b) concrete dams; (c) silos/containment structures; (d) cooling towers; (e) wind turbine foundations; (f) piles; (g) precast segments (top: immersed tunnel, bottom: bridge deck); (h) armor units; (i) bridge piers; and (j) retaining walls.

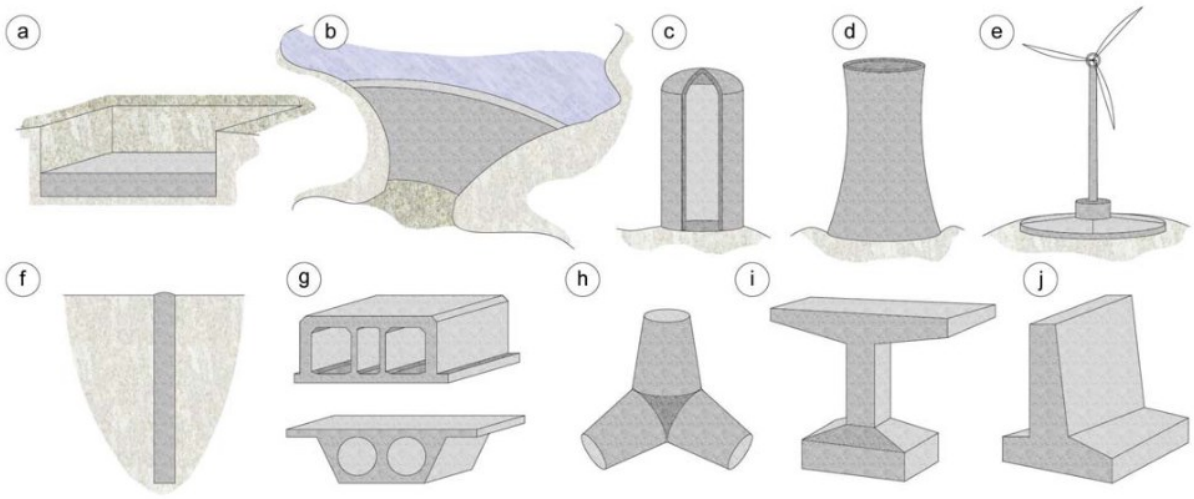

Source: Sfikas, Ingham and Baber (2017).

In very early ages of concrete (first hours), the increase of the temperature generated by the cement hydration reactions can lead to the appearance of cracks by the coupling between the thermal phenomenon (expansion-contraction of materials under non-uniform temperature distribution between the surface and the core of the structure due to the heat generated and heat exchanges) and the mechanical phenomenon (total or partial impediment of movement of the structure in the hardened state, for example, by the action of a temperature gradient). Cracks occur when the internal tensile stresses exceed the tensile strength of the concrete (WU *et al.*, 2011).

Besides thermal cracks in very early ages, another kind of phenomenon that may arise as a result of the temperature increase is the delayed ettringite formation (DEF). In this case, cracks do not appear immediately, but raising the internal temperature of the concrete above a certain limit (between about 65 to 70 ºC) prevents the natural formation of ettringite still in the fresh state (in which it is benign), so that ettringite will form within the concrete in the hardened state in the future, when in contact with water. The delayed ettringite formed is an expansive product (LAROSCHE, 2009), causing an increase in internal stress in the concrete structure, leading to cracking.

According to Emborg and Bernander (1994), the increase in the temperature of a concrete element depends on several factors. Among them are: the dimensions and geometry

of the structure; the thermal and mechanical properties of the early-age (young) concrete; the cement particle size; the placement and curing conditions (placement temperature and process, insulation mechanisms, and cooling schemes); the boundary conditions (heat transfer conditions); and the environmental conditions (temperature and wind speed). Thus, to predict and evaluate the thermomechanical behavior of concrete structures, it is important to consider the influence of as many relevant factors as possible to bring the predictions closer to the reality experienced daily at construction sites.

In the state-of-the-art on this subject, there are some methodologies for calculating and predicting the evolution of the internal temperatures and stresses of mass concrete structures, such as the Finite Difference Method (FDM) and the Finite Element Method (FEM), used to solve heat differential equations using the pertinent material thermal and mechanical properties. The FEM is more common in the studies consulted for the development of this study, as can be seen in Azenha (2009), Smolana et al. (2022), Sfikas, Ingham and Baber (2017), Huang et al. (2018), Gambale (2017), Couto (2018), among others. If properly used it can be a fast and accurate tool for predicting field behavior. This can be used for many engineering purposes, in different phases of the project (mix design, project design, construction planning, etc.), such as: calculating how much water should be replaced by ice before mixing; deciding the use and choosing the placement of cooling water circuits; deciding construction phases to avoid too-high concrete volumes placed at a given time and avoid high temperatures, among others.

During the construction of massive concrete structures, the monitoring of internal temperatures over time and the comparison between these data and the computer prediction models can allow the evaluation of the risk of thermal cracking and the choice of the best mitigating methods to be used. This is also important as a means to perform quality assessment and quality control of mass concrete structures (COUTO, 2018) and is also a way to validate the proposed models and/or identify differences between the construction and the project.

It is noteworthy that this study is connected with two approved projects developed in partnership: the French FONDEOL project ("*Problématiques propres aux Fondations d'éoliennes en zone littorale*") about wind tower foundations, carried out mainly by French universities, agencies with partner companies and, with the participation of Federal University of Ceará (UFC) as a partner; and FUNCAP/INSA-Rouen ("Challenges with respect to aerogenerators` foundation in coastal zones"), an international cooperation project between research groups in Ceará and Normandy region in France. Those projects are part of a strategy for the emergence of a Franco-Brazilian research center in Geotechnical Engineering and Civil

Engineering applied to renewable energies. Through those projects, an academic mobility in France was made possible during this MSc work. Moreover, industrial partnerships in the field were used for full-scale tests, such as partners responsible for the construction of wind farms and high-rise buildings in the state of Ceará, Brazil.

Finally, this research is relevant for the technical and scientific advances required to develop a plan for thermal analysis and monitoring of mass concrete structures that can assist in the casting stages of concrete and increase the performance and structural health of such structures. It contributes to future academic and engineering works on mass concrete.

1.2 Problem statement

According to Roso, Oliveira e Beuter (2021), the verticalization of urban spaces is not only connected to demographic growth and the decrease of available spaces in large urban centers but also relates to modernization and to the economic and political interests of the cities. Thus, to provide greater stability to buildings, which are increasingly taller and are mostly built in smaller urban spaces, there is a need for bulky concrete foundation structures and even the joining of foundation blocks into a single larger block due to the limited building area available. In this case, the foundation is potentially a mass concrete structure.

Wind tower foundations are another type of mass concrete structure that has received attention in thermomechanical studies. Due to the expansion of onshore wind farms in Brazil, especially in the Northeast region, where the wind source leads (ABEEÓLICA, 2022a), and due to the development of technologies that provide the construction of increasingly taller towers, it is necessary to build foundations with significantly high volumes of concrete.

Furthermore, it is worth mentioning that the wind source represents 10.8 % of the sources of energy in Brazil, presenting significant expansion rates, with the capacity of wind power installed expected to reach 34.69 GW until 2026 (ABEEÓLICA, 2022a). From the 827 existing wind farms, 88,27% are located in the Northeast region (ABEEÓLICA, 2022b), where the winds are more constant and have a stability of speed and direction (ABEEÓLICA, 2022a). Figure 2 shows the distribution of wind farms in operation in Brazilian states. The Brazilian Government (2022) states that the Northeast region is responsible for more than 90% of the national wind energy production.

Figure 2 - Distribution of wind farms in operation in Brazilian states

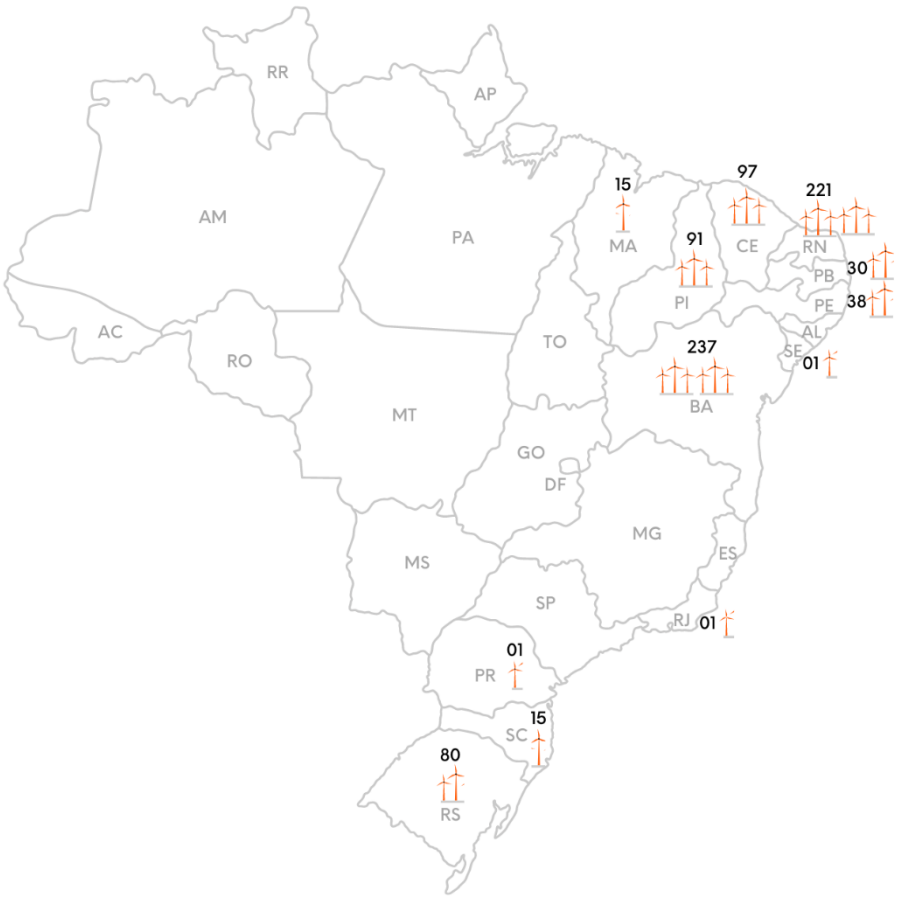

Source: Adapted from ABEEÓLICA (2022b).

Thus, there is an increase in the construction of massive concrete structures related to the urban development of cities (construction of high-rise buildings) and to the energy development (expansion of wind farms), which require measures to control thermal rise from the cement hydration process. It is essential, therefore, to predict its thermomechanical behavior to avoid structural failure because the building of this type of structure requires high financial costs, and its collapse can cause severe accidents (COELHO, 2012). Also, it is important to mention that early-age thermal cracking can be related to degradation phenomena that reduce the durability of structures. Cracks allow aggressive agents to enter the structure, such as CO_2, which causes carbonation of the concrete material, and Cl^- , which accelerates the corrosion of the reinforcing steel (BAMFORTH, 2007; BOBKO *et al.*, 2015).

Despite the increasing application of massive concrete structures in a variety of civil engineering fields, no Brazilian standard has been identified to guide professionals on precautions to take when building this type of structure, or to define criteria for construction

and projects. As a result, some builders are either unaware of or do not place enough priority on mitigating the risks associated with problems of thermal origin in massive elements. Additionally, such structures are frequently not visible after construction, making detection of degradation hard to perform.

It is relevant to mention that according to the reports of the construction partners of this study, one of the biggest challenges during the construction of massive concrete structures is the concreting stage, due to the high demand of time and manpower and, mainly, the unforeseen events that can occur during this process. In addition, the great distances between the concrete production site and the pouring site and the characteristics of the environment (temperature, wind speed, and humidity) can affect both the properties of the concrete and the pouring temperature, causing the need for corrections in the mix design. Concrete cooling mechanisms, such as the use of ice and liquid hydrogen, are also factors that can hinder and delay planned activities.

Therefore, despite being frequently neglected, it is necessary to emphasize the extreme importance of estimating the thermal behavior of these structures before construction, and also the development and monitoring of the execution of a concreting plan, including from mix design control to the monitoring of the internal temperatures of the structure analyzed.

Given that context, the relevance of this work is the implementation of a thermal study of mass concrete structures, aiming to verify the reliability of different computational tools and the influence of internal parameters (material properties) and external ones (environmental conditions) on the prediction results, comparing them with field measurements.

Thus, it is expected to spread knowledge in this area and thus guide engineers and future researchers about the importance and execution of performing this type of study before the casting of these large-volume elements. The work focuses on the following research questions:

- What are the main divergences that can be identified in thermal predictions when these are performed using different computational tools?

- Can the influence caused by the variation of input parameters (both from the material and from the ambient conditions) be considered significant in the results of predictions of the thermal behavior of mass concrete structures?

- Are the computational models capable of predicting thermal behavior with

sufficient accuracy? And what are the main improvements that can be applied in the process of predicting the thermal behavior of concrete structures to improve the reliability of this type of analysis?

1.3 Research objectives

1.3.1 Main Objective

The general objective of this research is to analyze the thermal behavior of massive concrete structures (a wind tower foundation and a high-rise building foundation) ranging from computational predictions to the field monitoring to identify the main challenges and improvements needed throughout this process.

1.3.2 Specific Objectives

To achieve the general objective, the specific objectives addressed in this research are presented below

1. To investigate differences in the results of thermal simulations of a wind turbine foundation performed in two finite element software packages: a commercial specific purpose software (b4cast) and a commercial customizable software programmed for thermal analyses (Ansys);
2. To evaluate and define which parameters of the concrete (e.g. thermal properties), of the external conditions (e.g. boundary conditions), and of the casting process (e.g. construction of the structure in layers) generate significant influence on the thermal behavior of a wind turbine foundation, from a parametric study;
3. To develop a case study on a high-rise building foundation applying from the development of computational prediction models to follow-up the casting process and the monitoring of the internal temperatures of a structure in the field.

1.4 Manuscript structure

This research is organized into 5 chapters. Chapter 1 presents considerations about the problem contextualization, objectives, and relevance of the study. After the Introduction, Chapters 2, 3, and 4 were presented in scientific article format, to facilitate the organization and publication process of the results found after the MSc defense. While Chapter 2 focuses on the

specific objective 1 (cf. Section 1.3), Chapter 3 focuses on the specific objective 2 , and Chapter 4 focuses on specific objective 3. This organization allows the reader to focus on a specific chapter in function of the treated specific objective.

Chapter 2 presents the comparative study between the thermal analyses of a wind turbine foundation performed using the two computational tools chosen for this research (Ansys and b4cast software packages), highlighting the convergences and divergences between them. To better understand the thermal behavior of the structure, the maximum global temperatures reached by the structure were first studied. Then, the heating/cooling profile of the foundation was observed by studying the isotherms and the thermal behavior of some internal points of the structure through time. Finally, the computational results were compared with the field monitoring data from a wind farm, at which concrete block construction was monitored.

Chapter 3 examines the effect of varying certain parameters on the thermal behavior of the structure studied in Chapter 2 with the purpose of reducing the divergences identified between the computational models and the monitoring data, primarily concerning the values of maximum temperatures reached by the structure.

Chapter 4 shows the case study performed on a high-rise building foundation, whose analysis starts from the computational predictions and proceeds to the follow-up of the casting methodology proposed for this structure. The post-casting analysis is highlighted, comparing the computational results to those measured in the field to validate the prediction model's reliability. In addition, an unexpected situation experienced on the day of the casting required adjustments of the simulations to assist in the decision-making process for the next casting steps. This is also discussed in Chapter 4.

The final considerations, as comments on the results keyed to each of the objectives of this work, are found in Chapter 5, which concludes this research by identifying the main contributions, challenges, limitations, possible improvements, and indicating paths for future work.

2 COMPARATIVE STUDY BETWEEN TOOLS FOR THERMAL ANALYSIS OF MASSIVE CONCRETE FOUNDATIONS

ABSTRACT

The construction of bulky concrete structures has been notorious in Brazil, such as wind tower foundations, due to the expansive growth of this sector, especially in northeastern of Brazil. Mass concrete structures need measures to control the thermal rise generated by the cement hydration reactions to avoid delayed ettringite formation (DEF) and cracks of thermal origin. Considering this need, it is possible to perform studies to predict the thermal behavior of these elements before casting, which contribute to the choice of materials and casting conditions, for example. These studies can be performed using computational tools, such as finite element software. Thus, given the several options of tools in the literature, the main objective of this study was to evaluate the thermal analyses performed in two chosen software (b4cast and Ansys), besides comparing the results searching for similarities and differences between them. Another fundamental point was to verify the reliability of the computational analyses by comparing them with field monitoring data sent by the construction company of the concrete structure chosen for this study. The results showed that the main differences identified between the software results were concerning the time for reaching the maximum temperatures in the structure, which occur earlier in b4cast and near the end of the study (168 h) in Ansys. In addition, the differences in temperatures between the two software increased with increasing placing temperatures, being more evident at points closer to the external environment. Regarding the reliability of the computational tools, the prediction models presented lower values than the field monitoring data, especially in the reach of maximum temperatures, highlighting the need for improvements in the models used to bring them closer to the reality experienced on-site.

Keywords: thermal analysis; mass concrete; finite element simulation.

2.1 Introduction

Mass concrete structures need to control heat generation, coming from the exothermic reaction of cement hydration, and the risk of cracking due to volumetric changes and temperature differences (ACI 207.1R, 2006). The mass concrete, as well as other, is composed of cement, aggregates, water and mineral and chemical admixtures. Its mixture dosage must be adequate to increase its durability and produce concrete with economic and technical feasibility to ensure appropriate workability and mechanical strength and to avoid temperature rises, dimensional instabilities and, consequently, cracking. Concrete can also be classified as a thermal mass material due to its ability to absorb, store and release heat very gradually (SHAFIGH; ASADI; MAHYUDDIN, 2018).

Due to social, economic, and technological growth, the construction of increasingly taller and larger buildings is noticeable, for example, skyscrapers, wind towers, bridges, dams, and tunnels. The dimensions of these buildings contribute to the use of massive concrete structures in some parts of their designs, such as in the foundations. As a highlight, the foundations of wind towers in northeastern Brazil can be mentioned, whose growth of this sector made this nation move from position 21st in 2009 (WWEA, 2010) to position 6th in 2021 in the ranking of installed capacity of onshore wind energy (GWEC, 2022). Also, according to the Global Wind Report 2022 (GWEC, 2022), Brazil was among the world's top five markets in 2021 for new onshore installations, behind only China and the United States. In that year, the global installed onshore wind capacity reached 780.28 GW.

Wind turbines are supported on reinforced concrete foundations and, due to technological advances that cause the increase of towers height, larger foundations of the order of hundreds of cubic meters and with high diameters are needed to ensure the stability of the tower (SILVA, 2014). These foundations are usually cast on-site, where the concrete is exposed to variable environmental conditions that can adversely influence their performance and durability (e.g. presence of soil water, possibly salted water in the case of coastal regions) (PERRY *et al*., 2017). Besides, these structures are susceptible to drying shrinkage due to exposure to wind and sun and may consequently crack (MEHTA; MONTEIRO, 2014).

During the early age of concrete (typically up to seven days), the thermal effect and problems during the casting process are the main causes of cracks, which can affect the mass concrete structures, compromising the useful life and structural stability. These cracks allow the penetration of deleterious agents into the structures (e.g. chlorides and sulfates) (BOURCHY *et al.*, 2018).

Azenha (2009) presents a description of the thermal and mechanical processes that happen in mass concrete structures, showing that the hydration reaction of cement is a complex process that results in the variation of concrete properties over time, such as porosity decrease and stiffness increase. Also, this author emphasizes that, during this process, the concrete relates internally with its neighboring particles, and externally with the surrounding environment, which affects the stress development.

Moreover, many factors can influence the thermomechanical behavior of these concrete structures, increasing the risk of early age cracking: cement content and type, concrete placement temperature, concrete properties, particle size of the cement, cement composition, restraint conditions, other concrete constituents and mix proportions (e.g., aggregates, moisture, and admixtures), section thickness, formwork and insulation, environmental conditions and curing schemes (BAMFORTH, 2007).

In addition to the cracks caused by the stresses of thermal origin, another phenomenon that arises as a result of temperature increase is the delayed ettringite formation (DEF), which can affect the performance and durability of structures.

It is possible to perform forecasts and evaluations of the internal temperature of large volumes of concrete by solving the heat equations associated with the problem (involving the heat of hydration of the cement as a source and propagating it by conduction through the volume of the structure and by convection on the surface).

In this way, it is possible to predict the evolution of the temperatures distributed in the concrete structure with time and the maximum temperatures and to determine the points considered critical for the appearance of cracks of thermal origin (where thermal stresses are higher, usually where temperature differences are higher and where mechanical restraints exist) (GAMBALE, 2017; COUTO, 2018; JU; LEI, 2019; ANISKIN; NGUYEN, 2020). Thus, there is the opportunity to previously identify critical situations through the study of these massive concrete structures before their construction (COELHO, 2012). In this way, numeric analysis can be done using some methods, such as the Finite Element Method (FEM) by through computational tools (e.g. Ansys, Abaqus, B4Cast, ConcreteWorks, among others software).

Therefore, this chapter aims to verify the differences between the results of thermal analysis of a bulky concrete foundation performed in more than one type of computational tool, as well as the reliability of these results. For this, two software were chosen, one with a specific commercial purpose to perform thermomechanical analysis and the other customizable for this type of analysis. The results were compared with each other and with field monitoring data,

aiming to identify convergences and divergences and, mainly, improvements for the study of the thermal behavior of this type of concrete structure.

2.2 Literature review

2.2.1. Thermal stresses and cracks

One of the most important factors to prevent the appearance of early age cracks in mass concrete structures is to reduce the hydration heat generated. These cracks arise when the tensile stress in the concrete exceeds its tensile strength (HA; JUNG; CHO, 2014).

Portland cement is a material composed of several components and, due to this, its hydration process is complex, having several chemical reactions that occur both in parallel and in series (KIM, 2010). Figure 3 illustrates the evolution of cement heat, which is divided into five stages.

Figure 3 – Heat evolution during the cement hydration process

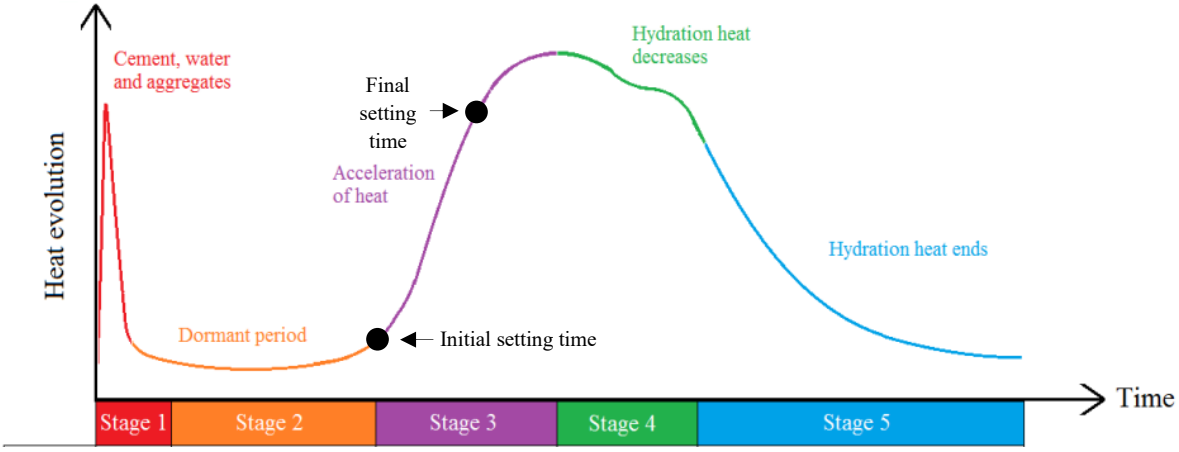

Source: Adapted from Lagundžija and Thiam (2017).

Cement hydration is spontaneous, exothermic, and thermally activated, i.e., besides producing internal heat, the reaction is accelerated by the increase in temperature. Several factors may influence hydration reactions (BAMFORTH, 2007; AZENHA, 2009; TAHERSIMA; TIKALSKY, 2017; LACARRIÈRE *et al.*, 2018; BEAUDOIN; ODLER, 2019):

- Mineral composition of clinker and cement consumption: the total amount of heat generated is proportional to the amount of cement constituents. Choktaweekarn and Tangtermsirikul (2010) showed that the amount of heat released by each component is in increasing order: C_2S, C_4AF, C_3S, C_3A;

- Presence of mineral admixtures (e.g. granulated blast furnace slag, pulverized fly ash, etc.): The less admixtures presence, the higher heat generation;
- Cement fineness (particle size distribution and specific surface): the thinner the grains, the faster the reactions;
- Water / cement ratio;
- Section thickness;
- Concrete placement temperature;
- Ambient conditions;
- Presence and type of chemical admixtures.

The concrete hardening process causes an increase in the internal temperature of concrete and a thermal imbalance with the environment around it. The mass concrete structure cools slowly in the core and quickly on the surfaces due to the proximity to the environmental air, thus generating significant thermal gradients (NGUYEN; BUI; HOANG, 2021). In addition, the surface mechanical strengths are lower than the core ones due to the faster cooling of the surface (BOBKO et al., 2015).

According to Azenha (2009), due this thermal imbalance, the processes of heat transfer through the mechanisms of conduction, convection and radiation are initiated (FIGURE 4). Through convection, a process that increases in the presence of the wind, heat exchange occurs between the structure and the external environment. However, the internal heat generation can be higher than the heat flow to the environment, thus hindering the thermal balance. Internally, there is the conduction process. Still according to Azenha (2009), the thermal balance will occur when the heat generated internally through the chemical reactions is lower than the heat flow between the structure and the environment.

Figure 4 - Main heat transfer processes in a mass concrete foundation

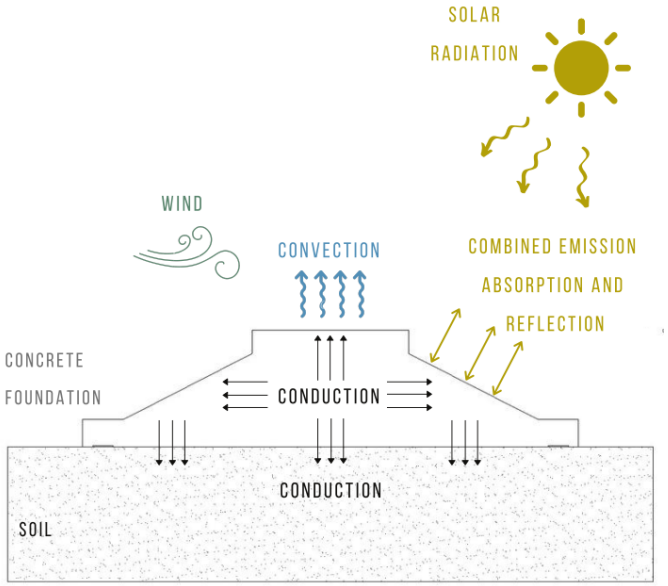

Source: Author (2022).

Conduction is the mode in which heat flow occurs from the hottest to the coldest part of the structure by direct molecular contact and not by gross motion (LEVENSPIEL, 2014). Heat transfer is called steady when the heat flow does not change over time. It is unsteady or transient when the heat flow varies with time (FORSBERG, 2021a). This type of heat transfer typically occurs inside solids (AZENHA, 2009). In a steady-state (when the temperature differences and heat fluxes driving the heat transfer remain constant with time), heat transfer can be expressed by Fourier's law (EQUATION 1) and depends on the nature of the material and the temperature differential (LEVENSPIEL, 2014). As the temperature of a mass concrete structure changes with time, its temperature distribution can be classified as a transient thermal process (KIM, 2010).

$$q_n" = -k\frac{\partial T}{\partial n} \tag{1}$$

where n designates the direction of the heat flow, e.g., x, y, or z in Cartesian coordinates; k is the thermal conductivity of the material; $q_n"$ is the rate of heat flow (W/m²) in direction n per unit area perpendicular to the heat flow and $\partial T/\partial n$ is the temperature gradient in direction n.

The convection heat transfer mode normally is between a surface and a surrounding fluid. This involves the combination of conduction between the surface and surrounding fluid

layer and of heat transport into the fluid in motion (FORSBERG, 2021a). The rate of heat transfer by convection is influenced by the difference in temperature between the surface of the structure and the fluid. Regardless of the process of heat transfer by convection, Equation 2, which represents Newton's law of cooling, is appropriate to calculate the convection transfer rate.

$$q" = h_c\,(T_s - T_\infty) \tag{2}$$

where $q"$ is the convective heat rate (W/m²), which is proportional to the temperature difference between the surface (T_s) and fluid (T_∞) temperatures; h_c is the convective heat transfer coefficient (W/m².K), which depends on the conditions in the boundary layer. This coefficient is directly proportional to wind speed (AZENHA, 2009). The convective heat transfer coefficient can be calculated according to Equation 3 (B4CAST, 2022).

$$h_c = \left({}^{1}/_{\alpha_k} + \sum ({}^{e}/_{\beta}) \right)^{-1} \tag{3}$$

$$\alpha_k = 20 + 14\,v \qquad if\ v \leq 5\ m/s$$

$$\alpha_k = 25.6\,v^{0.78} \qquad if\ v > 5\ m/s$$

where e is the thickness of formwork/insulation-material, β is the thermal conductivity of material and v is the wind speed.

According to Azenha (2009), when radiation hits an element, three things can happen: total or partial reflection, total or partial absorption and total or partial transmission. Besides, it can be emphasized that the thermal input provided by solar radiation has a high influence on the thermal behavior of mass concrete structures, such as wind turbine foundations, due to hydration heat that delays dissipation (AZENHA, 2009). According to the Stefan-Boltzmann Law of Radiation, the rate of thermal radiation is expressed by Equation 4.

$$q" = e\,\sigma\,(T_S^4 - T_\infty^4) \tag{4}$$

where $q"$ is the radiation heat rate (W/m²), e is the dimensionless emissivity or absorptivity of the structure (hotter structures emit energy and colder structures absorb), σ is the Stefan-Boltzmann constant (5.67x10-8 W/(m²K4)), T_s is the surface temperature and T_∞ is the surroundings temperature.

The analysis of heat transfer from concrete to the environment by convection and radiation is complex because they depend on several factors, mainly the boundary conditions, highlighting the characteristics of the surroundings (walls and ground surfaces), presence of formwork, curing blankets, ambient conditions and conduction of heat inside the concrete (GILLILAND; DILGER, 1997 apud RIDING, 2007).

ACI 207.1R (2006) reported that with the occurrence of this thermal phenomenon in this type of structure, stresses are developed within the concrete, which results in the change of volume. Thus, if the strains are restrained, cracks might arise in the concrete (FIGURE 5).

Figure 5 - Representation of the effect of internal and external restraints on the development of stresses and cracks in a foundation block: a) longitudinal section; b) cross section

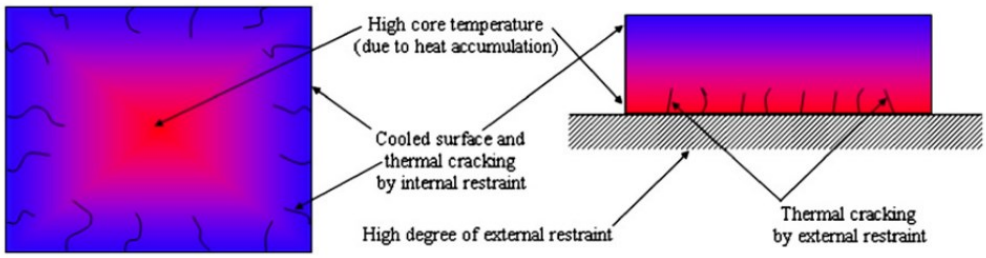

a) b)

Source: Amin *et al.* (2009).

Thermal stresses (compressive and tensile) vary according to the spatial and temporal evolution of temperatures. During the heating period, the core presents a higher temperature and a higher probability of expanding, thus appearing compressive stresses in the core and tensile stresses at the surface. However, during the cooling period, the tensile stresses predominate in the core and the compressive stresses at the surface (AZENHA, 2009).

The compressive stresses that arise in the core after placement are not so large, because at that moment, when the temperature increases significantly, the elastic modulus of concrete is low and the creep is high, which provides a relief of stress. In contrast, at the moment of cooling, the elastic modulus is high and creep is small, which leads to significant tensile stresses (BOFANG, 2014).

2.2.2. Temperature control

Thermal stresses are more significant when there is a large difference between the maximum (at the central core) and minimum (at the outside surface) temperatures in a mass concrete structure (ACI 207.2R, 2007; COELHO et al., 2014; BOBKO et al., 2015). According to ACI 207.2R (2007), thermal gradients are temperature changes and determined through a time history of temperature for a specific path through the structure. There are two types: mass gradients (between a concrete mass and a restraining foundation) and surface gradients (the result of surface cooling relative to internal temperatures).

Increasing the dimensions of mass concrete structures causes an almost adiabatic rise in internal temperature due to the difficulty of dissipating the generated heat (ACI 207.2R, 2007; BOBKO et al., 2015).

To avoid thermal increases harmful to concrete, it is recommended to use types of cement classified as low heat of hydration (LH), which, according to NBR 16697 (ABNT, 2018), they have total generated heat less than 270 J/g at 41 h of the test. According to ASTM C150 (ASTM, 2012), a cement classified as low heat of hydration should generate a maximum of 250 J/g at 7 days or 290 J/g at 28 days. And according to European standard EN 197-1 (BSI, 2011), the heat of hydration should be a maximum of 270 J/g at 7 days, when determined according to EN 196-8 (BSI, 2010), or 41 h, when determined according to EN 196-9 (BS, 2010). Furthermore, among the types of cement commercialized in the world, some are classified as LH.

According to Mehta and Monteiro (2014), to control the internal temperature of concrete is one of the main ways to avoid thermal cracking. To minimize thermal cracks, ACI 301 (2010) set a maximum temperature difference of 35 ºF (19.4 ºC) between the center of the element and average daily ambient temperature, not just the concrete surface. This standard recommends the development of a thermal control plan for the placement of mass concrete structures to limit both the temperature gradient and the maximum temperature.

The thermal control plans must evaluate the concrete mix (particularly the type and content of cement), guide the placement process and inform the maximum placement temperature of concrete and the possible mechanisms to reach it. In addition, it is relevant to inform about the control of superficial heat dissipation (curing procedures and formwork removal) and describe the entire process of temperature monitoring (equipment, procedures and locations for temperature sensors), including remedial measures when temperatures exceed pre-

established limits and when cracks appear (ACI 301, 2010; BOBKO et al., 2015; VIRGINIA DOT, 2016).

According to ACI 301 (2010), temperatures should be monitored every hour using sensors capable of measuring temperatures from 0 ºC to 100 ºC. The ambient temperature on-site should also be monitored. Temperatures should be measured from the moment the concrete is poured until the moment the difference between the average daily ambient temperature and the internal temperature of the concrete is less than 20 ºC. Finally, this standard guides to compare the values of temperatures and differences every 12 h and if they exceed the limits, the cause should be identified and action taken as soon as possible according to the control plan developed. The structure should be cured and protected for at least 7 days (BOBKO *et al.*, 2015). In practical terms, thermocouples (FIGURE 6) should be used embedded into concrete to measure internal concrete temperature.

Figure 6 - a) Thermocouple type K, with glass fiber insulation cable with a connector at one of its extremities, from Bagarel brand; b) Thermocouple installed in the foundation reinforcement

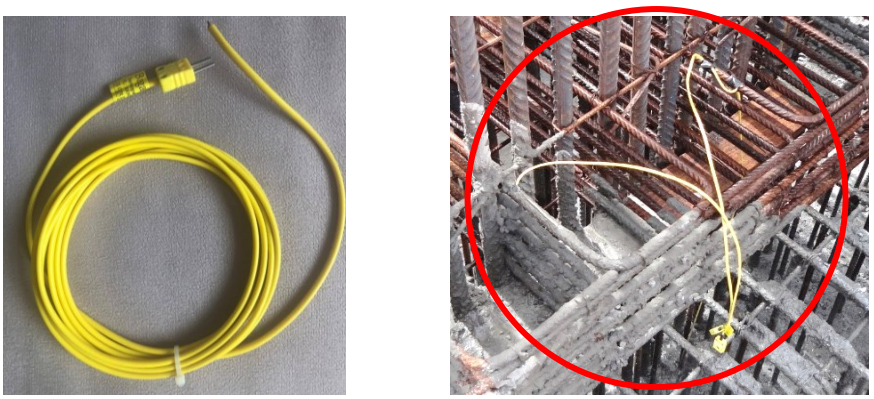

a) b)

Source: Cabral, Machado e Babadopulos (2020).

Regarding the concrete placing temperature, Virginia DOT (2016) states that it cannot exceed 35 ºC and Texas DOT (2014) states that it cannot exceed 24 ºC. As for the temperature monitoring step, a temperature sensor must be placed at the center of concrete mass (ACI 301, 2010) and, if necessary, at other points that can reach maximum temperatures (VIRGINIA DOT, 2016). In addition, ACI 301 (2010) requires the placement of another temperature sensor at a depth of approximately 5 cm from the center of the surface closest to the center of mass and one more to monitor the ambient temperature on site. Predicting possible

failures and aiming at safety, this standard recommends placing a pair of temperature sensors at each chosen point.

To reach the concrete placing temperatures and avoid damaging thermal rises, precooling techniques can be used, such as the cooling of aggregates using liquid nitrogen, cooling the concrete water, or replacing part of the mix water with ice. During mixing, the heat required to melt the ice is removed from other components of the mixture, thus reducing the placing temperature. Besides, to avoid high-temperature gradients, post-cooling techniques can be used by circulating cold water in pipes embedded in the concrete structure. Another technique is the use of materials, such as bidim blankets, to provide surface insulation of the structure to control heat loss from conduction, convection and radiation.

2.2.3. Delayed ettringite formation (DEF)

It is important to highlight that, during the cement hydration process, ettringite is formed after the hydration of aluminates and calcium sulfate. This phenomenon can be called early ettringite formation (EEF), which occurs homogeneously and immediately (within hours or days). Although it is an expansive phenomenon, the EEF does not harm the concrete because it occurs during its deformable state.

However, the early heating of the concrete can change the normal process of hydration reactions. When the internal temperature of the concrete varies from 60 ºC to 70 ºC approximately, the EEF is harmed and ettringite may be formed in the future when the concrete stays in touch with water. In this case, delayed ettringite formation (DEF) occurs (COLLEPARDI, 2003). Unlike EEF, DEF occurs in a heterogeneous way and after months or years. The volumetric expansion caused is deleterious to the concrete because it happens during its hardened state, causing an increase in internal stresses in the structure and may rupture it by exceeding the strength of the material (COLLEPARDI, 2003). Figure 7 shows a concrete foundation cracked due to DEF and Figure 8 shows the scanning electron microscopy (SEM) of the ettringite crystals formed.

Figure 7 - Concrete foundation cracked due to DEF phenomenon

Source: Hasparyk, Kuperman e Torres (2016).

Figure 8 - SEM of the ettringite crystals

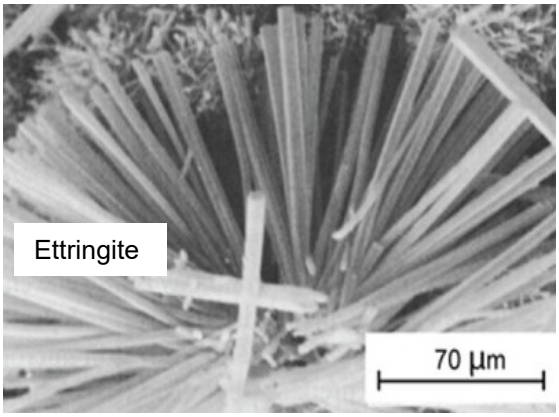

Source: Hasparyk, Kuperman e Torres (2016).

The absence of standards to verify the potential for delayed ettringite formation in concrete before its application highlights the importance of using methods to control the rise in internal temperatures of mass concrete structures before their casting (FUNAHASHI JUNIOR; GAMBALE, 2022). Therefore, to avoid the emergence of DEF and to perform effective monitoring of mass concrete structures, it is important to establish a maximum temperature limit to be observed. Some considerations of this temperature threshold can be found in the literature, such as 65°C (MEHTA; MONTEIRO, 2014) and 70ºC (TAYLOR; FAMY; SCRIVENER, 2001). These values prove the ACI 301 (2010) maximum temperature limit in concrete after placement, which should not exceed 70 ºC. For the analyses performed in this study, the adopted limit was 65 ºC.

2.2.4. Finite Element Method (FEM)

There are some methods used for the analysis of the thermal behavior of concrete structures, such as the finite difference method, finite element method (FEM), boundary element method and control volume approach. Finite element method is one of the most used for structural mechanics and stress calculation. Also, this method can provide better accuracy of complex geometries and boundary conditions by dividing the structure into smaller regions (finite element mesh creation). These regions can typically be triangular for two-dimensional objects or tetrahedral for three-dimensional objects (FORSBERG, 2021b). There is some software available in the market that can be used for finite element analysis, such as Ansys, Comsol, Diana, SolidWorks, Abaqus and b4cast.

Using FEM it is possible to estimate the evolution of the temperatures distributed in the concrete structure with time, the maximum temperatures and to determine the points considered critical for the appearance of cracks of thermal origin. Monitoring the temperature, over time, at some points of the structure, together with model predictions, allows the evaluation of the risk of thermal cracking and the choice of the best mitigating methods to be used.

To obtain the results of the FEM analyses, it is necessary to provide some input parameters to the software used, such as materials properties, casting conditions, curing conditions, and special in-service conditions (SFIKAS; INGHAM; BABER, 2018). The main results can be presented in graphs, showing the distribution and development of temperatures at any point in the structure over time. Computational analyses using FEM in concrete structures are mainly performed for the development of new structural designs and forensic engineering of existing structures (SFIKAS; INGHAM; BABER, 2018).

The estimation and diagnosis of thermal stress and possible cracks in a concrete structure is very relevant because, through it, it is possible to have technical and financial advantages, since problems will be avoided and the decisions taken will have a reliable basis, reducing construction and repair costs (AZENHA, 2009).

2.3 Methodological procedure

Aiming to achieve the specific objectives 1 of this dissertation, this section describes the research method that will be used to perform this part of the study, ranging from the choice of the two computational tools (Ansys and b4cast finite element software) to the comparison between the results of each software and the field monitoring data. Figure 9 shows the flowchart of the process designed to perform these activities. In this Chapter, four computer simulations were performed (S1, S2, S3, and S4). In the flowchart, it is shown in which steps they were used. These simulations were differentiated by the value of the placing temperature applied, which was equal to 15ºC, 25ºC, 35ºC, and 30ºC, respectively.

Figure 9 - Flowchart of this study

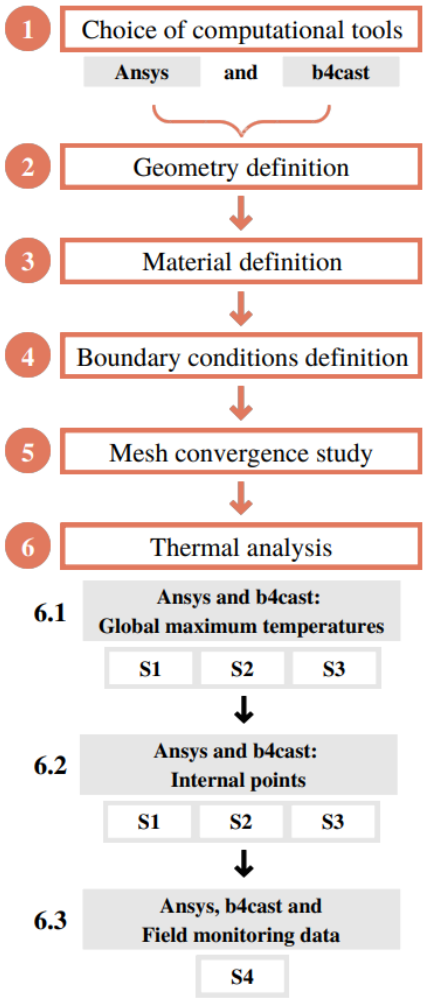

Source: Author (2022).

2.3.1. Selection of computational tools

The selection of the two computational tools to perform the thermal analyses was made with the purpose of comparing the results between the commercial specific purpose software (b4cast) and the commercial customizable software programmed for this type of analysis (Ansys). Given the several options found in the literature, these software were chosen due to their ease of use and learning, and the available licenses.

2.3.2. Geometry definition

The first step in performing the thermal analysis is to define the geometry that will be studied. It was chosen to analyze a foundation block of a wind tower of a wind farm located in the Brazilian northeast. According to the design provided by the construction company, the

structure has a base diameter of 18.30 m, a total height of 4.00 m, and a top diameter of 5.40 m, totaling a volume of 484.72 m³. Moreover, each foundation block would be made with the use of two concrete mixes, distributed as follows: from 0.00 m to 3.20 m height, the concrete mix of fck = 30 MPa, and from 3.20 m to 4.00 m, the concrete mix of fck = 40 MPa (FIGURE 10). The cement used in the mixes was Portland blast furnace.

Figure 10 - Cross section of the foundation block structure

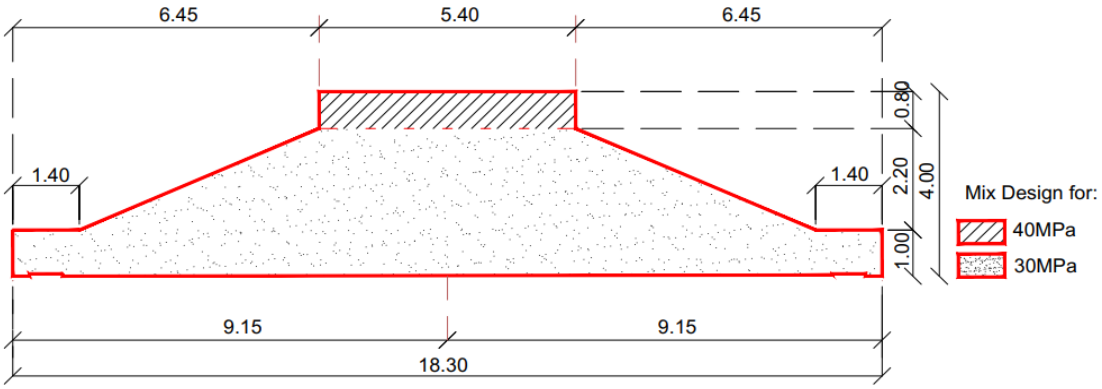

Source: Cabral, Machado e Babadopulos (2020).

The geometry was sketched in both Ansys (FIGURE 11) and b4cast (FIGURE 12) software. The design of the analyzed structure can be divided into three geometric figures: a base cylinder (called volume V1), a central cone trunk (volume V2), and a top cylinder (volume V3). Figure 13 shows this division. It is worth noting that, for the analyses, no time intervals between the casting of each part of the geometry were considered. In addition, there is a 0.10 m layer of regularization concrete and a 8.00 m layer of soil below the entire structure, which were considered in the design.

Figure 11 – Geometry of the evaluated foundation block defined in Ansys software

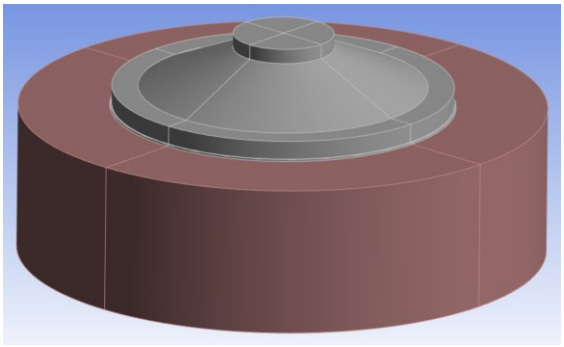

Source: Author (2022).

Figure 12 – Geometry of the evaluated foundation block defined in b4cast software

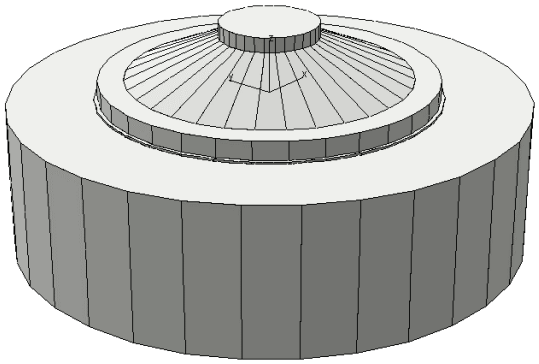

Source: Cabral, Machado e Babadopulos (2020).

Figure 13 - Division of the structure design

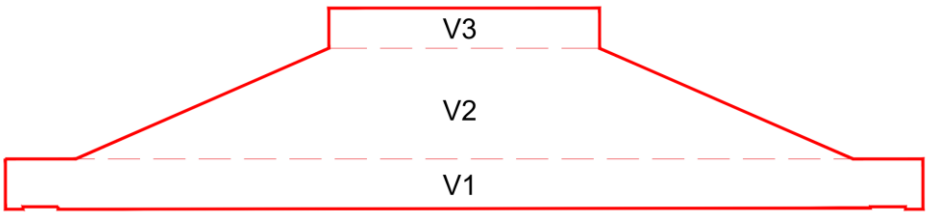

Source: Cabral, Machado e Babadopulos (2020).

2.3.3. Material definition

For the computer simulations, it is important to determine the properties of the concrete and correctly characterize the materials that compose it. The ability to estimate the thermomechanical response of cement-based materials is dependent on accurate thermal property determination (HONORIO; BARY; BENBOUDJEMA, 2018). The main thermal properties required for this type of analysis are coefficient of thermal expansion, specific heat or thermal capacity, thermal conductivity, and thermal diffusivity.

Another important point that needs to be implemented in thermal analyses of concrete structures is the rate of heat released during cement hydration, and it is possible to measure it through isothermal calorimetry, described in C1702 (ASTM, 2017), or Langavant's method, described in NBR 12006 (ABNT, 1990). In addition, there are Brazilian standards that establish tests to find most of the parameters mentioned above: NBR 12820 (ABNT, 2012) for thermal conductivity, NBR 12817 (ABNT, 2012) for specific heat, and NBR 9778 (ABNT, 2005) for density.

Due to the impossibility of performing laboratory tests to obtain the material properties, some of these values were obtained from the literature, according to the characteristics of the concrete mixes, and others were provided by the construction company of the foundation block and by the Laboratory of Civil Construction Materials (LMCC) of the Federal University of Ceará (UFC). Table 1 shows the values of the concrete properties implemented.

Table 1 - Concrete properties used in thermal analyses

Property	**Concrete Mix f_{ck} = 30 MPa**	**Concrete Mix f_{ck} = 40 MPa**
Density [(1)]	2322.00 kg/m³	2326.00 kg/m³
Specific Heat [(2)]	1.00 kJ/kg/ºC	1.00 kJ/kg/ºC
Thermal Conductivity [(3)]	9.55 kJ/m/h/ºC	9.55 kJ/m/h/ºC
Coefficient of Thermal Expansion [(4)]	10^{-5} / ºC	10^{-5} / ºC

Source:
[(1)] LMCC (2020); [(2)] Couto (2018); [(3)] Breugel (1998); [(4)] Mehta e Monteiro (2014); Couto (2018).

The heat of hydration curves used in the analyses were obtained through tests performed by LMCC, considering the influence of the admixture in the mixes design. The tests were performed on an isothermal conduction calorimeter TAM Air (TA Instruments) with eight channels and a computerized acquisition system. The procedure for this test was based on ASTM C1702 (ASTM, 2017), which is initiated after the weighting and the filling of the 20ml ampoules with the cement paste. The ampoules must then be inserted into the cells of this equipment, which must be at a constant temperature. It is worth mentioning that, during the tests, the electric power supply cannot be interrupted due to the continuous use of the computer for data acquisition and the air conditioning for local temperature control (GONÇALVES, 2018).

According to NBR 16697 (ABNT, 2018), the cement used was classified as low heat of hydration (LH). Figure 14 shows the curves with values in W/m³, which were implemented in the internal heat generation of the structure in Ansys. Figure 15 shows the curves with values in J/g, which were implemented in b4cast. The 30 MPa mix design has a cement content equal to 310 kg/m³, with 0.5% polyfunctional admixture, and the 40 MPa mix design has a cement content equal to 330 kg/m³, with 0.9% polyfunctional admixture.

Figure 14 - Heat of hydration curve of cement in W/m³ implemented in Ansys software

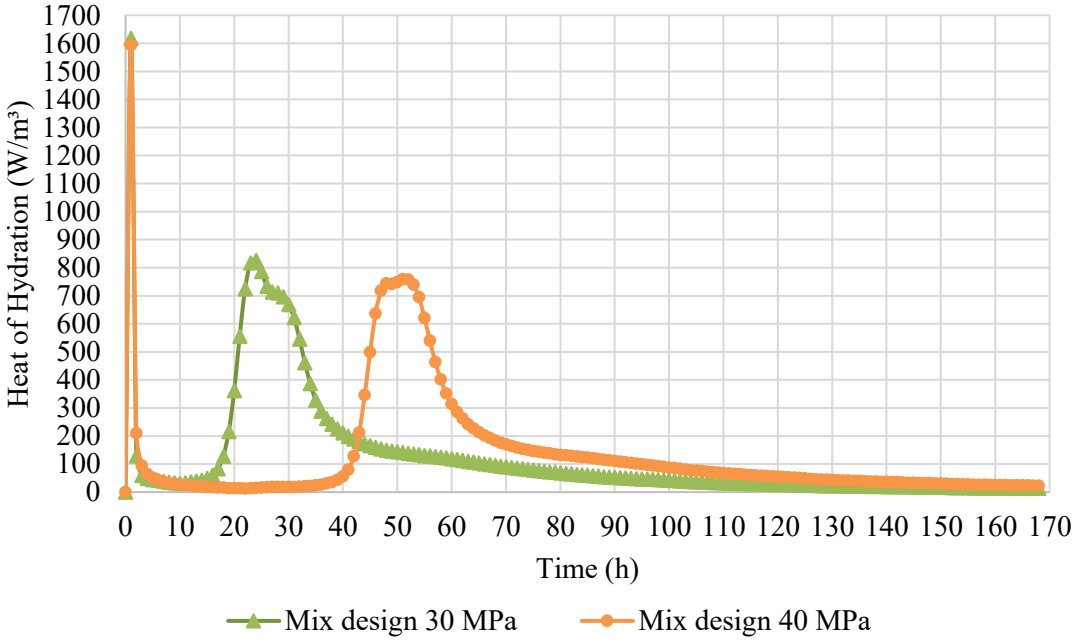

Source: LMCC (2020).

Figure 15 - Heat of hydration curve of cement in J/g implemented in b4cast software

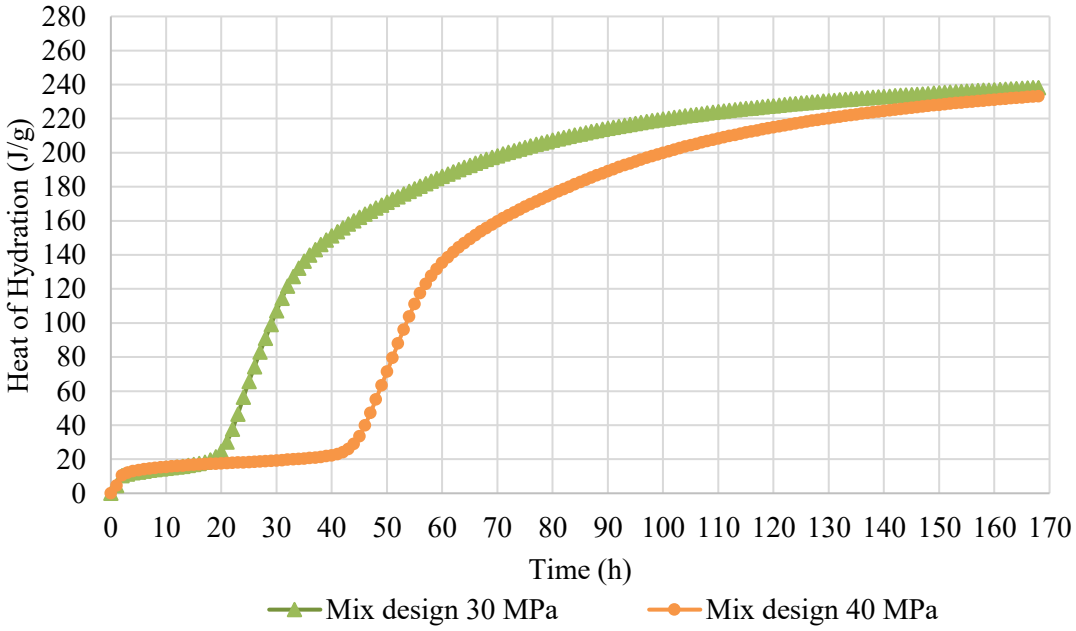

Source: LMCC (2020).

In contrast to what was expected for the behavior of the curves shown in Figures 14 and 15, it was noticed that the hydration heat curve of the 40 MPa mix design (with higher cement content) showed lower values than the heat curve of the 30 MPa mix design. The higher additive content in the 40 MPa mix and the small difference in the cement content (20 kg/m³) between the two mixes can justify this behavior. According to Zhang et al. (2018) and Antoniazzi, Mohamad, and Casali (2021), increasing the content of some additives in concrete can delay the setting time, generating a slower heating.

Finally, it was necessary to define the properties of the soil layer underneath the entire structure. According to the construction site of the foundation blocks, the soil is predominantly sandy. The thermal properties of the soil were obtained based on literature data and are described in Table 2.

Table 2 - Soil properties used in thermal analyses

Property	
Density [(1)]	1515.00 kg/m³
Heat Capacity [(2)]	0.80 kJ/kg/ºC
Thermal Conductivity [(3)]	0.97 kJ/m/h/ºC
Coefficient of Thermal Expansion [(6)]	10^{-5} / ºC

Source:
[(1), (2), (3)] Incropera *et al.* (2008); [(4)] Delage (2013).

2.3.4. Boundary conditions definition

The next step for carrying out the thermal analyses was to apply the boundary conditions to the foundation block geometries, to improve the accuracy of the results.

To define the convection temperatures, the city temperature of the wind farm site was researched. According to the data obtained from climate forecasts, the average temperatures in this city vary between 28ºC and 32ºC, and may eventually exceed 32ºC. Thus, to define the worst thermal situations in the geometries, it was chosen that the ambient surface temperature of the foundation block geometries would be 32 ºC.

Another point that must be considered is the influence of wind speed. According to the climate forecasts, the wind speed in the city of the building site varies between 5.60 m/s and 9.70 m/s. In this way, the maximum value of 9.70 m/s was adopted.

Finally, it was considered that, on the sides of the geometries of the largest base cylinder (V1) and the top small cylinder (V3) (FIGURE 16), there are steel formworks of 14 mm thick, which will be in contact with the concrete up to 48 hours after the casting of concrete. In addition, the application of wet curing during the first 7 days after casting was considered.

Figure 16 – Steel formworks on the sides of the geometries V1 and V3

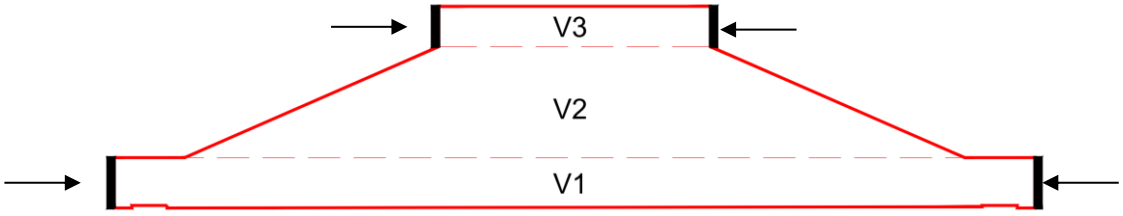

Source: Author (2022).

It is emphasized that, for the analyses described in this chapter, heat exchange by radiation was not considered.

2.3.5. Mesh convergency study

To ensure more accurate simulations, in addition to the boundary conditions and material properties, the discretization of meshes is extremely important. A point that is linked to the quality of the FEM analyses is the number of elements created for each case study, i.e., the size of the mesh. The relationship between the number of elements and the precision of the analysis is given by the convergence of the mesh (PATIL; JEYAKARTHIKEYAN, 2018).

The more refined the mesh, the more time and computational effort is required to perform the analyses. Thus, it is necessary to balance the refinement of adequate mesh with computational resources. This is done using a mesh convergence study. The mesh will converge when further mesh refinement produces a negligible change in the solution. First, the structure should be discretized, producing the mesh. Later, its results should be analyzed, then, this mesh should be refined and it should be verified if the results obtained are similar to the previous ones and, if so, the first mesh can be used for the analysis of the results (COELHO, 2016).

For the mesh convergence study, it was chosen to vary the mesh size from 1.00 m to 0.40 m. Sizes smaller than 0.40 m were not feasible due to the limit of software elements, in

the case of Ansys (student version), and computational capacity, in the case of b4cast. Figures 17 and 18 show the mesh refinement done for this study.

Figure 17 – Mesh refinement in Ansys software

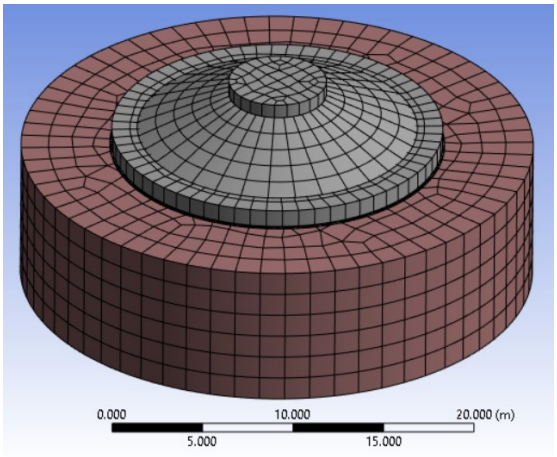

a) 1.00 m

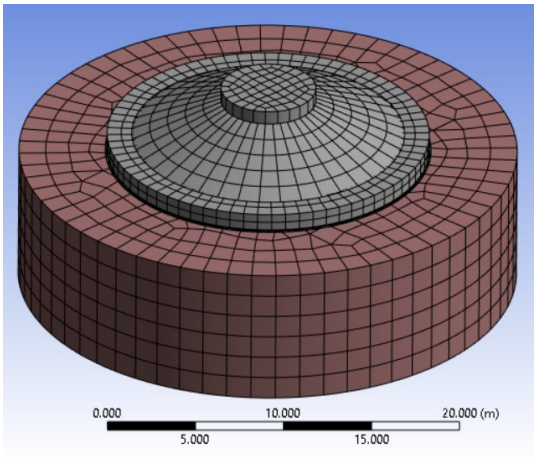

b) 0.80 m

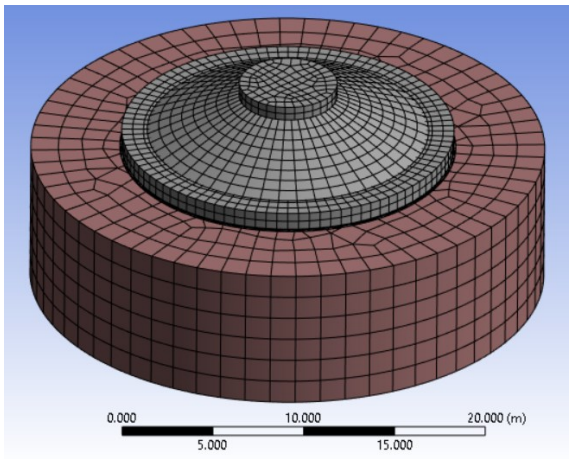

c) 0.60 m

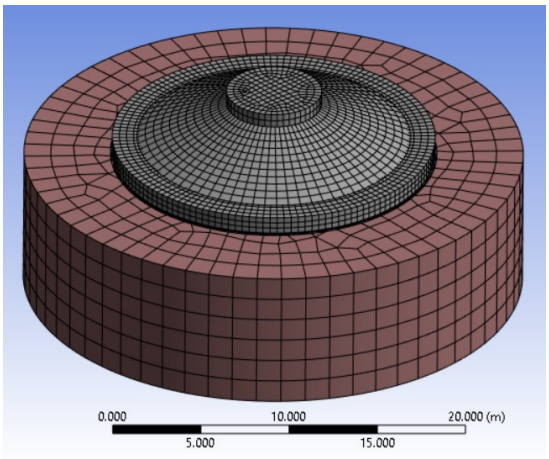

d) 0.40 m

Source: Author (2022).

Figure 18 – Mesh refinement in b4cast software

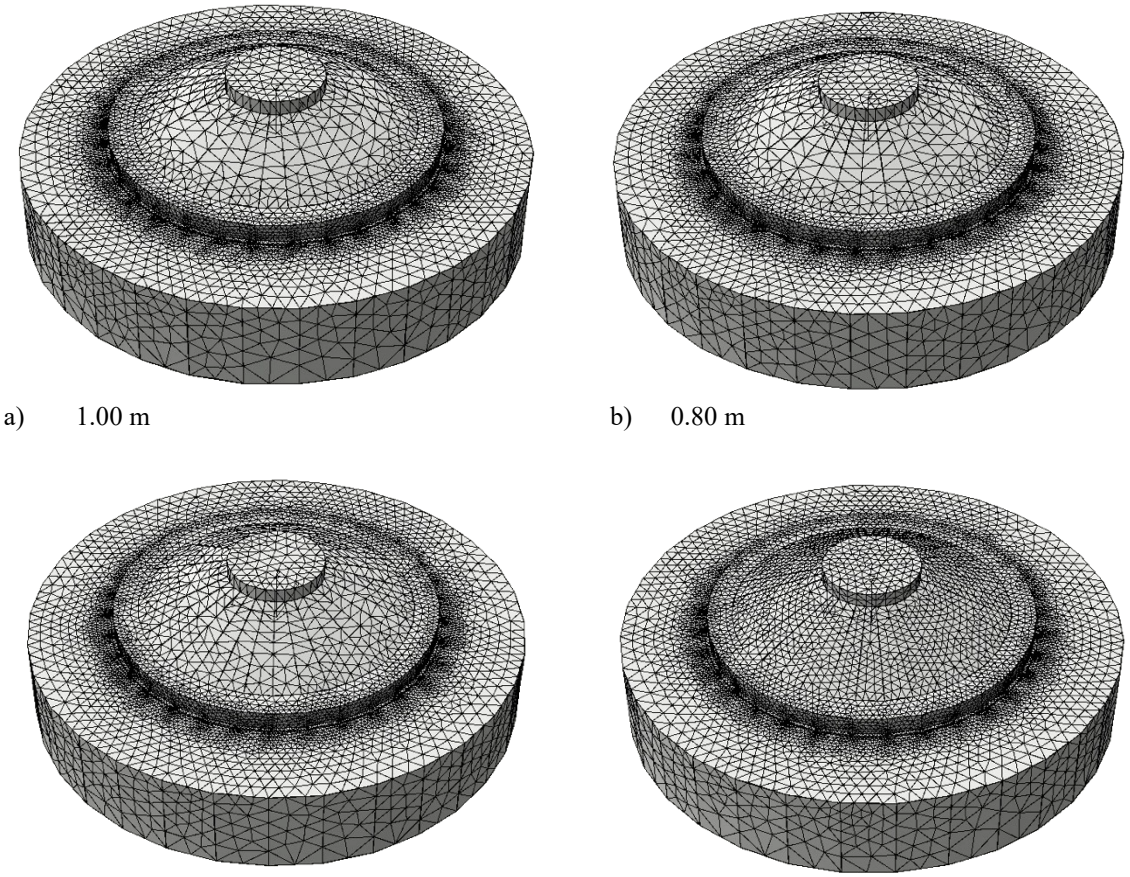

a) 1.00 m b) 0.80 m

c) 0.60 m d) 0.40 m

Source: Author (2022).

The global maximum and minimum temperature data of the structure were analyzed in each test, and the results of the mesh convergence study are presented in Figures 19 and 20 for Ansys and b4cast software, respectively.

Figure 19 – Mesh convergence study in Ansys software

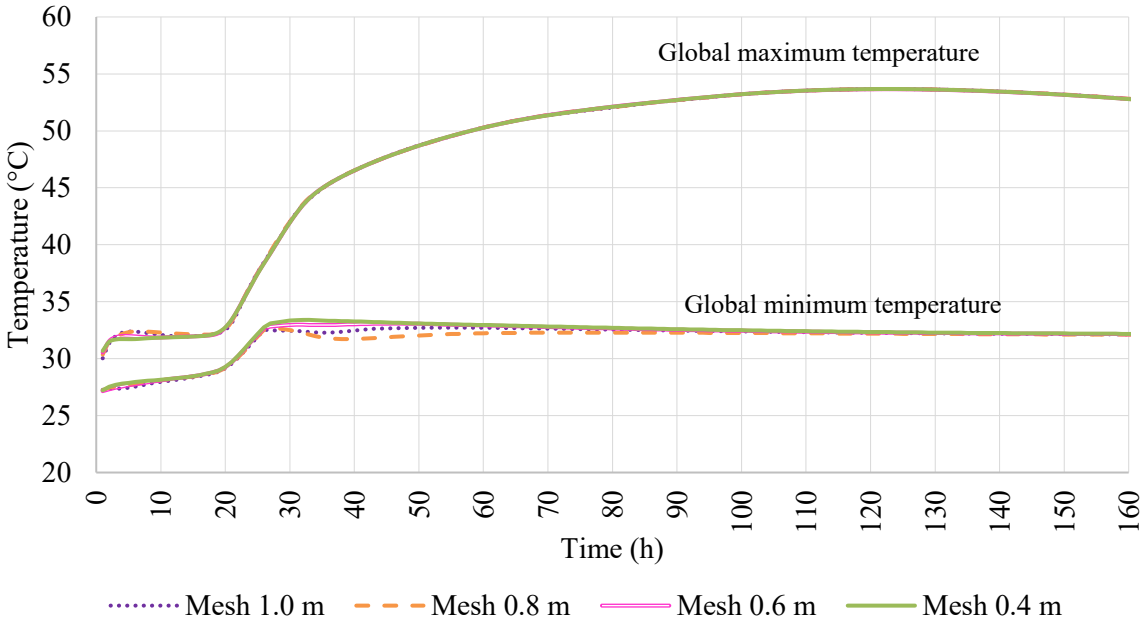

Source: Author (2022).

Figure 20 – Mesh convergence study in b4cast software

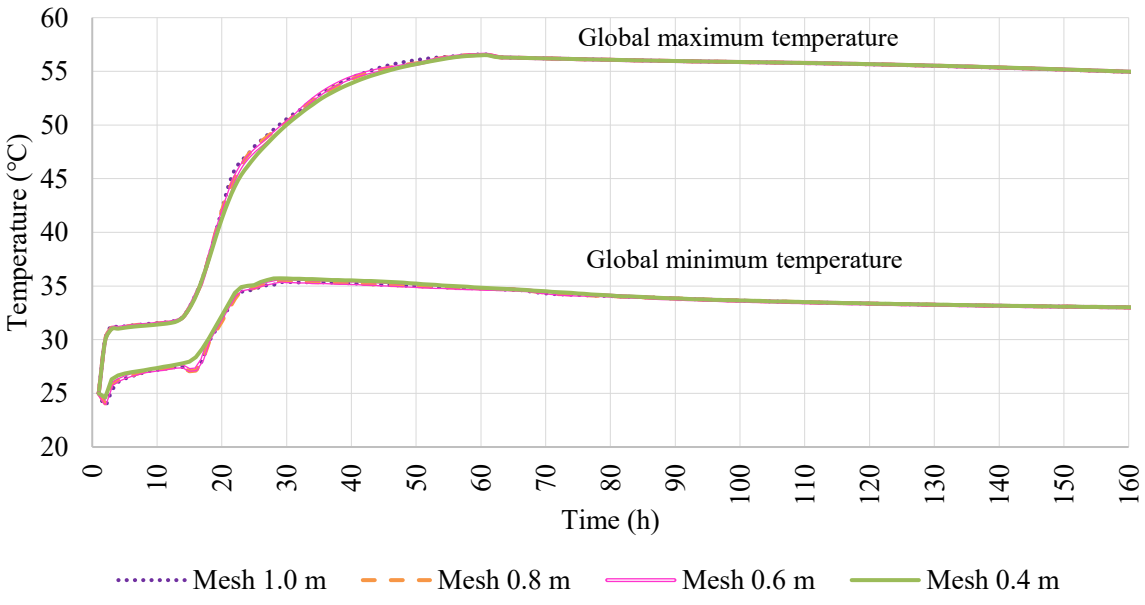

Source: Author (2022).

According to Figure 19, in the analysis of minimum temperatures, a divergence between the less refined meshes (1.00 m and 0.80 m) and the more refined meshes (0.60 m and 0.40 m) was observed between 30 h and 50 h of the study. In the analysis of maximum

temperatures, a small divergence between these meshes was observed only in the first 20 h of the study. The 0.60 m and 0.40 m meshes showed excellent convergence, with an average difference of 0.02 °C and a maximum difference of 0.28 °C. Thus, for a lower computational effort, it was chosen to use the 0.60 m mesh to perform the following simulations.

According to Figure 20, in the analysis of minimum temperatures, a divergence between the less refined 1.00 m mesh and the other more refined meshes was noticed in the first 20 h of the study. In the analysis of maximum temperatures, uniformity was observed for the analysis of all meshes, with small deviations between 20 h and 50 h. Given the results, to standardize, it was also chosen to use the 0.60 m mesh in the b4cast simulations.

2.4 Thermal analysis results

To perform the thermal analyses and define the optimal placing temperatures and the time of the peak temperatures, initially, 03 simulations were performed (S1, S2, and S3) varying the concrete placing temperature of the entire foundation block (parts V1, V2 and V3) at 15 ºC, 25 ºC, and 35 ºC, respectively. The highest temperature (35 °C) is the maximum allowed according to the Virginia DOT (2016). The minimum temperature (15 ºC) was chosen due to the environmental conditions of the construction site city and, consequently, the challenge of casting concrete with temperatures lower than this value. In addition, for the simulations, 30 ºC was considered as the initial temperature of the soil and the regularization concrete layer.

After defining the materials, geometries, and boundary conditions of the structure, the mesh with a distance between each node of 60 cm was generated both in b4cast and Ansys software. The thermal analyses of the concrete structure were then started.

To compare the results obtained between Ansys and b4cast software, the maximum global temperatures reached by the structure were analyzed, to determine the ideal placing temperatures for each part of the foundation block. Next, internal points in critical heating zones were chosen to evaluate the thermal rise experienced by the concrete over time in each of the studied software. Finally, to verify their reliability, a new study was performed comparing the results from computer analyses with the field monitoring data of a foundation structure, received from the wind farm construction company.

2.4.1. Ansys and b4cast: Global maximum temperatures

The first part of this study was mainly performed to define the ideal concrete placing temperatures for each part of the structure. For this, the maximum global temperatures reached by the concrete in each part of the structure versus the concrete placing temperatures (15 °C, 25 °C, and 35 °C) considered in each simulation (S1, S2, and S3, respectively) were presented. The upper limit chosen for the concrete temperature during cement hydration was 65 °C (MEHTA; MONTEIRO, 2014). Figures 21, 22, and 23 present this comparison of the maximum global temperatures for parts V1, V2, and V3, respectively. Table 3 shows the summary with the overall maximum temperatures reached by each part of the structure in simulations S1, S2, and S3, and the time to reach these temperatures. Table 4 shows the absolute difference between the results of global maximum temperatures from Ansys and b4cast software in the three simulations performed for each part of the structure.

Figure 21 – Global maximum temperatures reached by V1 in simulations S1, S2 e S3 with the placing temperatures 15 °C, 25 °C, and 35 °C, respectively

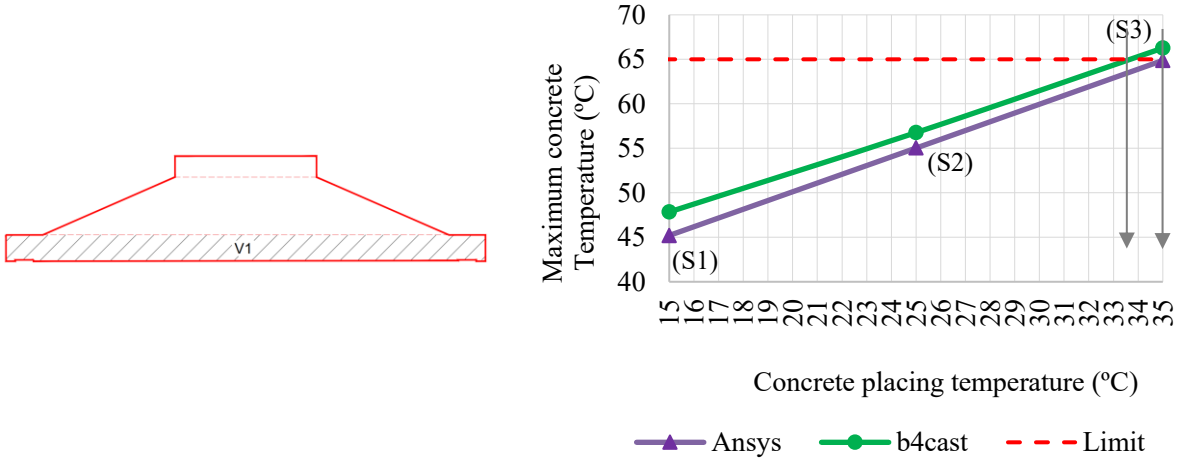

Source: Author (2022).

Figure 22 – Global maximum temperatures reached by V2 in simulations S1, S2 e S3 with the placing temperatures 15 °C, 25 °C, and 35 °C, respectively

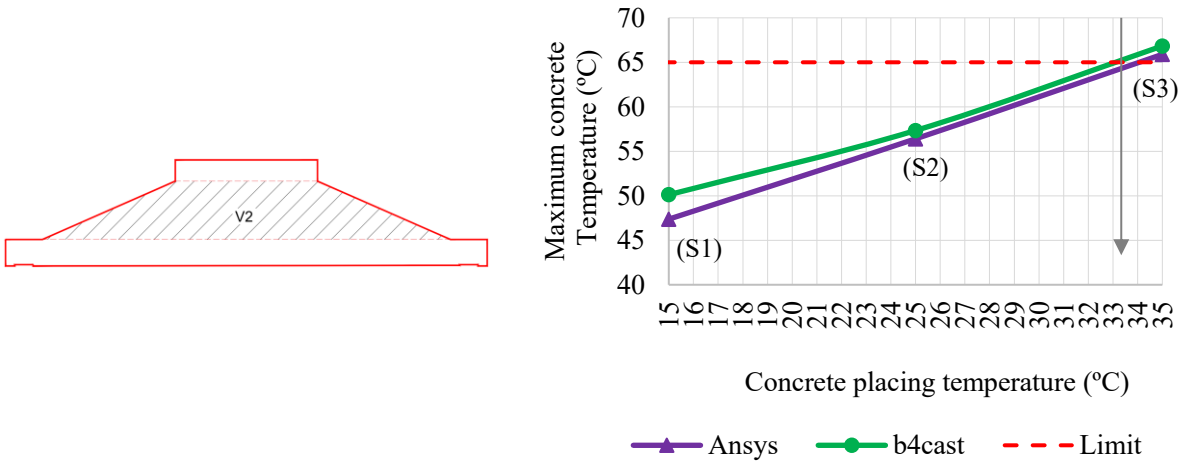

Source: Author (2022).

Figure 23 – Global maximum temperatures reached by V3 in simulations S1, S2 e S3 with the placing temperatures 15 °C, 25 °C, and 35 °C, respectively

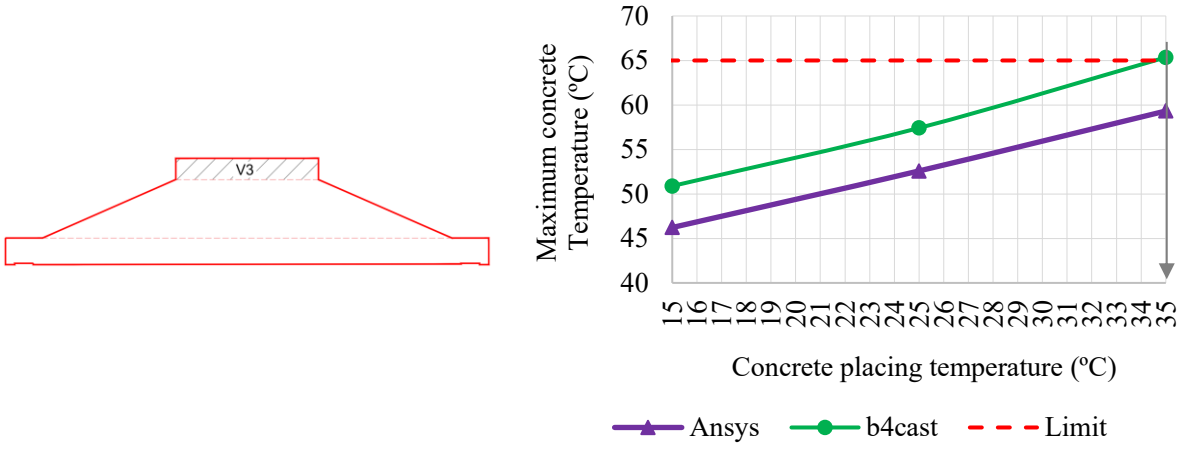

Source: Author (2022).

Table 3 – Global maximum temperatures reached and time to reach them in V1, V2 and V3 in simulations S1, S2 and S3 performed in Ansys and b4cast software

Simulation	Part	Ansys		b4cast	
		Global maximum Temperature (°C)	Time (h)	Global maximum Temperature (°C)	Time (h)
S1	V1	45.2	168	47.8	81
	V2	47.4	166	50.1	74
	V3	46.2	104	50.9	62
S2	V1	55.0	168	56.8	55
	V2	56.4	163	57.4	59
	V3	52.6	100	57.4	52
S3	V1	64.8	164	66.3	38
	V2	65.9	148	66.8	38
	V3	59.3	88	65.4	41

Source: Author (2022).

Table 4 – Absolute difference between the results of global maximum temperatures from Ansys and b4cast software in V1, V2 and V3 in simulations S1, S2 and S3

Simulation	Part	|Ansys – b4cast|
		Temperature (°C)
S1	V1	2.60
	V2	2.70
	V3	4.70
S2	V1	1.80
	V2	0.90
	V3	4.80
S3	V1	1.50
	V2	0.90
	V3	6.10

Source: Author (2022).

According to Figures 21, 22, and 23, and Table 3, it is possible to demonstrate what was already expected, that is, when the placing temperature increases, the maximum temperature reached by the structure also increases. Regarding the values of maximum temperatures, it is also observed that the results obtained in b4cast were higher than those of Ansys in all cases analyzed. Table 4 shows that the largest differences were identified in the V3 geometry, with a maximum value of 6.10 °C in simulation S3, with a higher placing temperature (35 °C). Despite the implementation of the same environmental properties and parameters to perform all simulations, it is not sure if the heat exchange process (conduction and convection) occurs in the same way in the two software, because b4cast is not customizable. Thus, it is in

the V3 geometry that there is an intense heat exchange process, since there is influence from both the external environment and the heating of the V2 part.

Table 3 shows that the higher the value of the applied placing temperature, the less time it took for the structure to reach its maximum global temperature in both Ansys and b4cast, following what is expressed in ACI 207.2R (2007). In addition to this, a major difference between the two software is highlighted: the simulations performed in b4cast showed that the structure reaches its maximum temperatures much earlier than the simulations performed in Ansys.

Another point is that, in Ansys, the time to reach the maximum temperatures was very close, or even at the end of the analyses, at 168 h. This behavior observed in the Ansys results does not characterize the behavior of real structures in general, which present temperature peaks before 168 h, as can be seen in the analyses made by Coelho (2012), Couto (2018), and in the next Sections of this Chapter. This suggests that more research on the boundary conditions is required to address this late peak of temperature obtained in Ansys.

Furthermore, through this preliminary analysis, it is possible to estimate the ideal placing temperatures for the structure. Considering the maximum limit of 65 ºC previously established for the maximum concrete temperatures, it can be seen in Figures 21, 22, and 23 that, according to the b4cast software, the ideal concrete placing temperature for geometries V1, V2, and V3 is equal to 33 °C, 33 °C, and 35 °C, respectively. About the Ansys software, geometry V1 admits to being cast at 35 °C, geometry V2 at 33 °C, and V3 at a temperature above 35 °C. The slight difference between these results showed a convergence between the software regarding the definition of the ideal placing temperatures for the concrete structure.

In addition to observing the global maximum temperatures in each part of the structure, the isotherms obtained by each software referring to each simulation were analyzed. The isotherms of simulation S1, with the placing temperature of 15 °C, are shown in Figures 24a and 24b for b4cast and 24c and 24d for Ansys. The isotherms of simulation S2, with the placing temperature of 25 °C, are shown in Figures 25a and 25b for b4cast and 25c and 25d for Ansys. And the isotherms for simulation S3, with the placing temperature of 35 °C, are presented in Figures 26a and 26b for b4cast and 26c and 26d for Ansys. For each simulation, the isotherms at the time of reaching the highest temperatures and at the end of the simulations, i.e., at 168 h, were also presented.

Figure 24 – Isotherms of simulation S1, with the placing temperature of 15 °C

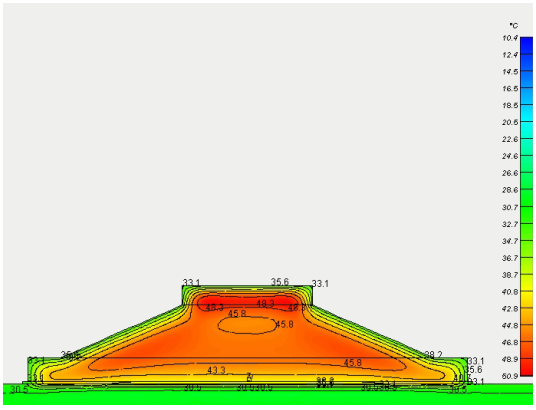

a) b4cast - maximum temperature time: 62 h

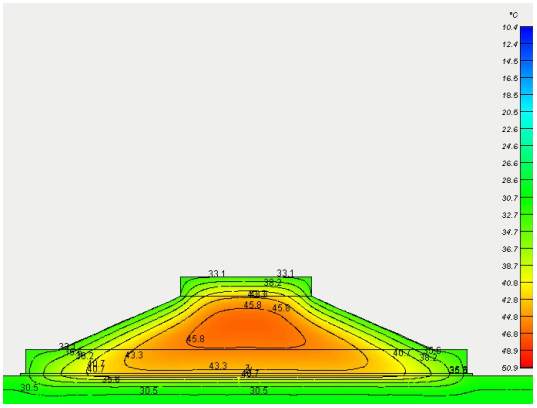

b) b4cast - simulation timeout: 168 h

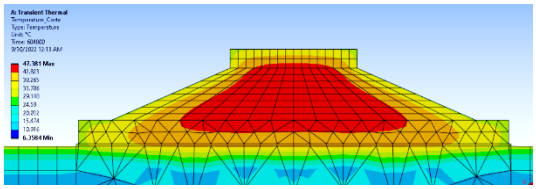

c) Ansys - maximum temperature time: 166 h

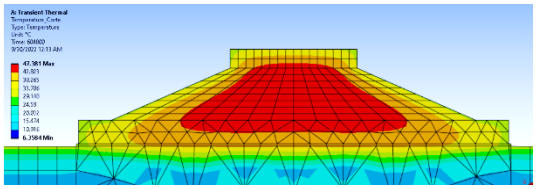

d) Ansys - simulation timeout: 168 h

Source: Author (2022).

Figure 25 – Isotherms of simulation S2, with the placing temperature of 25 °C

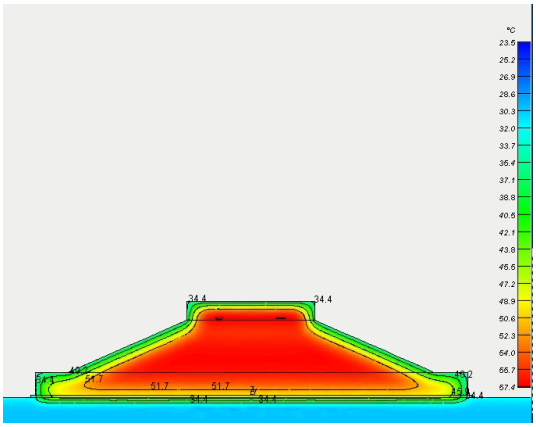

a) b4cast - maximum temperature time: 59 h

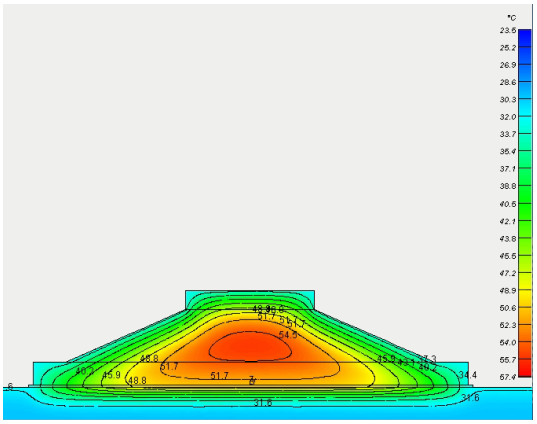

b) b4cast - simulation timeout: 168 h

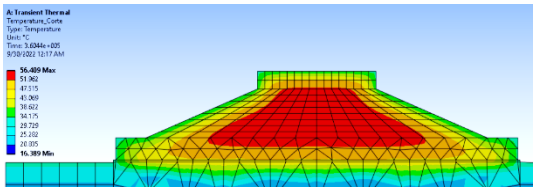

c) Ansys - maximum temperature time: 163 h

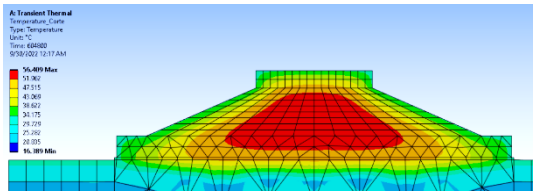

d) Ansys - simulation timeout: 168 h

Source: Author (2022).

Figure 26 – Isotherms of simulation S3, with the placing temperature of 35 °C

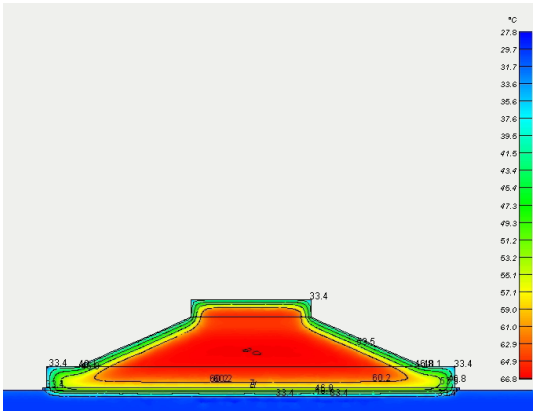

a) b4cast - maximum temperature time: 38 h

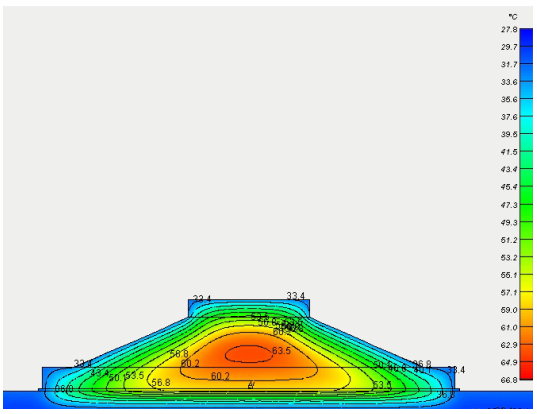

b) b4cast - simulation timeout: 168 h

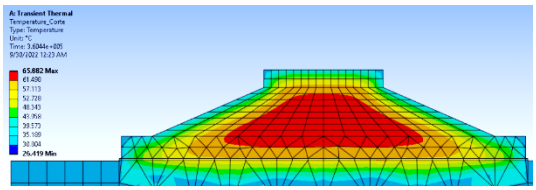

c) Ansys - maximum temperature time: 148 h

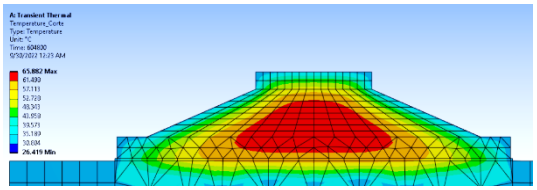

d) Ansys - simulation timeout: 168 h

Source: Author (2022).

It was also observed that, for Ansys, there was little difference between the isotherms of the moment of reaching the maximum temperatures and the final moment of the simulation, which can be justified by the shorter time interval between them. For b4cast, however, this difference was greater, where it is possible to see more uniform heating of the whole structure at the moment of reaching maximum temperatures and cooling of the areas closer to the external environment at 168 h of analysis.

Despite the differences observed between the isotherms of the two software, it is important to highlight the similarity between the thermal behaviors in all cases studied, which can be better observed in the isotherms of 168 h of analysis. At this instant, it is noticeable, for all simulations performed both in Ansys and b4cast, the occurrence of the highest temperatures near the geometric center of the structure (in geometry V2) and the cooling of geometry V3 and the edges of the structure, which present an easier heat exchange due to their proximity to the external environment. In addition, the influence of the heating of the center (located in geometry V2) on the geometry V1 is also observed in the isotherms of 168 h.

2.4.2. Ansys and b4cast: Internal points - thermal increase over time

In the following, according to the observation of the thermal behavior of the foundation block, three central points (A in V1, B in V2, and C in V3) and one point at the edge of the geometry (D in V3) were chosen, shown in Figure 27, to verify the thermal rise experienced by them and compare the results obtained in Ansys and b4cast. The central points were chosen because they are in more critical regions for reaching the maximum temperatures, and the point at the edge was chosen to analyze the heat exchanges with the outside and the temperature differences between the center and the edge. The evolution of the temperatures of points A, B, C, and D over time was observed in simulations S1, S2, and S3 (with placing temperatures of 15 °C, 25 °C, and 35 °C, respectively) and are presented in Figures 28, 29, 30 and 31, respectively.

This part of the study was important to observe the thermal behavior of the structure over time in each software, analyzing the temperature differences and thermal gradients between the core and the edge of the concrete foundation as a function of time.

Figure 27 – Selected internal central points

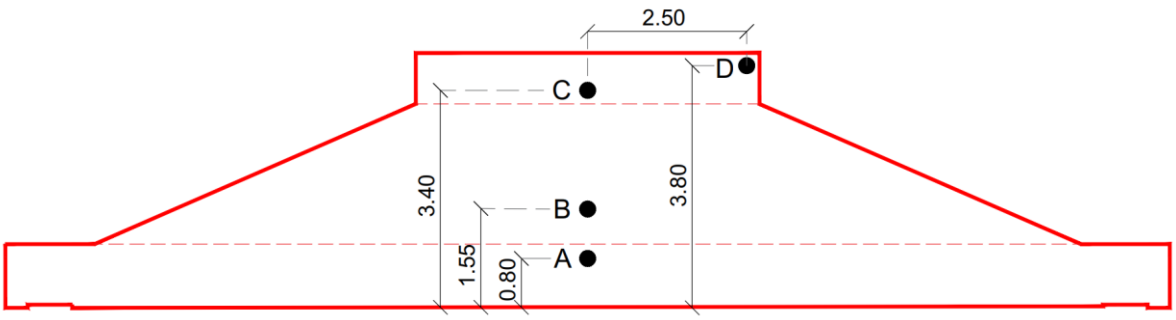

Source: Author (2022).

Figure 28 – Temperature rise of point A (a) over time for simulations S1 (b), S2 (c) and S3 (d)

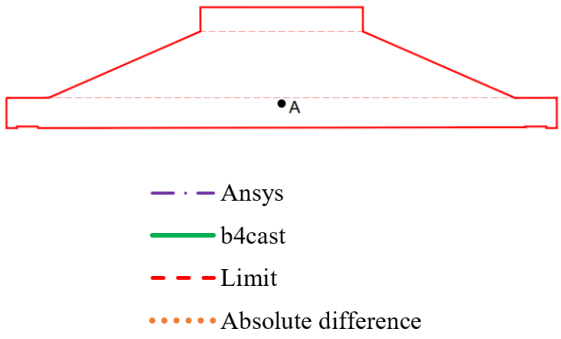

a) Point A and legend

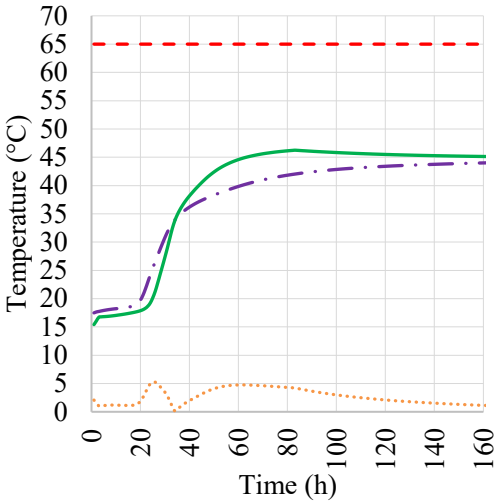

b) Temperature rise of point A in simulation S1, with placing temperature equal to 15 °C.

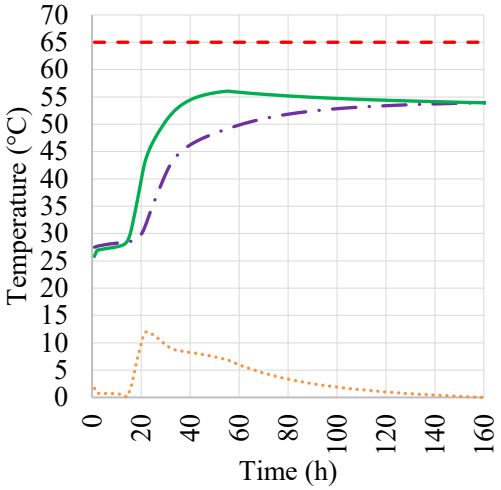

c) Temperature rise of point A in simulation S2, with placing temperature equal to 25 °C.

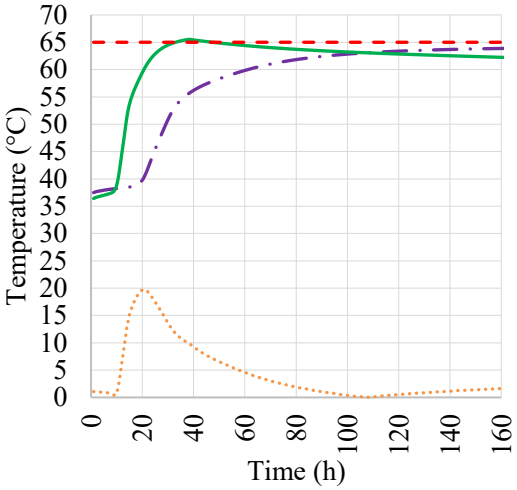

d) Temperature rise of point A in simulation S3, with placing temperature equal to 35 °C.

Source: Author (2022).

Figure 29 – Temperature rise of point B (a) over time for simulations S1 (b), S2 (c) and S3 (d)

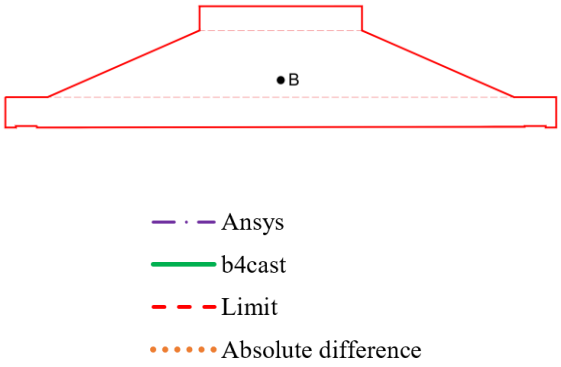

a) Point B and legend

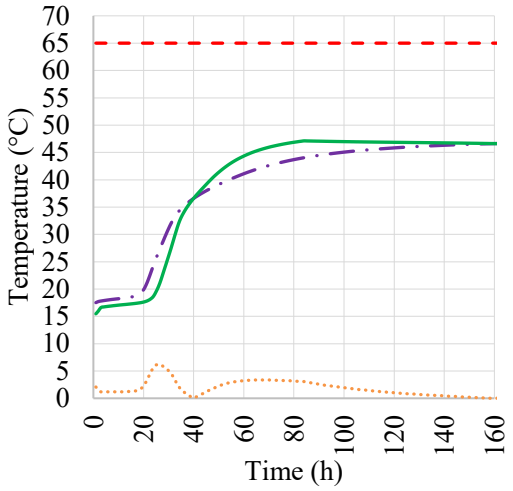

b) Temperature rise of point B in simulation S1, with placing temperature equal to 15 °C.

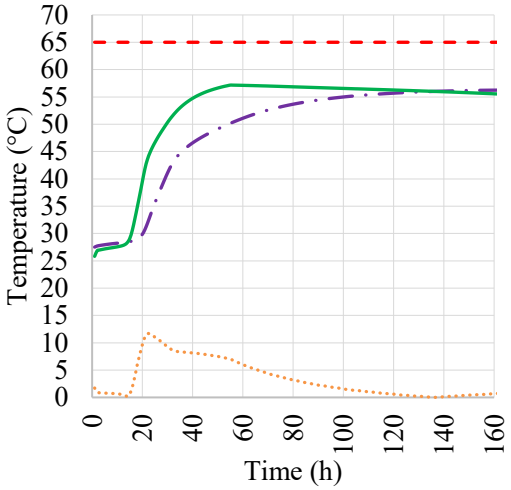

c) Temperature rise of point B in simulation S2, with placing temperature equal to 25 °C.

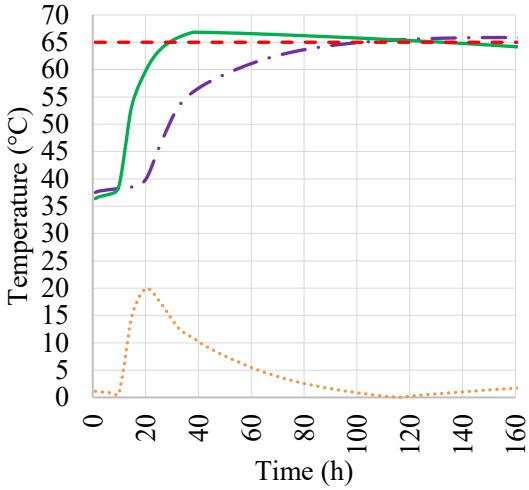

d) Temperature rise of point B in simulation S3, with placing temperature equal to 35 °C.

Source: Author (2022).

Figure 30 – Temperature rise of point C (a) over time for simulations S1 (b), S2 (c) and S3 (d)

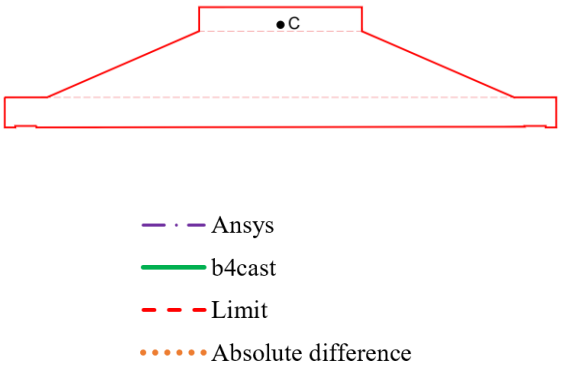

a) Point C and legend

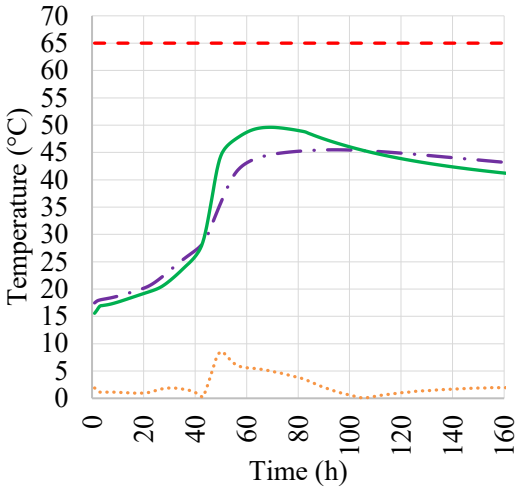

b) Temperature rise of point C in simulation S1, with placing temperature equal to 15 °C.

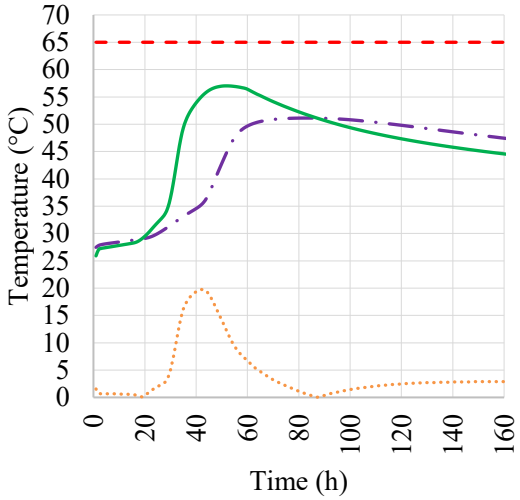

c) Temperature rise of point C in simulation S2, with placing temperature equal to 25 °C.

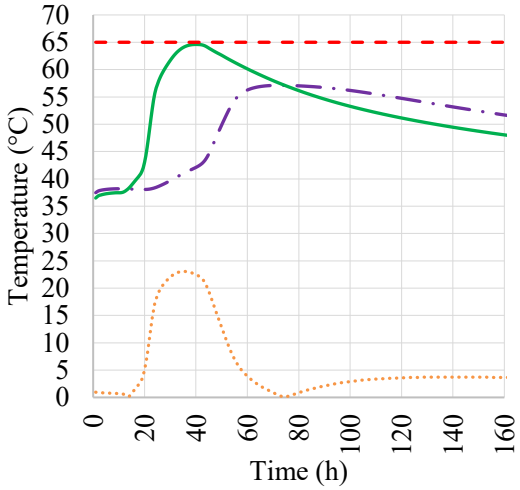

d) Temperature rise of point C in simulation S3, with placing temperature equal to 35 °C.

Source: Author (2022).

Figure 31 – Temperature rise of point D (a) over time for simulations S1 (b), S2 (c) and S3 (d)

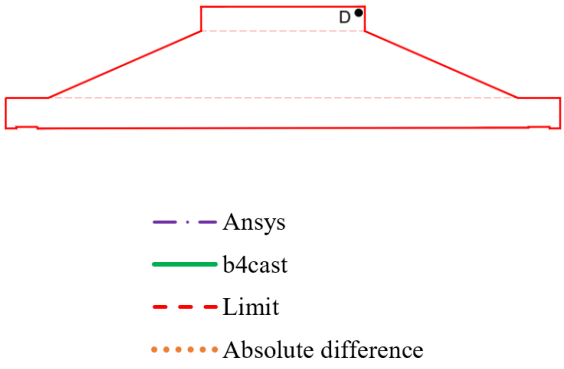

a) Point D and legend

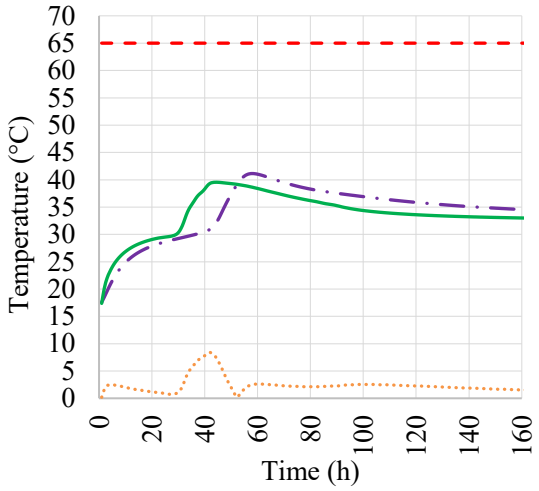

b) Temperature rise of point D in simulation S1, with placing temperature equal to 15 °C.

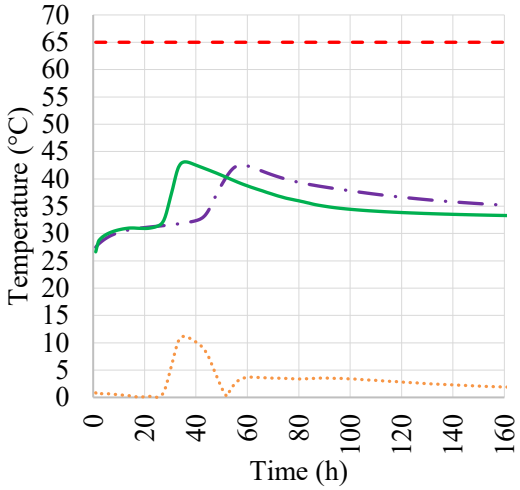

c) Temperature rise of point D in simulation S2, with placing temperature equal to 25 °C.

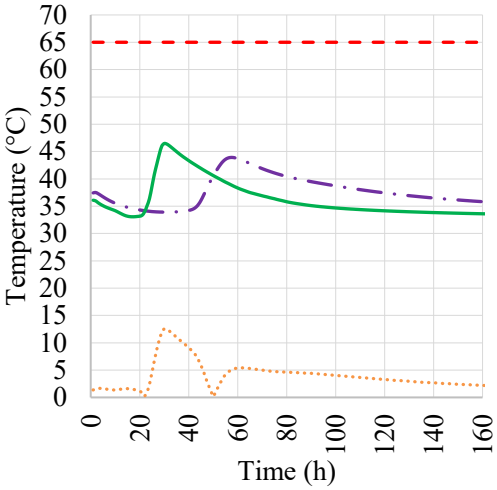

d) Temperature rise of point D in simulation S3, with placing temperature equal to 35 °C.

Source: Author (2022).

In general, when looking at Figures 28, 29, 30, and 31, the convergence in the trend of the temperature curves as a function of time between the Ansys and b4cast results is noticeable for all cases. As with the analysis of the global maximum temperatures (presented in Figures 21, 22, and 23), the higher the placing temperature, the higher the thermal elevation of the points. In addition, the results obtained from b4cast were superior for most of the time of the analyses, especially regarding the temperature peaks. The curves of the results obtained in Ansys showed a slower heating of the structure during the simulations performed in this software.

Analyzing the results obtained in both software, it can be seen that Point B (Figure 29) was the one that presented the highest temperature peaks, exceeding the limit of 65 ºC at some points in simulation S3. By analyzing the graphs in Figures 28 and 29, it can be noted the difficulty of the cooling of Points A and B, which is justified by the location of these points in the structure, in the center of geometries V1 and V2, causing the heat dissipation to the external environment a challenge. Although Point A is affected by the thermal rise in the central area of the structure, there is a small difference in the behavior of Point A when comparing it to Point B. This can be explained due to the heat exchange between Point A and the ground.

Regarding Point C, more intense heating was expected, since it is located in geometry V3, which is composed of 40 MPa concrete, i.e., with higher cement consumption. This was not identified due to the behavior of the heat curve of this mix design (Figures 14 and 15), due to the small volume of this geometry and its faster cooling because of its location closer to the external environment and because, after the launch of V3, no other volume of concrete was cast, so there is no influence of a new volume of concrete on its temperature rise. Finally, about point D, the lowest maximum temperatures and the highest cooling for both software are observed, since it is the point that is more influenced by the outside.

Although the results of the analyses performed in b4cast showed the fastest and highest temperature peaks in almost all cases, it was observed that the results of this software showed a faster cooling of the structure at Points C and D (closer to the external environment) in all three simulations performed. Despite the implementation of the same parameters in both software, according to these results, it can be concluded that the heat exchanges between the structure and the external environment were more intense in the analyses conducted in the b4cast software.

Besides the thermal behavior, the differences between the temperature values as a function of time obtained in each software were observed to verify their compatibility. Similarly to the analysis of the global maximum temperatures, the differences between the results obtained in Ansys and b4cast at points A, B, C and D increased as the concrete placing temperature increased. In an opposite way, the time intervals for the maximum differences to occur reduced with the increase of the placing temperature.

Analyzing the absolute differences between the results over time in Figures 28, 29, 30, and 31, very similar behavior can be seen at Points A and B, due to the proximity between these points, distinguishing them from the behavior at C and D. Table 5 presents the absolute maximum values between the temperature differences over time obtained from Ansys and

b4cast software for points A, B, C, and D. Besides, the time at which this maximum difference occurred is presented.

Table 5 – Maximum absolute differences between the results obtained in Ansys and b4cast for Points A, B, C, and D and time at which the maximum differences occurred

Simulation	Point	|Ansys – b4cast|	
		Temperature (°C)	Time (h)
S1	A	5.25	25
	B	6.26	26
	C	8.57	50
	D	8.40	42
S2	A	11.97	23
	B	11.97	22
	C	19.75	42
	D	11.16	35
S3	A	19.72	21
	B	19.94	22
	C	23.08	35
	D	12.55	32

Source: Author (2022).

According to Table 5, the absolute maximum differences were greater for Point C in all three simulations, exceeding 20 °C in S3. Furthermore, the maximum differences between the temperatures obtained in Ansys and b4cast occurred between 20 h and 50 h of analysis.

According to ACI 301 (2010), the difference between the internal temperatures of the structure and the average environmental temperature must be less than 19.4 °C to prevent the emergence of harmful stresses in the concrete due to high temperature gradients. Thus, since the ambient temperature was considered constant in the study presented in this chapter, to analyze the temperature gradients in the center of the structure in each software, it was chosen to use the differences between the temperatures at Point B (representing the core of the structure) and Point D (representing the edges in direct contact with the outside). Figure 32 illustrates the study of thermal gradients for the wind turbine foundation.

Figure 32 – Thermal gradients between Points B and D over time for simulations S1 (b), S2 (c) and S3 (d)

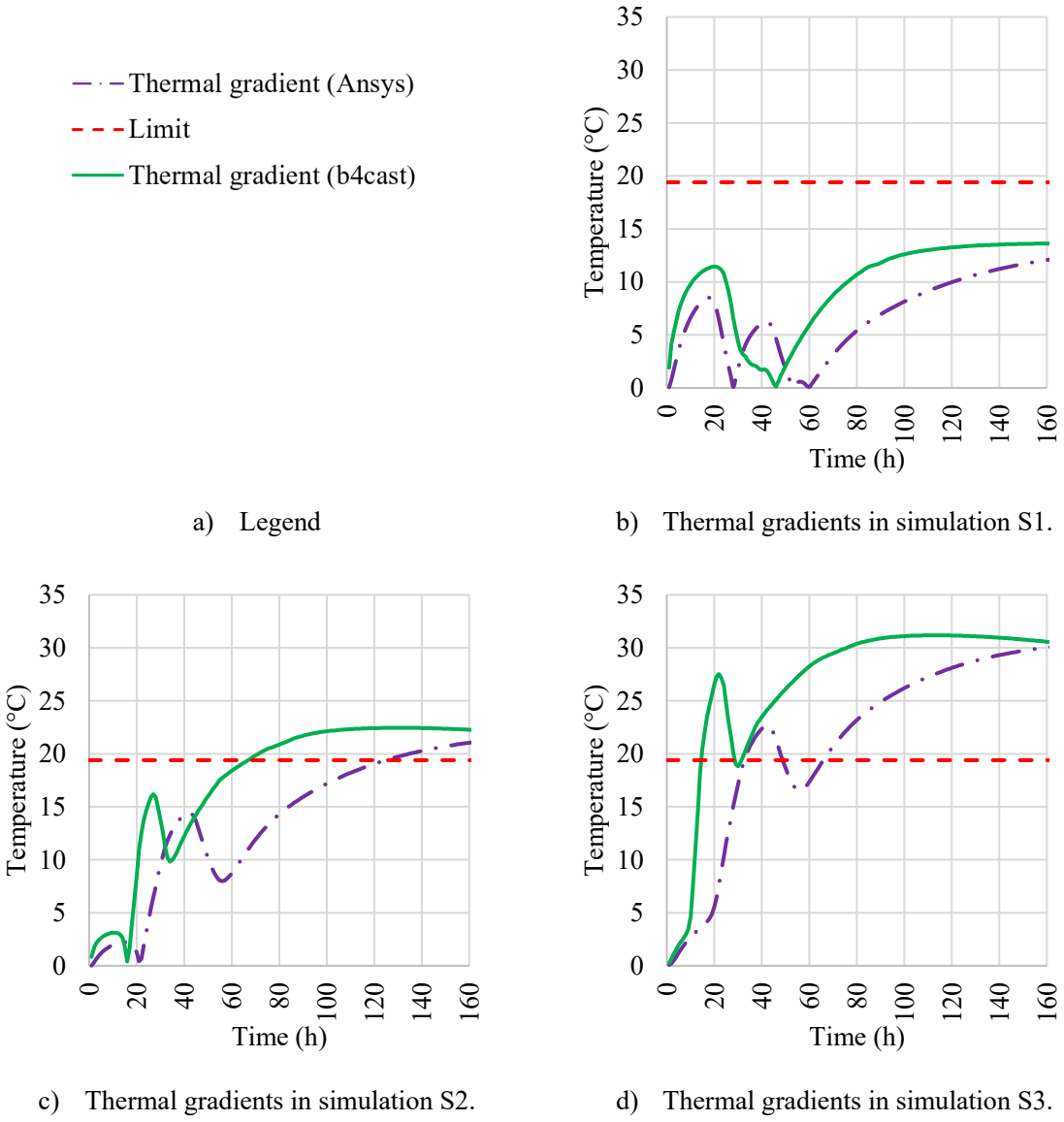

a) Legend

b) Thermal gradients in simulation S1.

c) Thermal gradients in simulation S2.

d) Thermal gradients in simulation S3.

Source: Author (2022).

Figure 32 shows the influence of concrete placing temperatures on thermal gradients is also confirmed, since they were higher as the placing temperatures increased. It is noteworthy that the thermal gradients were larger in the analyses performed at b4cast, which may be a point in favor of security in this software. Moreover, from the placing temperature of 25 °C (S2) the gradients exceeded the 19.4 °C limit, which deserves attention. The use of insulating materials at the edges could delay the heat dissipation from these areas, thus reducing the temperature differences between the edges and the core of the structure.

2.4.3. Ansys, b4cast and Field monitoring data

To finalize the study described in this chapter, it was chosen to perform a comparison between the monitoring data sent by the wind farm construction company and the results of the simulations performed in Ansys and b4cast software. According to the construction company, the temperature sensors were positioned on the coordinates indicated in the casting plan and attached with wires to the reinforcement of the foundation structure. The temperature acquisition devices were positioned on top of the structure and inside wooden boxes or plastic tubes for their protection and to ensure their operation during the days of analysis.

To do the comparison, a new simulation was performed in each software (S4), because the concrete placing temperature used in the field was different from the temperatures applied in simulations S1, S2, and S3. By analyzing the data received, it was noticed that the maximum field placing temperature reached 30 °C in some of the foundation blocks. Therefore, this value was considered in simulation S4. For the comparison with the results of this simulation, it was chosen the monitoring data of one of the foundation blocks (Block 01), which presented maximum temperatures higher than the limit of 65 °C.

Regarding the analysis points, the construction company installed four thermocouples (T01, T02, T03, and T04) to monitor the internal temperature rise in the concrete structure. The location of these points is shown in Figure 33 and it was used to extract the software results and, later, perform the comparison with the field data, presented in Figure 34. The maximum temperature values reached in the field and the computational analyses and the time to reach them after the beginning of the casting for T01, T02, T03, and T04 were analyzed and are presented in Table 6.

Figure 33 – Positioning of the thermocouples installed for monitoring the temperatures of the foundation blocks in the field

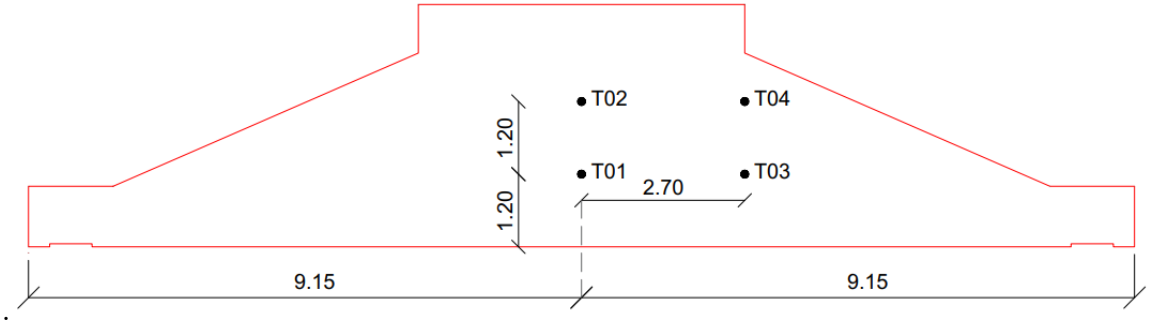

Source: Author (2022).

Figure 34 – Comparison between the field monitoring data from Block 01 and the S4 computer simulation results obtained in Ansys and b4cast for thermocouples T01 (a), T02 (b), T03 (c) and T04 (d)

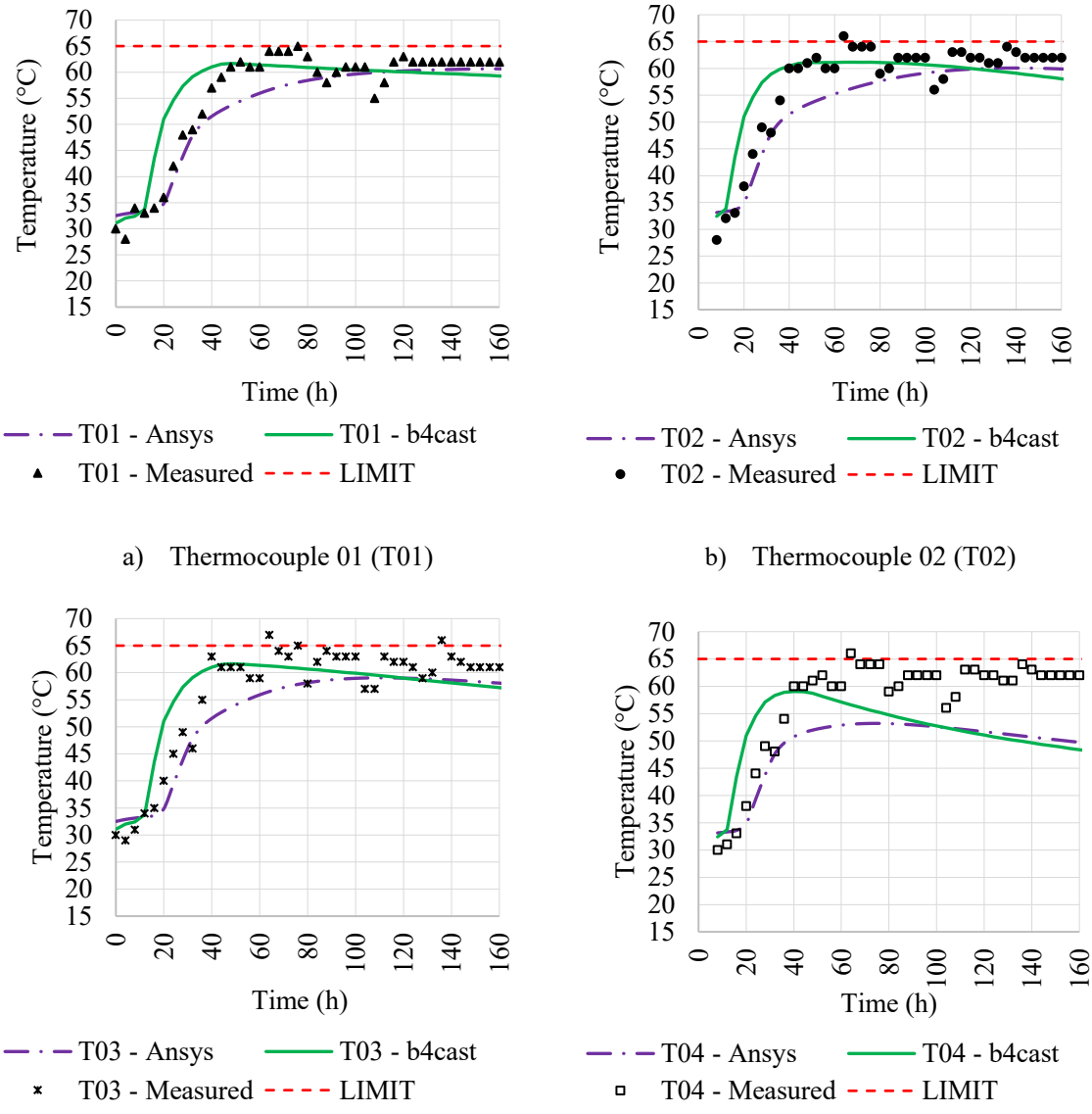

a) Thermocouple 01 (T01)

b) Thermocouple 02 (T02)

c) Thermocouple 03 (T03)

d) Thermocouple 04 (T04)

Source: Author (2022).

Table 6 – Maximum temperatures and time to reach them obtained from field monitoring and Ansys and b4cast software results for each thermocouple

Thermocouple	Field monitoring		Ansys		b4cast	
	Maximum Temperature (°C)	Time (h)	Maximum Temperature (°C)	Time (h)	Maximum Temperature (°C)	Time (h)
T01	65	76	60.65	164	61.68	48
T02	66	64	60.07	140	61.14	68
T03	67	64	59.05	112	61.66	48
T04	66	64	59.19	136	59.04	40

Source: Author (2022).

According to Figure 34 and Table 6, concerning the time to reach the maximum temperatures in the structure, the results from the b4cast software came closest to the field monitoring data if compared with Ansys results. For the thermocouples T01, T03, and T04, the maximum temperatures obtained in the b4cast software occurred at times lower than the instant for reaching the maximum temperatures in the field. For thermocouple T02, this time was very close, with a difference of only 4 hours. For the Ansys software, the maximum temperatures occurred at times higher than the field monitoring in all thermocouples.

It is important to point out that, in Figure 34, it is observed that the beginning of heating of the structure monitored in the field occurs in approximately 20 h and coincides with the beginning of heating of the structure in the S4 simulation performed in Ansys. However, after this time, the internal temperatures of the monitored structure rise to a peak, and the Ansys curve shows a slow heating until the end of the analysis. Thus, there is a distancing of these curves after 20 h of analysis.

Regarding the maximum temperature values, it was observed that for points T01, T02, T03, and T04, the results from the b4cast and Ansys software presented convergence with each other. However, these values were lower than the field monitoring data. Overall, the b4cast results in this simulation (S4) were the closest to the reality of the structure measured in the field.

Table 6 shows that the thermocouples T02, T03, and T04, installed in the field, presented points that exceeded the limit of 65 °C, which was not observed in the computer simulations, which presented results below this limit in the simulation performed (S4), with a placing temperature of 30 °C. Thus, it can be seen that, despite coincident values in some points (FIGURE 34), the simulations performed in this chapter could not accurately predict the value of the maximum temperature reached by the structure, which is one of the main results in

thermal studies due to the risk of DEF and the emergence of thermal stresses and, consequently, cracks.

When analyzing the results at the points of the thermocouples T01 (FIGURE 34a), T02 (FIGURE 34b), and T03 (FIGURE 34c), it is possible to see that the behavior of the curves from computer models and field measurements presented similarities in trend and differences in the position of the y-axis (temperature). This is expected since no effect of temperature variation on the thermophysical parameters of the material was considered. So the main effect on the heat equations is that of the original placing temperatures before the variations.

Regarding the point of the T04 thermocouple, Figure 34d shows the differences in the position of the y-axis (temperature) and also divergences in the trend, since the field monitoring data for this point did not show the expected cooling observed in the computational results for this point, which is closer to the external environment and, consequently, has a more favorable heat exchange. On the other hand, this cooling was observed in the monitoring data of the T04 thermocouple in the field monitoring of other blocks, as can be seen in Figure 35 for two other blocks (B02 and B03).

Figure 35 – Comparison between the field monitoring data and the S4 computer simulation results obtained in Ansys and b4cast for the T04 thermocouple in Blocks 02 (a) and 03 (b)

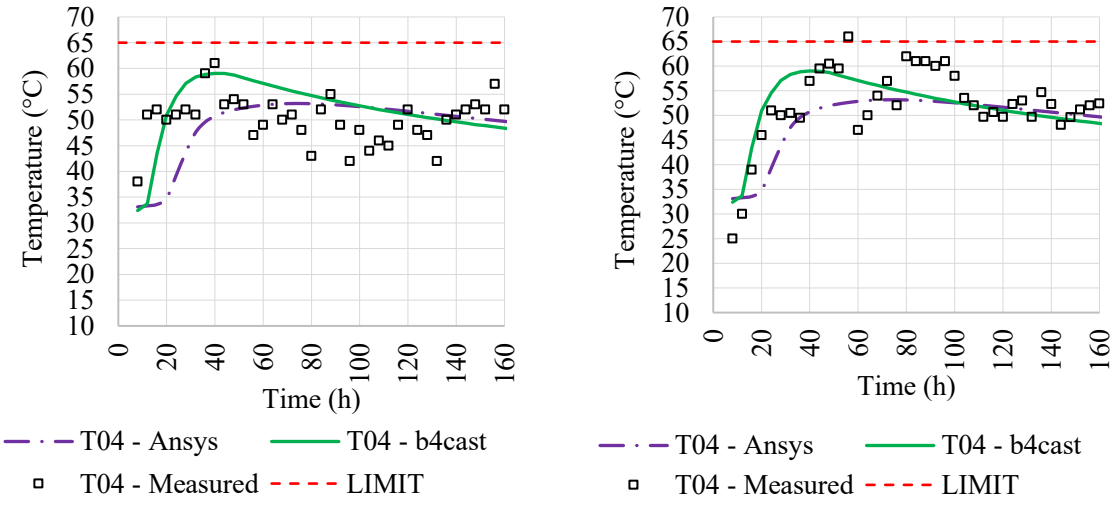

a) Thermocouple 04 - Block 02

b) Thermocouple 04 - Block 03

Source: Author (2022).

Despite the similarity in trend with the computational data at some points, it was identified that the field measurements presented relevant oscillations that may be due to many reasons, such as variation in the position and time of concrete casting; evaporation of water that

removes heat from the system, variations in concrete composition, heat flow during casting, air temperature variations, wind speed variations, heat exchange by radiation, etc. It is noticeable, therefore, that the oscillations occur similarly at intervals of about 24 hours.

Regarding the values of the absolute differences between the monitoring data of Block 01 and the results of the computational analyses over time, these were calculated and are presented in Figure 36. In addition, the values of the maximum absolute differences and the time in which they occurred are presented in Table 7.

Figure 36 – Absolute temperature differences between the monitoring data of Block 01 and the results obtained in Ansys (a) and b4cast (b) over time

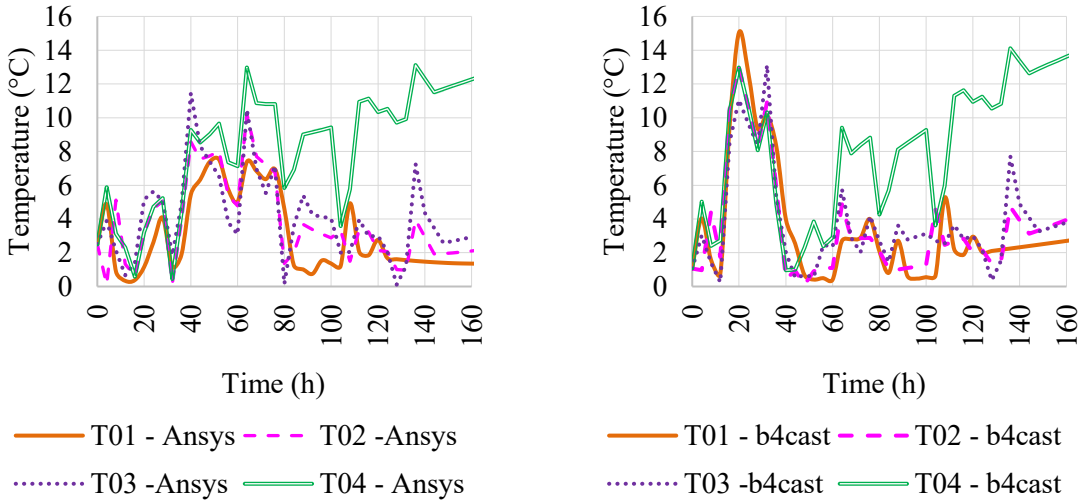

Source: Author (2022).

Table 7 – Maximum absolute differences between the monitoring data of Block 01 and the results obtained in Ansys and b4cast and time at which the maximum differences occurred for thermocouples T01, T02, T03, and T04

Thermocouple	**|Field monitoring – Ansys|**		**|Field monitoring – b4cast|**	
	Temperature (°C)	**Time (h)**	**Temperature (°C)**	**Time (h)**
T01	7.53	52	15.05	20
T02	10.22	64	13.01	20
T03	11.45	40	13.11	32
T04	13.11	136	14.11	136

Source: Author (2022).

About the differences observed in Figures 34 and 36 and Table 6, it is observed that between the field monitoring data of Block 01 and the results of the computer simulations performed in Ansys (FIGURE 35a) the maximum absolute difference values were equal to

13.11 °C at the T04 thermocouple (closest to the exterior) at 136 h, due to the higher cooling of the structure in the computational results, which was not observed in the field. As for b4cast, the highest difference was equal to 15.05 °C at thermocouple T01 (at the core) at 20 h, due to the more accelerated heating of the core observed in the analysis performed in this software.

It is important to note that, about thermocouple T04, there is an increase in the differences over time after 60h in the results of the two software (FIGURE 36), unlike the other thermocouples, which show a decrease in the differences values between the field monitoring data and the computer results. This may have occurred due to some external influence, such as variations in environmental conditions or the possible use of some insulation method (not informed by the construction company).

Based on the results reported, it is evident that it is necessary to modify the computational models used, such as implementing changes in the thermophysical properties of concrete, variations in environmental temperature, and wind speed, and even changes in the casting process of the structure, to bring the computational models closer to the on-site experience.

2.5 Final comments

This chapter focused on identifying the differences between the results of thermal analyses of a mass concrete foundation performed in two computational tools (b4cast and Ansys software). In addition, the results were compared with field monitoring data obtained during the construction of foundation blocks.

According to the studies carried out for comparison between the software, despite some differences identified, a convergent thermal behavior was noticed between the results. The main differences identified were in the geometry that is more influenced by the external environment (V3), showing a slightly divergent heat exchange behavior between the two software. The main conclusions regarding the results obtained in the computational analyses were:

- in general, the results of the analyses performed in b4cast presented higher results in most of the cases analyzed when comparing them with the results of the analyses performed in Ansys;
- the higher the placing temperature applied in the simulations, the higher the maximum temperature reached by the structure, a fact observed in the analyses made in both software;

- a convergence was observed between the trend of the curves of the two software about the obtained values of maximum global temperatures as a function of the applied placing temperature;
- concerning the moment of reaching the maximum temperatures, a reduction in time was observed as the placing temperature increased in b4cast and Ansys;
- b4cast software reached the maximum temperatures earlier than Ansys, getting closer to the results measured in the field;
- despite the difference identified in the maximum heating times between the software, the thermal behavior (heating and cooling profile) was similar between them, especially when observed at the end of the simulation, with the presence of the highest temperatures in the region near the geometric center of the structure (in geometry V2) and with the cooling of the extremities areas that are closer to the external environment, besides the influence of the core heating especially in geometry V1;
- the absolute temperature differences between the b4cast and Ansys results increased with increasing placing temperature, with the largest differences identified at the point of the structure located in geometry V3, composed of another type of concrete, close to the environment and which receives influence from the heating of the core of the structure, presenting a maximum difference equal to 23 °C;
- a more intense cooling of the structure after temperature peak was noticed in the results obtained in the b4cast software, which situation was more evident in the analysis of the points located closer to the external environment.
- the difficulty in dissipating the heat generated by the cement hydration reaction at the inner points of the structure, located in the core (B) and close to the soil (A) for both software, was proven when compared to points located closer to the outside;
- the higher cement consumption of geometry V3 was not so relevant in the increase of its internal temperatures in the analyses performed in both software, since its heat curve, small volume of concrete and its location concerning the ease of heat exchange were more relevant to contribute to its rapid cooling and lower elevation of temperatures;
- regarding computational effort, the time required for the analyses in b4cast was at least two times as long as the time required for the analyses in Ansys.

Concerning the second part of the study to verify the feasibility of computer simulations using field monitoring data, a convergence was observed about the heating of the structure. However, there was a need for changes in the computational model developed, aiming

for a closer approximation to the realistic experience and, consequently, better reliability of the thermal analysis results. Among the main changes that should be made in a new study, changes in the thermal properties of the concrete, the boundary conditions related to the external environment, and in the configurations of the casting process stand out. The main conclusions were:

- regarding the maximum temperature values, it is observed that the results obtained from the b4cast software were closer to the field data;
- although the preliminary study showed the possibility of casting the concrete with temperatures above 30 °C, it was noticed that, in practice, casting the structure with a maximum placing temperature equal to 30 °C resulted in internal temperatures higher than the limit of 65 °C, which showed the need for improvements in the computational model;
- regarding the time to reach the maximum temperatures in the structure, the field monitoring of thermocouples T01, T03, and T04 showed times higher than the results obtained by b4cast. For thermocouple T04, a difference of only 4h between them was identified. Regarding the comparison with the Ansys software, the thermocouples from the field monitoring reached maximums at lower times than those of this software.
- oscillations of approximately 24h were identified only in the results of the field monitoring and, because of this, realized the importance of implementing an investigative parametric study to verify the influence of environmental variations, boundary conditions, and even the casting procedure in the results of computer simulations.

3 MODELING OF MASSIVE CONCRETE FOUNDATION USING FIELD MONITORING DATA AND PARAMETRIC STUDIES

ABSTRACT

To make further progress in research and better investigate the behavior of structural elements, it is important to verify how the variation of certain factors influences the results obtained. Some of the main factors to be studied are the casting process (in one or more layers), the initial temperature of the fresh concrete placement, the content and type of cement used, the presence of insulation methods, the thermal properties, and the environmental conditions. Due to several factors, some laboratory tests to obtain the thermal properties of the materials and the monitoring of the climatic conditions in the field are not performed. Besides this, the concrete casting process and the concrete mix design may suffer adaptations in the field. Therefore, literature data, climate predictions, and simplifications are usually implemented as input data, which may not correctly characterize the structure in the finite element software used to perform the thermal analysis. As a result, there is a possibility of divergence between computational results and field measurement data. Using the thermal analysis of a massive concrete structure that presented differences between these data, a study was developed based on the variation of input parameters to verify the influence of each one on the rise of internal temperatures of the structure in question, thus promoting an approximation between the forecast data and the field monitoring data. The study showed that, among the thermal properties analyzed, the variation of specific heat generated more influence on the results obtained. Furthermore, despite a small improvement, it was observed that the division of the structure into concrete layers reduced the differences between computational predictions and field measurement. On the other hand, the results of the study carried out with the application of the variation of some environmental conditions (temperature and wind speed) were not satisfactory, highlighting the need for monitoring climatic conditions in the field and further investigative studies with the variation of other boundary conditions in the search for increasing the reliability of computational predictions.

Keywords: thermal analysis; mass concrete; finite element simulation; parametric study.

3.1 Introduction

An important point in the thermal analysis of mass concrete structures is the evaluation of the influence of material characteristics. This can be done by implementing computational parametric studies, varying the thermal parameters, the cement content and type, the concrete placing temperature, the thermal insulation conditions at the boundaries of the concrete, and the environmental conditions (GAMBALE, 2017; ZHAO *et al.*, 2021). Furthermore, it is interesting to investigate how the casting process (e.g., division of the structure into layers, executed with time intervals between them) influences the thermal behavior of these types of structures (JU; LEI, 2019; ANISKIN; NGUYEN, 2019).

According to the analyses presented in the previous chapter, it is possible to confirm the influence of the concrete pouring temperatures on the thermal rise of the structure. Furthermore, a divergence between the results of the computer simulations and the field monitoring data was noticed, especially concerning the values of the maximum temperatures reached, which were higher than the adopted safety limit of 65 °C. Therefore, there was a need to make changes to the defined computational model to bring it closer to the field reality. Because some of the input parameters used in the simulations were taken from the literature, such as the thermal properties of the materials, it is believed that the values considered in the simulations may not effectively characterize the materials used in the construction of the foundation block under study.

According to Azenha *et al.* (2021), thermal capacity or specific heat and the thermal conductivity are the most relevant thermal properties of concrete for thermal simulations. Some characteristics prevent the rise of the internal temperature of mass concrete, thus reducing the probability of occurrence of cracks. Among them, high thermal conductivity, high density, and high specific heat can be highlighted (COELHO et al., 2014). The ability to estimate the thermal response of cement-based materials is dependent on accurate thermal property determination (HONORIO; BARY; BENBOUDJEMA, 2018). For this, it is important to know the precise thermal properties of each constituent of the concrete.

Another point that should be mentioned concerns the environmental conditions (temperature and wind speed) applied in the previous study: they were considered constant throughout the time of the analyses in Chapter 2, while they are actually cyclic as seen in the periodic variations in the field measurements. The oscillations identified in the field monitoring were not identified in the computer simulations performed due to these simplifications. In the

field, the possible influence caused by variations in environmental parameters on the thermal behavior of the structure was highlighted.

According to Funahashi Junior *et al.* (2010), in addition to the influence of material characteristics, geometries, and environmental conditions, other basic parameters that can influence the design and analysis of mass concrete structures are related to the casting methodology. For example, it is possible to divide the casting process into layers with the implementation of a time interval between the placing of each one, in order to avoid too high temperatures. In the computational model used in Chapter 2, variations in the casting process were not considered, and, seeking greater reliability of computational results, it is evident the need to implement such study.

Therefore, this chapter aims to verify the influence of the variation of some input parameters on the results of the thermal analysis of the wind tower foundation block studied in Chapter 2. Through this study, the parameters that most approximated the predicted results with the computational model to the results measured in the field were identified to reduce the divergences identified in Chapter 2, mainly concerning the reach of maximum temperatures. This was done in a way to increase the reliability of the results.

3.2 Methodological procedure

Aiming to achieve specific objective 2 of this dissertation, this section describes the research method that will be used to perform this part of the study, with emphasis on the analysis of the variation of some input parameters used in the computer simulations seeking to verify the influence of these variations in the thermal behavior of the structure and to approximate the results obtained in them to the results of the field monitoring. At each stage, the results obtained were compared with the measured results. For this comparison, the points where the thermocouples were installed on-site were used to output the results of the computational analyses (FIGURE 37).

Figure 37 – Positioning of the thermocouples installed for monitoring the temperatures of the foundation blocks in the field

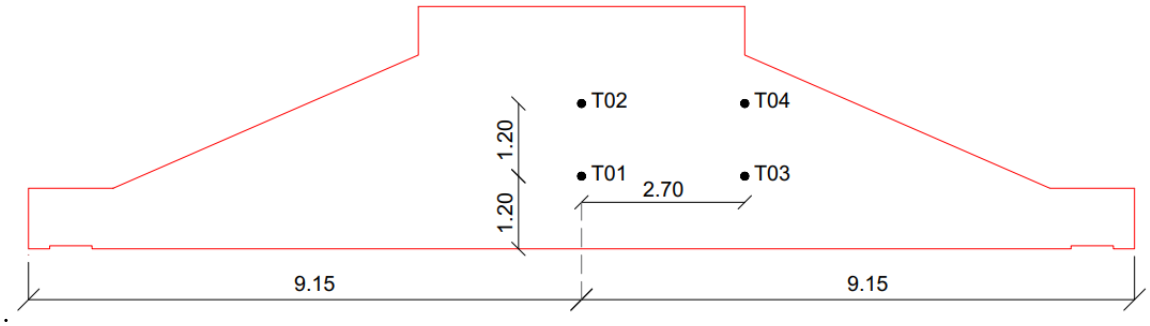

Source: Construction Company of Wind Farm (2021).

In addition, it was chosen to use only b4cast software in the analyses presented in this chapter due to the fact that it is widespread for consulting in field applications and because it presented, in general terms, a closer match to the field measurement data. The placing temperature considered in each simulation performed in this new study was 30 °C. In this chapter, 14 new simulations were performed, named S5 to S18. To perform the new simulations, the methodology described in Chapter 2 was used, performing the parameter changes described in Figure 38.

The study presented in this chapter was developed in three stages: I) variation of the thermal properties of concrete, where simulations S5 to S16 were performed; II) variation of the casting methodology, where simulation S17 was performed; and III) variation of environmental conditions, where simulation S18 was performed.

At the end of each step, the simulation that presented the closest results to the data measured in the field was chosen to be used as a reference in the next step (SX, SY, and SZ in Figure 37). For the first step of the study, reference values were chosen, over which variations of -30%, -20%, -10%, +10%, +20%, and +30% were applied. Simulation S4, developed in Chapter 2, was chosen as the reference for the first analysis developed (variation of the thermal conductivity coefficient). The choice of simulations SX, SY, and SZ was made according to the results described in sections 3.3.1, 3.3.2, and 3.4.

Figure 38 – Flowchart of this parametric study

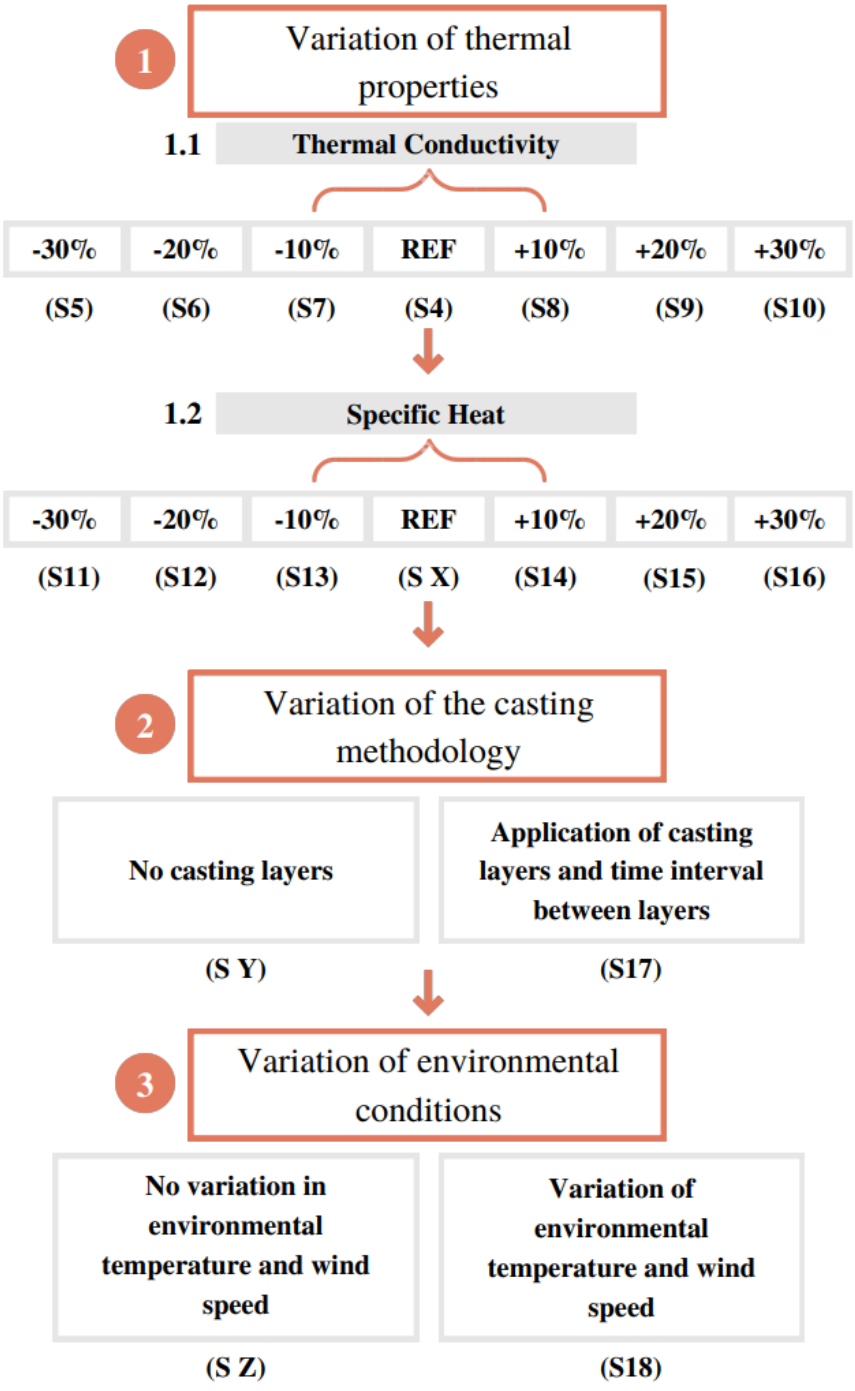

Source: Author (2022).

3.3 Parametric study results – variation of thermal properties

The thermal behavior is one of the main characteristics that differentiate mass concrete from a common structural concrete (ACI COMMITTEE 207, 2006). Some thermal properties of concrete are fundamental to study that behavior, such as specific heat, thermal conductivity and thermal diffusivity. According to Azenha *et al.* (2021), thermal capacity and thermal conductivity are the most relevant thermal properties of concrete for thermomechanical simulations.

According to NBR 12817 (ABNT, 2012), specific heat is described as the amount of energy required to raise the temperature of a unit mass of material by 1°C (or equivalently 1K), and it can be expressed in Joule per gram times degree Celsius (J/g °C). The referred standard determines a test method for obtaining this parameter.

Coelho *et al.* (2014) state that the ability of concrete to store heat is expressed by the specific heat and describe some parameters that influence the value of the specific heat: temperature, the density, moisture content and characteristic maximum size of coarse aggregate. Also, they noted, through analysis in mass concrete, that a lower specific heat value provides a higher thermal rise because less heat is needed for the temperature to increase. Meanwhile, for a higher specific heat value, the thermal rise is lower.

In the literature, it is possible to find values for the specific heat used for thermomechanical simulations in concrete foundation structures. ACI 207.2R (ACI COMMITTEE, 2007) showed some examples of concrete mixes with minimum specific heat values close to 0.9 kJ/(kg ºC), while Couto (2018) used 1.0 kJ/(kg ºC) and Gonçalves (2018) adopted 1.2 kJ/(kg ºC).

Thermal conductivity is the thermal property that measures the ability of materials to conduct heat (ACI COMMITTEE 207, 2007). According to NBR 12820 (ABNT, 2012), this property is measured by the ratio between heat flow per unit area of the material in the direction perpendicular to this area and the temperature gradient in the direction of flow. It can be expressed in Watts per meter per Kelvin (W/(m.K)). The referred standard determines a test method for obtaining this parameter.

The thermal conductivity of concrete can be influenced by some parameters, such as content and type of aggregate, w/c ratio, age, temperature, moisture condition of the specimen, porosity and density (BREUGEL, 1998; KIM *et al.*, 2003; ACI COMMITTEE 207, 2007). According to experimental results presented by Kim *et al.* (2003), the main factors

affecting thermal conductivity are aggregate volume fraction and moisture condition of the specimen. Besides, age does not change conductivity considerably, except for a very early age. In the literature, it is possible to find a variation of the thermal conductivity coefficient of concrete ranging from 1.9 W/(m.K) to 3.5 W/(m.K) according to the type of aggregate used (BREUGEL, 1998).

According to NBR 12818 (ABNT, 2012), thermal diffusivity is an index that indicates how easily concrete allows temperature variations to propagate spatially, expressing the ability to diffuse heat in all directions. The referred standard determines a test method for obtaining this parameter and expresses that thermal diffusivity (h^2) can be analytically obtained through the ratio of thermal conductivity (k) to the product between the specific heat (c) and the density (γ) of the material, according to Equation 5. The higher the value of this index, the easier the heat will move throughout the concrete (ACI COMMITTEE 207, 2007).

$$h^2 = \frac{k}{c \,.\, \gamma} \tag{5}$$

As presented in Chapter 2, some thermal properties were taken from the literature. As the main objective of this chapter is to investigate the influence of the main input parameters on the thermal behavior of the mass concrete structure and to define a computational model closer to reality, it was chosen to vary the values of the specific heat and the thermal conductivity coefficient of the concrete. The value of the density of the concretes of the foundation block under analysis was obtained from the mix design report, and the diffusivity was calculated in the b4cast software from the other parameters using Equation 5.

3.3.1. Results of the variation of the thermal conductivity coefficient of concrete

The first parameter chosen to initiate the new study was the thermal conductivity coefficient. In simulation S4, performed in Chapter 2, 9.55 kJ/m/h/°C (BREUGEL, 1998) was used as the input value for this parameter in the b4cast software. For this study, it was chosen to make six variations, which resulted in six new simulations, which were named S5, S6, S7, S8, S9, and S10. Table 8 shows the values used for the thermal conductivity coefficient in each of those simulations. Regarding the input values of the other properties (density, specific heat, and coefficient of thermal expansion), they were considered constant and equal to the values presented in Table 1 of Chapter 2. Furthermore, there was no variation investigated in the

properties of the soil below the concrete block. The properties used were those indicated in Table 2 of Chapter 2.

Table 8 - Variation of thermal conductivity coefficient of concrete in simulations S5, S6, S7, S8, S9 and S10

Simulation	**S5 (-30%)**	**S6 (-20%)**	**S7 (-10%)**	**S4 (Reference)**	**S8 (+10%)**	**S9 (+20%)**	**S10 (+30%)**
Thermal Conductivity (kJ/m/h/°C)	6.69	7.64	8.60	9.55	10.51	11.46	12.42

Source: Author (2022).

After the implementation of the input parameters in the b4cast software, the six new simulations with the variation of the thermal conductivity coefficient values were performed, obtaining curves of the internal temperatures over time at points T01, T02, T03, and T04 (cf. Figure 36), which are presented in Figures 39, 40, 41 and 42, respectively for each point.

Figure 39 – Influence of the thermal conductivity coefficient variation in the internal temperature of the concrete foundation at the point of the T01 thermocouple

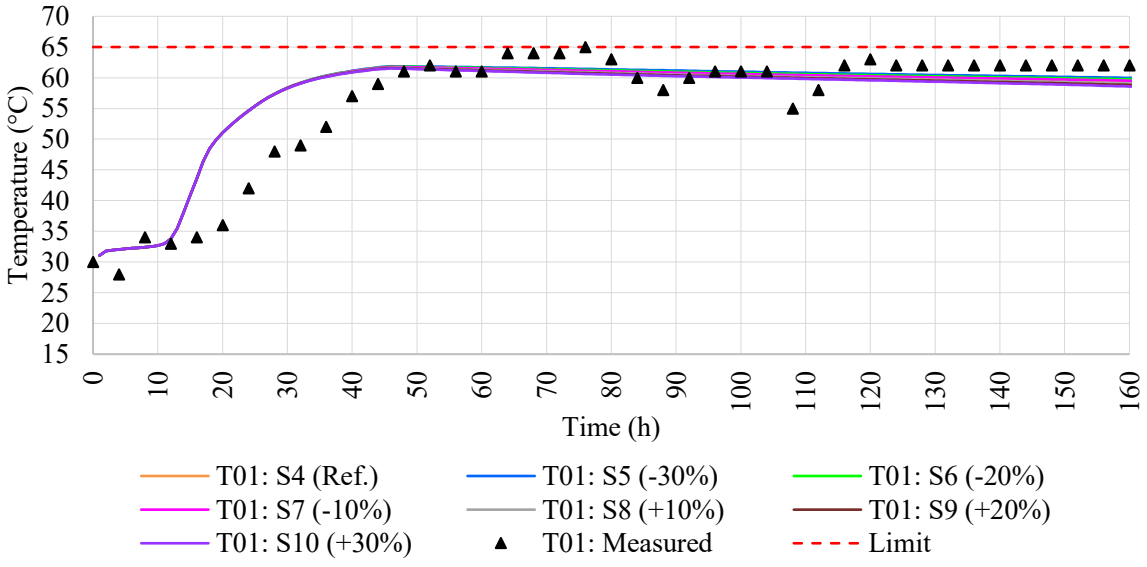

Source: Author (2022).

Figure 40 – Influence of the thermal conductivity coefficient variation in the internal temperature of the concrete foundation at the point of the T02 thermocouple

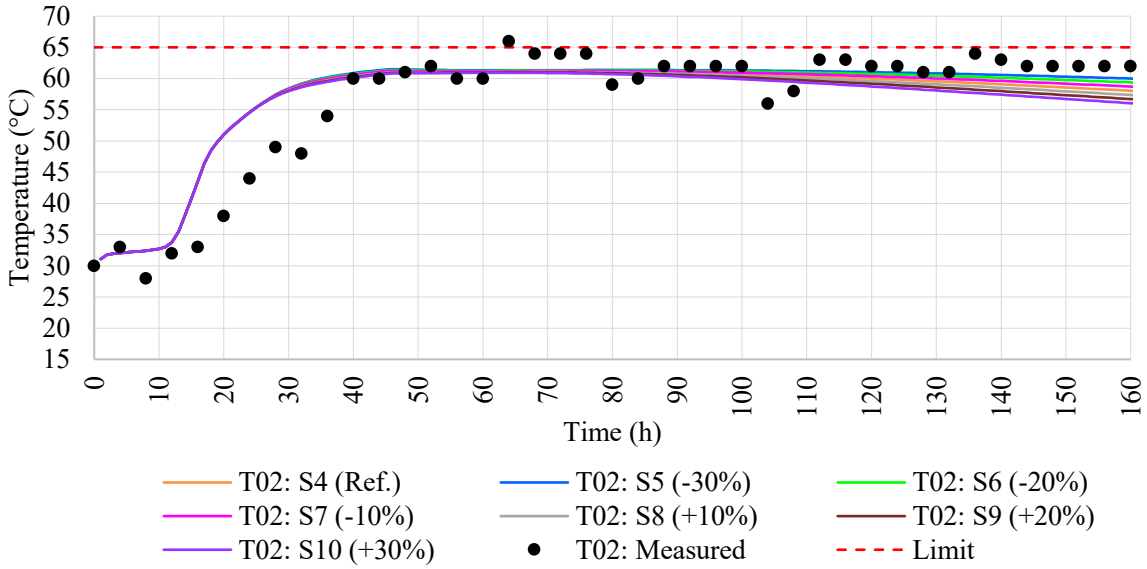

Source: Author (2022).

Figure 41 – Influence of the thermal conductivity coefficient variation in the internal temperature of the concrete foundation at the point of the T03 thermocouple

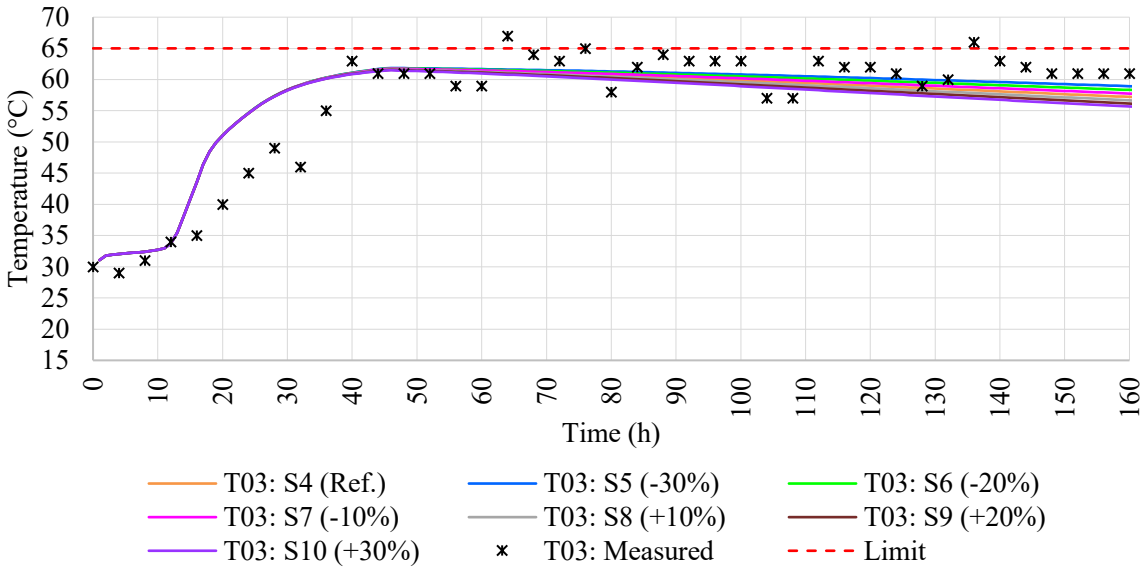

Source: Author (2022).

Figure 42 – Influence of the thermal conductivity coefficient variation in the internal temperature of the concrete foundation at the point of the T04 thermocouple

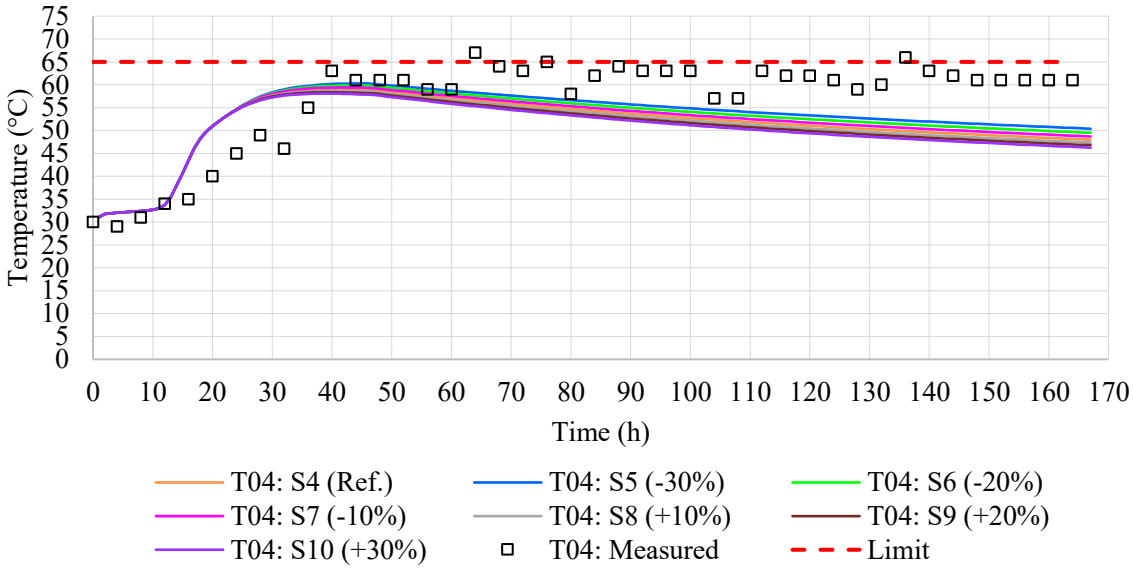

Source: Author (2022).

Analyzing the curves presented in Figures 39, 40, 41, and 42, it was noticed that the variation of the thermal conductivity parameter did not present a significant influence on the increase of internal temperatures reached by the foundation block. It was observed that the reduction in the value of the thermal conductivity coefficient of concrete every 10% generated an increase in internal temperatures of less than 1 ºC. This behavior was expected, because the lower the value of this parameter, the higher the difficulty of the concrete to transport the heat generated in the core (location of maximum temperatures) to the edges and thus cool the structure (COELHO, 2014).

The differences between the curves increased over time, being higher at the end of the study (160h). The maximum differences between the curves were calculated for simulations S5 and S10, which presented the highest and lowest thermal elevations, respectively. The maximum differences between them at points T01, T02, T03, and T04 were equal to 1.50 °C, 4.20 °C, 3.40 °C, and 4.15 °C, respectively. It can be seen that the smallest differences occurred at the innermost points (T01 and T03), which shows that the closer to the core, the smaller the influence of the variation of the thermal conductivity coefficient concerning the thermal behavior of the structure, due to the normal difficulty of the heat generated at this location to be transported to the edges of the structure.

One of the main points in thermal studies of mass concrete structures is the prediction of the maximum internal temperatures reached by these elements, due to the risk of delayed ettringite formation (DEF) (COLLEPARDI, 2003). In Chapter 2, it was shown that the monitoring of the structure in the field presented points with maximum temperatures higher than the safety limit of 65 °C, differently from what was observed in the results of the S4 simulation performed. The main focus of Chapter 3 is to change the computational model used in this simulation, seeking to bring it closer to the field results, especially regarding the reach of maximum temperatures, through parametric studies. Thus, a study was done comparing the differences between the maximum temperatures of the data measured in the field and each new simulation with the variation of thermal conductivity coefficient values, to identify which of the simulations most closely matched the monitoring data. Table 9 presents the results, highlighting the lowest temperature values at each point.

Table 9 – Differences between maximum temperatures reached in field monitoring and in simulations performed with the variation of thermal conductivity coefficient

Simulation	**Thermocouple point**			
	T01	**T02**	**T03**	**T04**
S5 (-30%)	3.13 °C	4.50 °C	5.15 °C	5.72 °C
S6 (-20%)	3.18 °C	4.63 °C	5.19 °C	6.16 °C
S7 (-10%)	3.23 °C	4.76 °C	5.25 °C	6.58 °C
S4 (Ref.)	3.28 °C	4.86 °C	5.30 °C	6.96 °C
S8 (+10%)	3.34 °C	4.93 °C	5.36 °C	7.31 °C
S9 (+20%)	3.41 °C	5.00 °C	5.43 °C	7.62 °C
S10 (+30%)	3.47 °C	5.07 °C	5.50 °C	7.92 °C

Source: Author (2022).

Despite the slight variation between the results (most with less than 1°C difference), it can be seen that simulation S5, with a 30% reduction in the value of the thermal conductivity coefficient concerning the reference value considered, was the one that presented the closest to the maximum temperature values reached by the structure in the field at points T01, T02, T03 and T04. Thus, the thermal conductivity value equal to 6.69 kJ/m/h/ºC will be considered in the simulations that will be performed in the next step of this study. The simulation that will be used as a reference in the study of the variation of the specific heat (SX in Figure 38) will be S5.

3.3.2. Results of the variation of the specific heat of concrete

The second parameter chosen for this study was the specific heat of concrete. In the chosen reference simulation (S5), performed in Section 3.3.1, 1.00 kJ/kg/ºC (COUTO, 2018) was used as the input value for this parameter in the b4cast software. For this study, it was chosen to make six variations, which resulted in six new simulations, which were named S11, S12, S13, S14, S15, and S16. Table 10 shows the values used for the specific heat in each of these simulations. Regarding the input value for the thermal conductivity coefficient, it was considered equal to 6.69 kJ/m/h/ºC according to the analysis performed in the previous Section. As for the input values of the other properties (specific mass and coefficient of thermal expansion), they were considered constant and equal to the values presented in Table 1 of Chapter 2. Besides, there was no change in the properties of the soil below the concrete block, being used those indicated in Table 2 of Chapter 2.

Table 10 – Variation of specific heat of concrete in simulations S11, S12, S13, S14, S15, and S16

Simulation	**S11 (-30%)**	**S12 (-20%)**	**S13 (-10%)**	**S5 (Reference)**	**S14 (+10%)**	**S15 (+20%)**	**S16 (+30%)**
Specific heat (kJ/kg/ºC)	0.70	0.80	0.90	1.00	1.10	1.20	1.30

Source: Author (2022).

After the implementation of the input parameters in the b4cast software, the six new simulations with the variation of the specific heat values were performed, obtaining curves of the internal temperatures over time at points T01, T02, T03, and T04, which are presented in Figures 43, 44, 45, and 46, respectively for each point.

Figure 43 – Influence of the specific heat variation in the internal temperature rise of the concrete foundation at the point of the T01 thermocouple

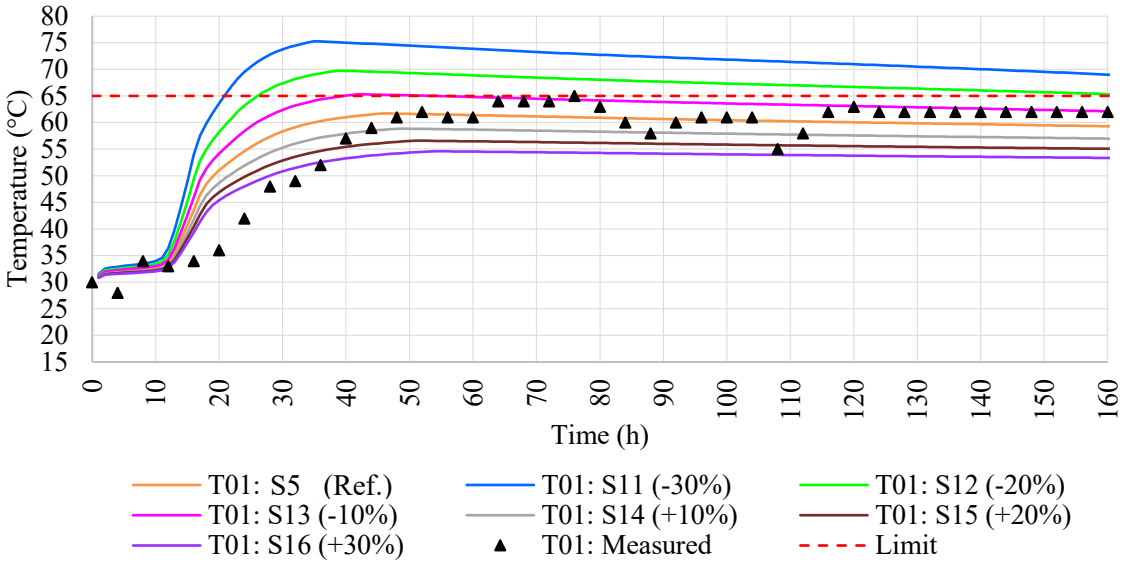

Source: Author (2022).

Figure 44 – Influence of the specific heat variation in the internal temperature rise of the concrete foundation at the point of the T02 thermocouple

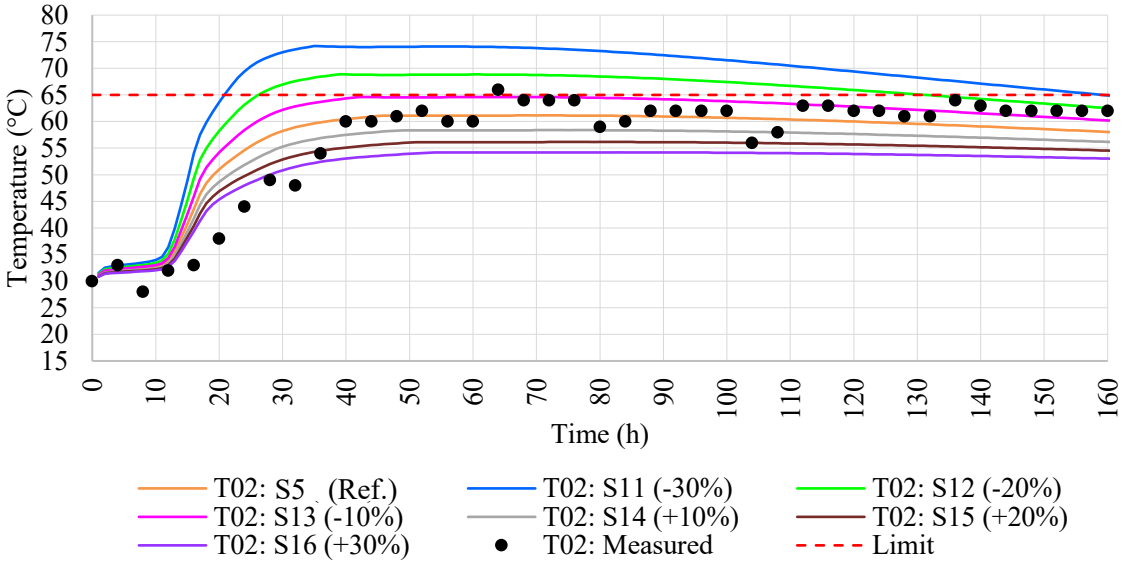

Source: Author (2022).

Figure 45 – Influence of the specific heat variation in the internal temperature rise of the concrete foundation at the point of the T03 thermocouple

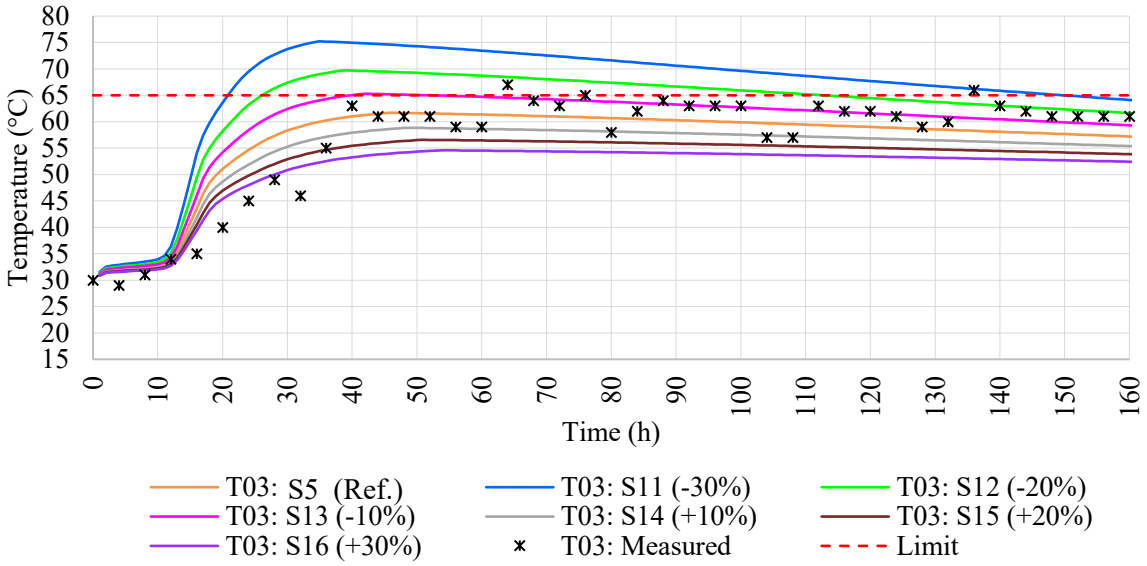

Source: Author (2022).

Figure 46 – Influence of the specific heat variation in the internal temperature rise of the concrete foundation at the point of the T04 thermocouple

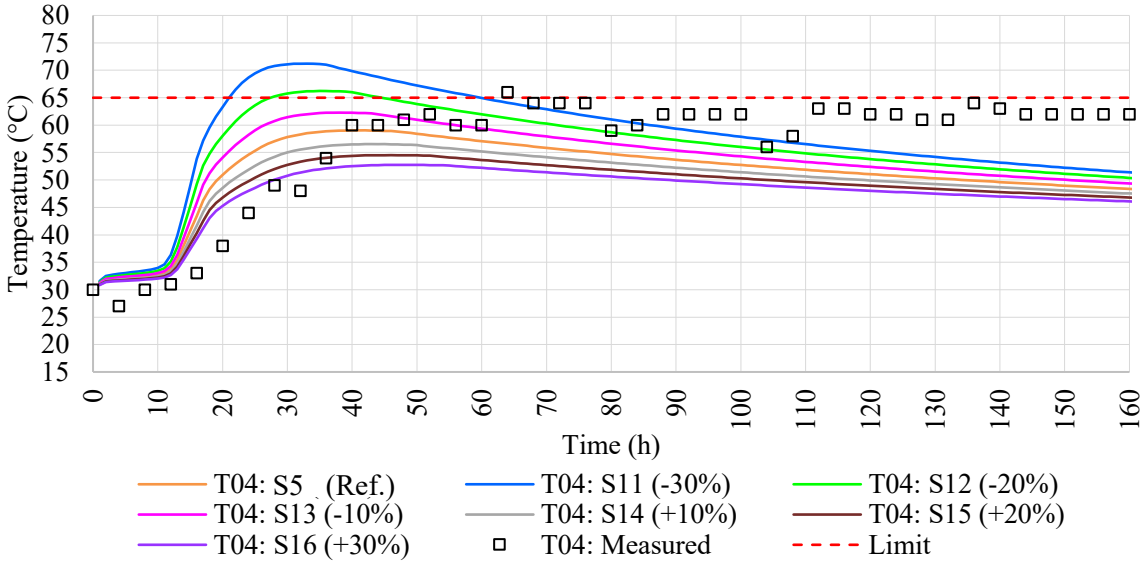

Source: Author (2022).

Analyzing the curves presented in Figures 43, 44, 45, and 46, it was noticed that the variation of the specific heat parameter presented a significant influence on the increase of internal temperatures reached by the foundation block. It was observed that the reduction in the specific heat value of the concrete every 10% was able to generate an increase of up to 6.4 ºC. This behavior can be justified by the fact that the specific heat is related to the amount of heat required to elevate by one degree the temperature of a unit of mass of the structure, thus, concretes with lower values of this parameter require a smaller amount of heat to increase their internal temperatures (COELHO, 2014).

The differences between the curves reduced over time. In the beginning, differences are higher. The maximum differences between the curves of simulations S11 and S16 were calculated, which presented the highest and lowest thermal elevations, respectively. The maximum differences between them at points T01, T02, T03, and T04 were equal to 23.00 °C, 22.24 °C, 22.97 °C and 20.94 °C, respectively. It can be seen that the largest differences occurred at the innermost points (T01 and T03), which shows that the closer to the core, the greater the influence of the variation of the specific heat concerning the thermal behavior of the structure since the core is the place of the highest rise of temperatures.

As demonstrated previously (cf. Section 3.3.1), a study was made comparing the differences between the maximum temperatures of the data measured in the field and each new simulation with the variation of the specific heat values of the concrete. This was done to identify which of the simulations was closest to the monitoring data. Table 11 presents these results, highlighting the lowest values at each point.

Table 11 – Differences between maximum temperatures reached in field monitoring and in simulations performed with the variation of specific heat

Simulation	Thermocouple point			
	T01	**T02**	**T03**	**T04**
S11 (-30%)	10.27 ºC	8.20 ºC	8.24 ºC	5.21 ºC
S12 (-20%)	4.75 ºC	2.89 ºC	2.73 ºC	0.22 ºC
S13 (-10%)	0.51 ºC	0.98 ºC	1.51 ºC	2.42 ºC
S4 (Ref.)	3.28 ºC	4.86 ºC	5.30 ºC	6.96 ºC
S14 (+10%)	6.14 ºC	7.62 ºC	8.16 ºC	9.47 ºC
S15 (+20%)	8.41 ºC	9.85 ºC	10.42 ºC	11.47 ºC
S16 (+30%)	10.40 ºC	11.80 ºC	12.41 ºC	13.25 ºC

Source: Author (2022).

According to Table 11, it can be seen that simulation S13, with a 10% reduction in the specific heat value concerning the reference value considered, was the one that presented the closest to the maximum temperature values reached by the structure in the field at points T01, T02 and T03. Thus, the specific heat value equal to 0.90 kJ/kg/ºC will be considered in the simulations that will be performed in the next step of this study. The simulation that will be used as a reference in the study of the variation of the casting methodology (SY in Figure 38) will be S13.

3.4 Parametric study results – variation of the casting methodology

As mentioned previously, all simulations performed until now (S1 to S16) were done considering that the whole structure would be cast simultaneously (at 0h), without splitting it into layers. However, this configuration did not closely represent the construction process experienced on-site. According to the details provided by the construction company, the casting occurs in a continuous process over a single day, for a duration of approximately 14 hours. Also, it should be noticed that there is a time (approximately 15 min) interval required for the arrival and emptying of each of the 8m³ concrete mixer trucks. Thus, the casting process occurs in layers, which are filled over time.

Therefore, a new simulation was performed (S17), dividing the geometry into 11 layers ranging from 0.30 m to 0.40 m thick (FIGURE 47) to represent the construction process more accurately and to analyze the differences between the two simulations (S13 with the single-layer geometry and S17 with the layers division), comparing the results with the field monitoring data. The computational effort required to perform the analyses in the b4cast software made it impractical to divide the structure into more layers.

The time interval between the placing of each layer implemented in simulation S17 was calculated according to the volume of concrete in each one and the number of truck mixers needed to fill them. A time interval of 15 min as, then, considered between each of truck mixer, over a total period of 14 h. Figure 48 shows the new geometric configuration used in simulation S17 and Figures 49, 50, 51, and 52 the results obtained for points T01, T02, T03, and T04, respectively.

Regarding the input parameter values of simulation S17, 6.69 kJ/m/h/ºC was used for the thermal conductivity coefficient and 0.90 kJ/kg/ºC for the specific heat, according to the analyses performed previously. As for the input values of the other properties (specific mass and coefficient of thermal expansion), they were considered constant and equal to the values presented in Table 1 of Chapter 2. Besides, there was no change in the properties of the soil below the concrete block, being used those indicated in Table 2 of Chapter 2.

Figure 47 – Splitting the foundation block into 11 casting layers

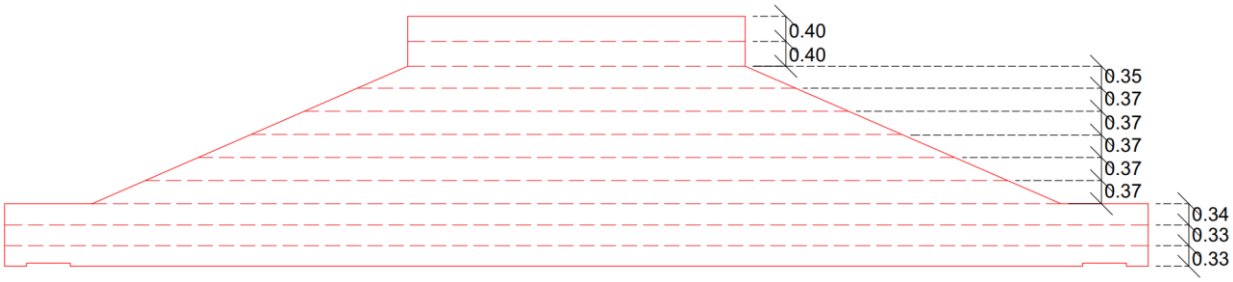

Source: Author (2022).

Figure 48 – New geometric configuration used in simulation S17

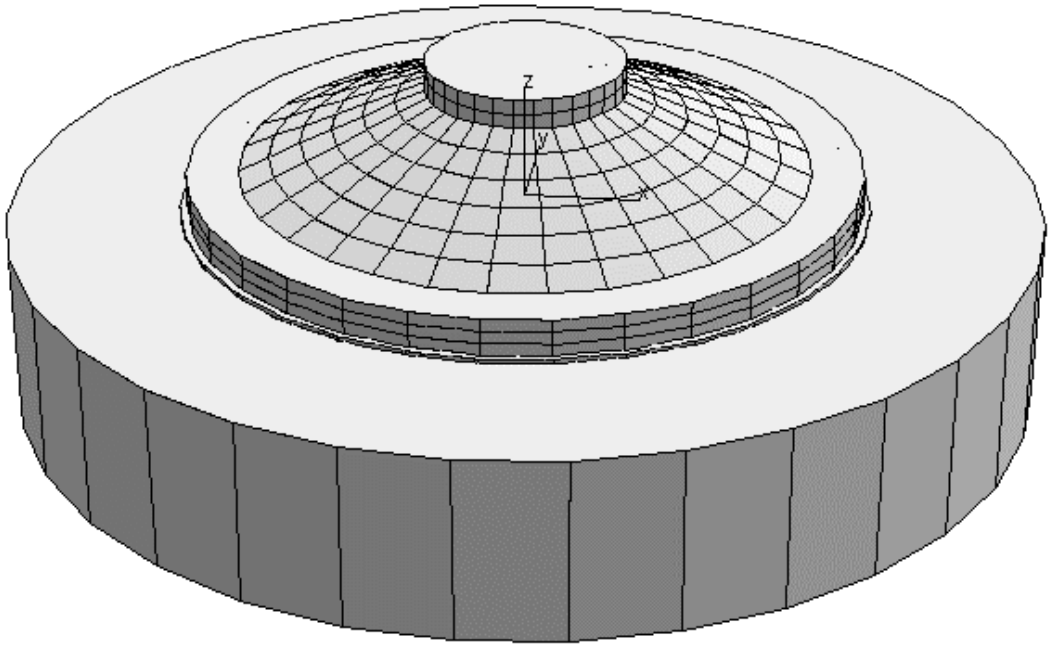

Source: Author (2022).

Figure 49 – Influence of splitting the casting in layers, with the application of time intervals between them at the point of the T01 thermocouple

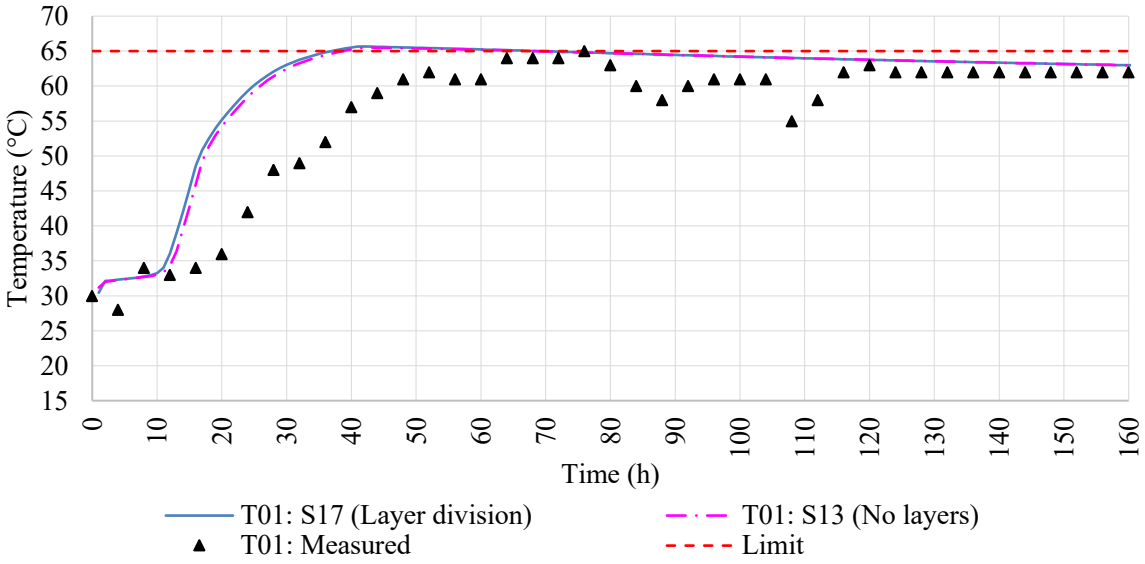

Source: Author (2022).

Figure 50 – Influence of splitting the casting in layers, with the application of time intervals between them at the point of the T02 thermocouple

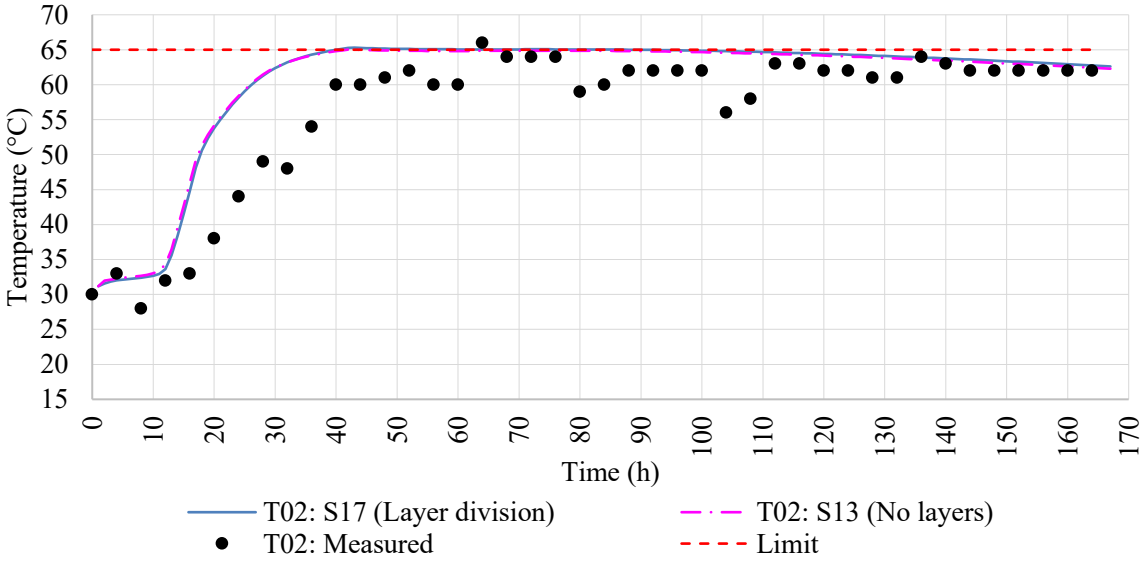

Source: Author (2022).

Figure 51 – Influence of splitting the casting in layers, with the application of time intervals between them at the point of the T03 thermocouple

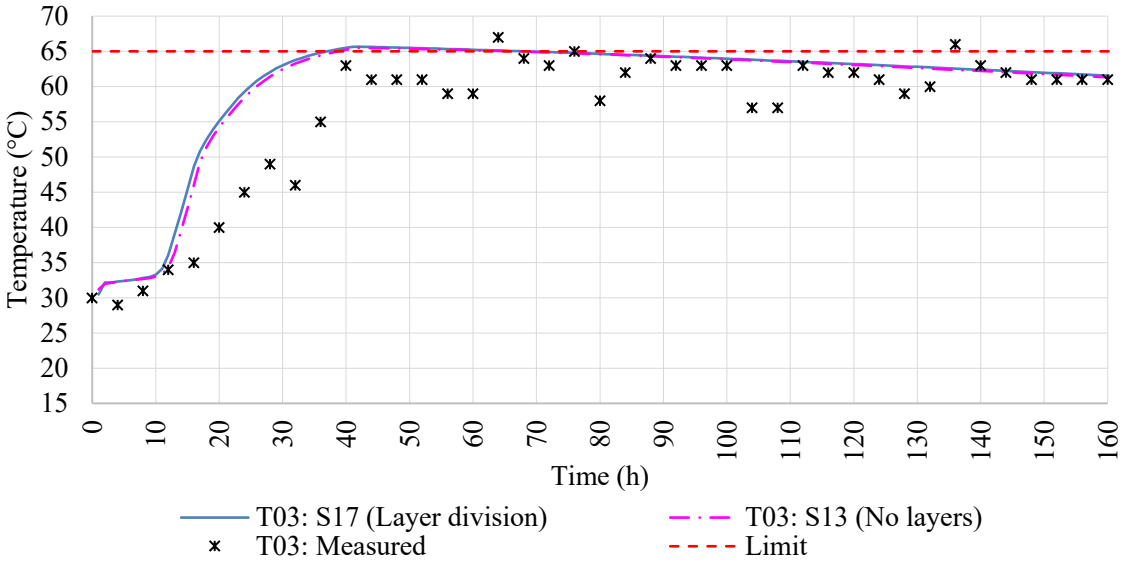

Source: Author (2022).

Figure 52 – Influence of splitting the casting in layers, with the application of time intervals between them at the point of the T04 thermocouple

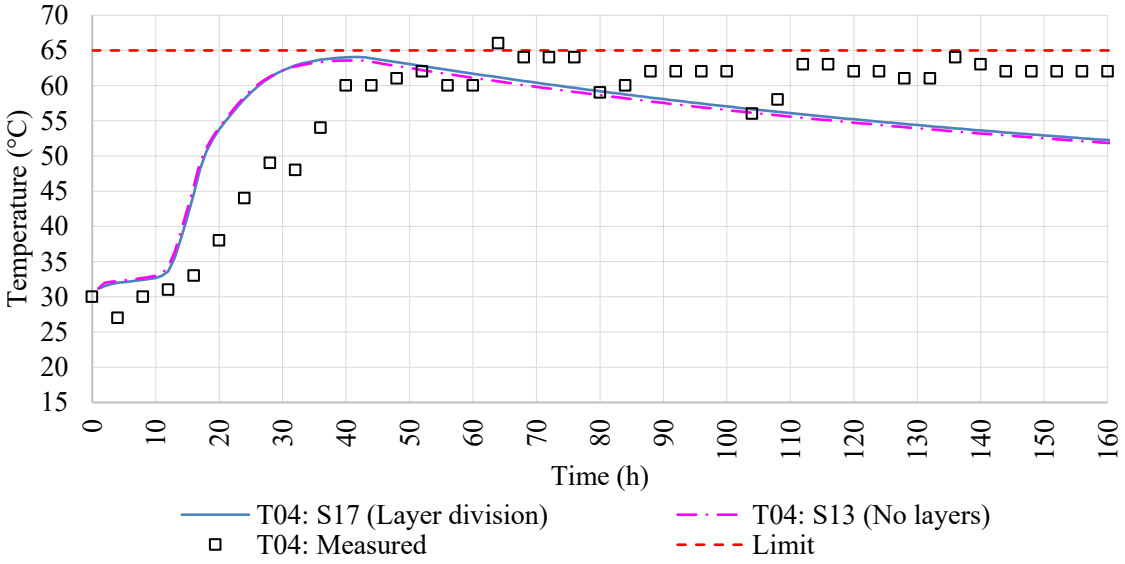

Source: Author (2022).

Analyzing Figures 49, 50, 51, and 52, it can be seen that the new casting configuration did not generate any considerable influence on the results obtained, which can be justified by the short time interval considered between the layers, which did not exceed 3 hours. It is believed that the influence is greater as the time interval between layers increases since the lower layers cool down over time. This analysis will be done in the next chapter. Nevertheless, the results here suggest that the delay observed between the simulated and the measured temperature increases is not explained by the casting plan difference between simulation and field. Then, explanation based on differences on materials (such as additives contents) used in the field may be necessary.

It can be seen at the innermost points (T01 and T03) that the curve of simulation S17 (with the division of the concreting into layers) showed slightly higher temperature values (about 3 °C) up to 40 h of analysis, approximately. This can be justified by the fact that when a layer is cast within a short time interval after the casting of the previous layer, the previous layer has not yet cooled down, and thus has a higher temperature. This, therefore, contributes to a faster thermal rise of the subsequent layers especially at points closer to the core. For points T02 and T04, closer to the external environment, there were no changes in temperature values until 40 h of the study. However, it was noticed that at point T04, from 40 h on, just after the peak, the S17 simulation presented slightly higher temperatures than S13, showing a slower cooling due to the influence of the previous layers that are warmer.

Regarding the field monitoring data, although the simulations curves are above them in most of the points, it is observed that, in some moments, the monitoring exceeded the limit of 65 ºC, showing the need to reduce the concrete placing temperature so that the maximum temperatures reached by the structure are below that limit. Moreover, it is worth noting, concerning the behavior of the curves, that the results of the field measurements show slower heating over time in the four points, which can be justified by the use of additives at the time of casting for corrections to the mix design, which may cause the delay of the cement hydration process. This information about possible changes in the content of additives, and consequently in cement and in concrete calorimetry, was not available and is also not considered in the b4cast software.

As in the previous Sections, a study was made comparing the differences between the maximum temperatures of the data measured in the field and the simulations S13 (without the division of the structure in concrete layers) and S17 (with the division in layers), to verify if the division in layers influenced the reduction of the differences between the maximum temperatures. Table 12 presents these results, highlighting the lowest values at each point.

Table 12 –Differences between the maximum temperatures reached in the field monitoring and in the simulations performed with and without the division of the structure into casting layers

Simulation	Thermocouple point			
	T01	T02	T03	T04
S17 (Layer division)	0.66 ºC	0.70 ºC	1.34 ºC	1.93 ºC
S13 (No layers)	0.51 ºC	0.98 ºC	1.51 ºC	2.42 ºC

Source: Author (2022).

Despite the small variation between the results (less than 1 ºC), it can be seen that simulation S17, with the division of the structure in casting layers and the implementation of time intervals between the placing of each layer, was the one that presented the closest to the maximum temperature values reached by the structure in the field at points T02, T03, and T04. Thus, it was chosen to continue the study using S17 (SZ in Figure 37), because it also best represents the casting process experienced in the field.

3.5 Parametric study results – variation of environmental conditions

The last step of this study was to investigate the influence on the computational results generated by the variation of some environmental conditions (temperature, wind speed, and, consequently, convection coefficient). The idea was to address the oscillations that were observed when monitoring the internal temperatures of the structure in the field.

Until the previous section, the ambient temperature and wind speed were considered constant in all simulations performed. Results as close as possible to the wind farm placement were obtained from data generated by weather forecasting agencies to perform a new simulation (S18). According to The Weather Channel (2021) forecasts, the local temperature ranges between 28°C and 32°C, and the wind speed ranges between 5.56 m/s and 9.70 m/s. The variation of these parameters over time, which was implemented in the software, is shown in Appendix A.

The results of the thermal rise of the structure over time at points T01, T02, T03, and T04 obtained in simulation S18 were compared both with those of simulation S17, which has constant environmental conditions and with the results of field measurements, to verify convergences and divergences between them. The curves obtained are shown in Figures 53, 54, 55, and 56 for points T01, T02, T03, and T04, respectively.

Figure 53 – Temperature over time at thermocouple point T01 with changing environmental conditions

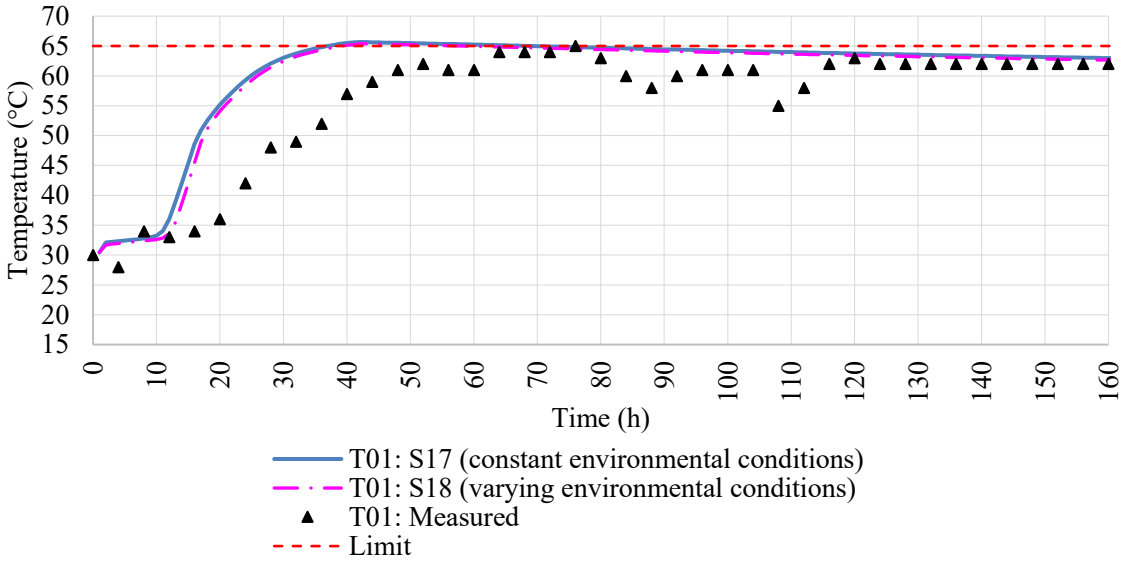

Source: Author (2022).

Figure 54 – Temperature over time at thermocouple point T02 with changing environmental conditions

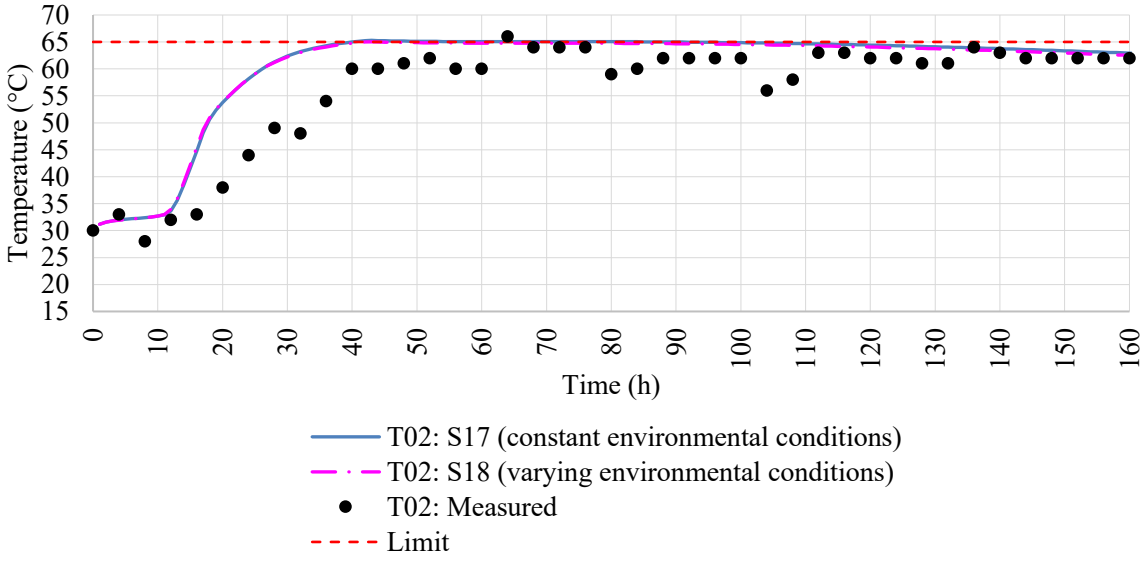

Source: Author (2022).

Figure 55 – Temperature over time at thermocouple point T03 with changing environmental conditions

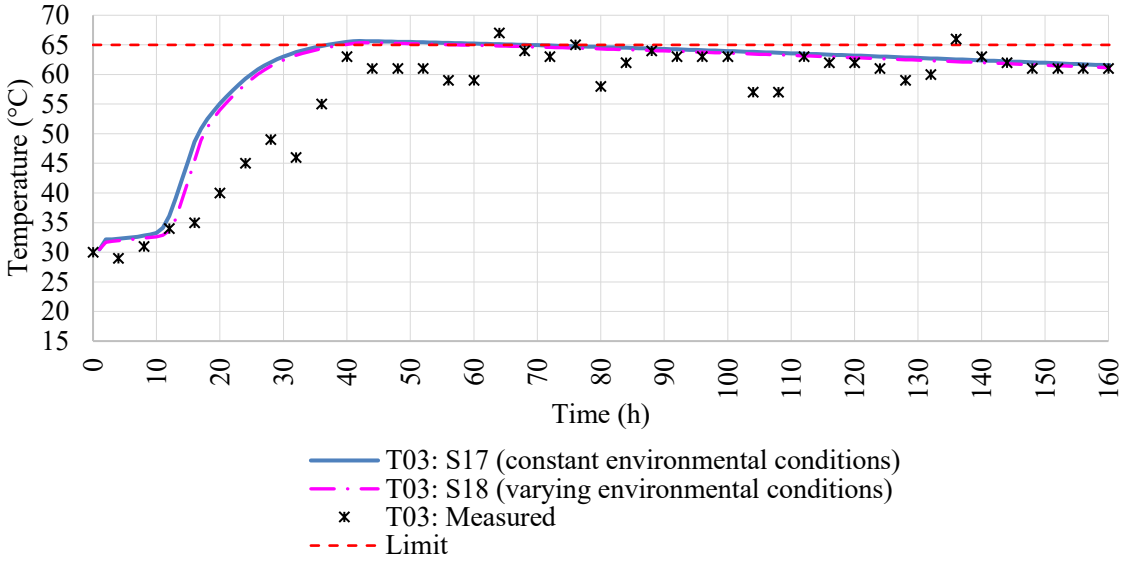

Source: Author (2022).

Figure 56 – Temperature over time at thermocouple point T04 with changing environmental conditions

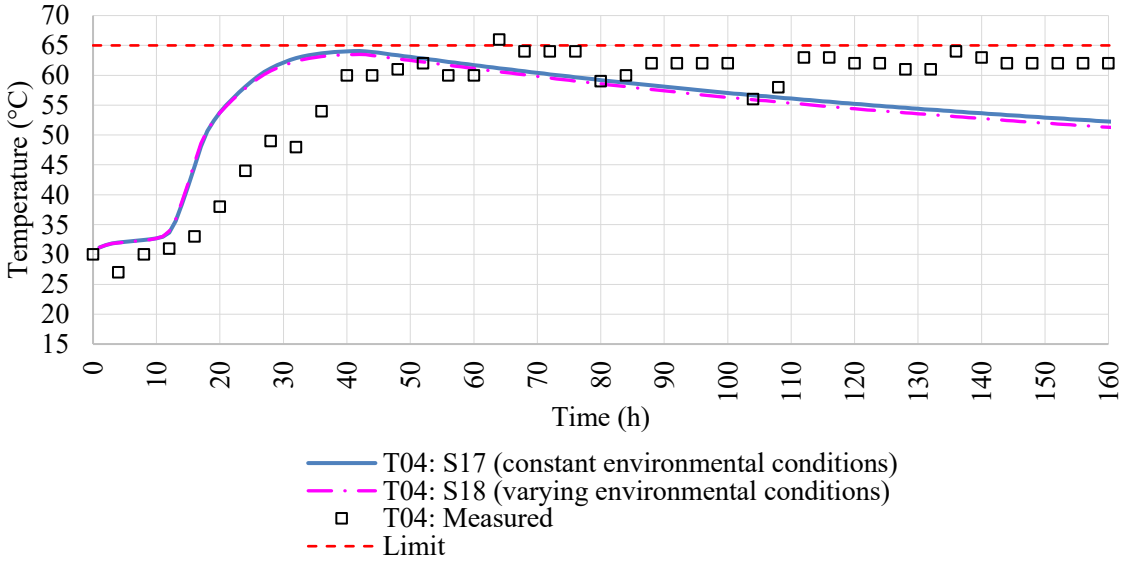

Source: Author (2022).

As mentioned previously, it was expected to observe oscillations in the internal temperatures of the concrete structure with the implementation of ambient temperature and wind speed variations in simulation S18. However, the results of this simulation did not present such oscillation, and results were quite similar to those of simulation S17 (less than XºC difference), in which the variation of environmental conditions was not applied. It seems that other input parameters, such as solar radiation, which was not considered in this work, would be necessary in order to explain the observed oscillations.

Finally, as in the previous Sections, a study was performed comparing the differences between the maximum temperatures of the data measured in the field and the simulations S17 (without the variation of environmental conditions) and S18 (with the variation of environmental conditions) to verify whether the implementation of this variation reduced the differences between the maximum temperatures. Table 13 presents these results, highlighting the lowest values at each point.

Table 13 – Differences between maximum temperatures reached in field monitoring and in simulations performed with and without the variation of environmental conditions

Simulation	**Thermocouple point**			
	T01	**T02**	**T03**	**T04**
S17 (Constant environmental conditions)	0.66 ºC	0.70 ºC	1.34 ºC	1.93 ºC
S18 (Varying environmental conditions)	0.37 ºC	0.98 ºC	1.63 ºC	2.50 ºC

Source: Author (2022).

It can be seen that the S18 simulation, with varying environmental conditions, did not contribute to reducing the differences between the maximum temperatures reached by the structure in the field and the computational results. The low amplitude in the values of the climate predictions used in the software may not have represented, in a practical way, the reality experienced in the field on the day of the casting, highlighting the importance of monitoring both the temperatures in the structure and the temperatures and wind speeds outside. Moreover, it is emphasized that, in the simulations performed, the effects of solar radiation were not considered, which may have influenced the thermal behavior of the structure during the monitoring time in the field, since the construction site has high solar exposure, which is oscillatory by nature.

3.6 Final comments

This chapter focused on carrying out studies varying some of the computational model input parameters in order to approximate their results with the data from the monitoring of the foundation block in the field. This was done because divergences, especially concerning the values of the maximum temperatures obtained, were identified in the study presented in Chapter 2. It was chosen to vary the thermal properties (thermal conductivity coefficient and specific heat), the casting methodology (dividing the structure into layers and applying a time interval between the placing of each one), and the environmental conditions (temperature and wind speed).

In general, it was observed that the variation of parameters can cause significant differences in computational predictions of the thermal behavior of massive concrete structures, which was expected. This highlights the importance of conducting tests to determine material properties and providing as much information as possible on both of the casting process and the environmental conditions in order to obtain better reliability of predictive models. In the impossibility of obtaining those data in advance, on alternative would be to develop a mock-up prototype on a smaller scale with the same materials and the same casting conditions of the actual structure to perform a previous optimization of the computational models. With this, it is expected to obtain a greater convergence between the simulation data and the monitoring data. The main conclusions regarding the results obtained in this chapter were:

- regarding the thermal properties, it was noticed that the reduction of the input values of the thermal conductivity coefficient and specific heat caused both an increase in the value of the internal temperatures of the structure in the simulations.
- it was observed a significant influence of the variation of the specific heat of concrete in the elevation of the internal temperatures of the structure, presenting maximum differences of up to 23 °C between the highest temperatures in the performed simulations. Differences are clear in the core of the structure. On the other hand, the variation of the thermal conductivity coefficient did not show a significant influence on the thermal behavior of the structure, in which differences of less than 2 °C in the highest temperatures were observed among the simulations performed in the study;
- concerning the study of the casting methodology, it was noticed that, despite the small differences (less than 1ºC), the simulation performed with the division of the casting in layers and the application of time intervals for the placing of each layer showed more

proximity to the data from field measurements concerning the reach of maximum temperatures. This suggests that it may be important to implement in the models these conditions, which are closer to the casting reality;

- due to the short time interval applied between the concreting of each layer, there was no significant influence of this change on the results. Importance of more research on this topic was emphasized;
- the oscillations in internal temperatures identified in the field measurements were not observed in the simulation performed with the variation of environmental conditions, going against what was expected. It is hypothesized that the effect of variable solar radiation onto the foundation (not investigated) is the main reason behind the oscillations;
- the importance of monitoring the climatic conditions was highlighted, since forecasts may not correctly represent the conditions experienced on the days of field monitoring. Furthermore, the importance of further studies to investigate the influence of other parameters, such as the heat exchange by radiation, is emphasized.

4 DEVELOPMENT AND APPLICATION OF A CASTING PLAN FOR A MASSIVE CONCRETE FOUNDATION OF A HIGH-RISE BUILDING

ABSTRACT

Another type of massive concrete structure is the foundations of high-rise buildings, whose increasing verticalization in Brazil enhances the need for larger foundations to provide more stability to the buildings. This chapter describes the development of a case study applied to a piled raft foundation of a high-rise building that is being built in the city of Fortaleza/CE, in northeastern Brazil. For this purpose, it was aimed to verify, besides the reliability of the method for predicting the thermal behavior of the structure, the main challenges that involve the whole process of casting and monitoring mass concrete elements. The procedure adopted included the execution of the computational thermal analysis, with the definition of the casting methodology, the follow-up of the application of this process, and the instrumentation and field monitoring of the internal temperatures reached by the structure. The results showed the importance of this follow-up and confirmed the reliability of the predictive model used. Moreover, the possible influence of the use of admixtures on the thermal behavior of the concrete structure and the need to implement parameters that correctly characterize the materials and the boundary conditions was highlighted to bring the computational predictions closer to the reality experienced in the field.

Keywords: thermal analysis; mass concrete; finite element simulation; casting control plan.

4.1 Introduction

Other types of massive concrete structures that should be highlighted are the foundations of high-rise buildings. The verticalization of urban spaces is not only connected to demographic growth and the decrease of available spaces in large urban centers but also relates to modernization and to the economic and political interests of the cities (ROSO *et al.,* 2021). Thus, to provide greater stability to buildings, which are increasingly taller and are mostly built in smaller urban spaces, there is a need for bulky concrete foundation structures and even the joining of foundation blocks into a single larger block due to the limited building area available.

Poulos (2016) states that foundation design suffers considerable influence from some characteristics of high-rise buildings, such as the vertical loads supported by the foundation structures (weight of the building), the differential settlements due to the influence of the neighborhood of low-rise buildings, the magnitude of the lateral forces from cyclic wind loading, which generates moments in the foundations, and the particularities of the dynamic responses of this type of buildings.

There are predictions that, by the year 2025, there will be towers built over 1300 min height in the world, which will surpass the Burj Khalifa, the tallest building built to date, with 828 m in height.

According to the Council on Tall Buildings and Urban Habitat (2022), there has been a noticeable evolution in the height of Brazilian buildings in the last few years. In terms of completed buildings over 150 m high, Brazil is the 16th tallest country in the world and the 1st in South America. In addition, 97 % of the buildings are made of concrete, and there are high-rise buildings (over 200 m high) being built and expected to be completed by 2028.

In this way, it is evident the growth of the use of massive concrete structures in various segments of the construction industry. Due to the necessary precautions about the thermomechanical behavior of this type of structure to avoid the development of pathological manifestations, such as the emergence of cracks and the formation of delayed ettringite (DEF), and aiming to increase the performance and durability of structures, the importance of conducting predictive studies capable of assisting the definition of the concrete mix designs, the casting processes, the curing and isolation methodology, and even the decision making during and after casting is highlighted.

Therefore, for this Chapter, it was chosen to perform a case study, applying the methodologies described throughout this research work, in a high-rise building foundation that is being built in northeastern Brazil. The thermal predictions were performed in a finite element

software and, after its results, the application of the defined casting process was followed in practice. Based on the results, it was aimed to verify the reliability of the predictive method and to list the main challenges experienced during the construction of this type of structure.

4.2 Methodological procedure

Aiming to achieve specific objectives 3 of this dissertation, this section describes the research method that will be used to perform this part of the study, with emphasis on the development of a case study to analyze, in practice, the entire construction process, from computational thermal analysis to the field monitoring of a massive concrete foundation.

According to the structure's characteristics, the construction company informed us that it would not be possible to do the whole casting process in a single stage due to the impossibility of supplying the concrete, being able to divide it into some steps. Thus, one of the focuses of the computational study was to define both the number of layers and, consequently, the ideal time interval between the placing of each one, and the ideal temperature of placing the concrete of the structure, based on the estimated temperature limit of 65 °C (MEHTA; MONTEIRO, 2014).

After that, points were defined for the measurement of the internal temperatures of the structure over time through the installation of thermocouples. The follow-up of the casting of concrete was performed in each of the stages and the monitoring data were collected for subsequent comparison with the simulation results. In addition, it was chosen to use only b4cast software in the analyses presented in this chapter due to its wider range of use for consulting in field applications. To perform the simulations, the methodology described in Chapter 2 was used. Figure 57 presents the flowchart of the methodology applied in this Chapter.

Figure 57 – Flowchart of the case study

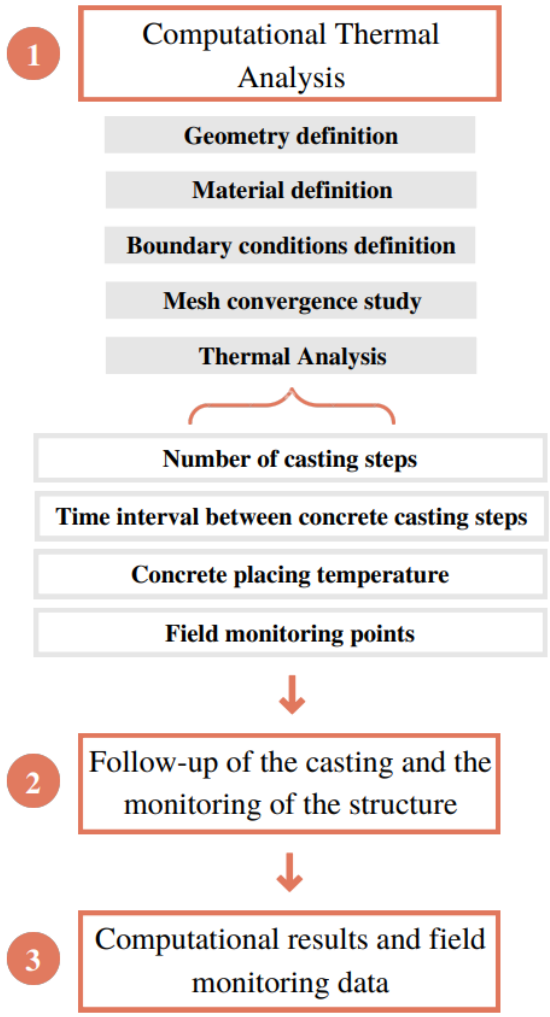

Source: Author (2022).

4.2.1. Geometry definition

The first step in performing the thermal analysis is to define the geometry that will be studied. It was chosen to analyze a piled raft foundation of a high-rise building (Acqualina) that is being constructed in the city of Fortaleza/CE, in the Brazilian northeast. This building will have 49 floors, of which 2 are underground, and will be approximately 150 m in height (FIGURE 58). It will become one of the tallest buildings in Fortaleza when it is finished. The construction is expected to be finished in 2024.

Figure 58 – 3D model of the Acqualina building facade

Source: Construction Company of the building (2021).

The concrete raft is a type of foundation that works as a continuous slab designed to support loads of all the columns and all the walls, as well as any pressure from the water table. This element is usually used to replace direct foundations when, by project imposition, they need to be very close to each other or overlap. The raft is usually used in buildings with few floors, but it is possible to find examples of tall buildings, whose projects present the piled raft as the best structural solution, as is the case of the structure chosen for the case study.

According to the design provided by the construction company, the foundation in this study has an irregular polygonal base (FIGURE 59), with an area of 642.6 m² and a height of 2.75 m, thus totaling a volume of 1767.15 m³ of concrete.

Figure 59 – Raft floor plan (dimensions in meters)

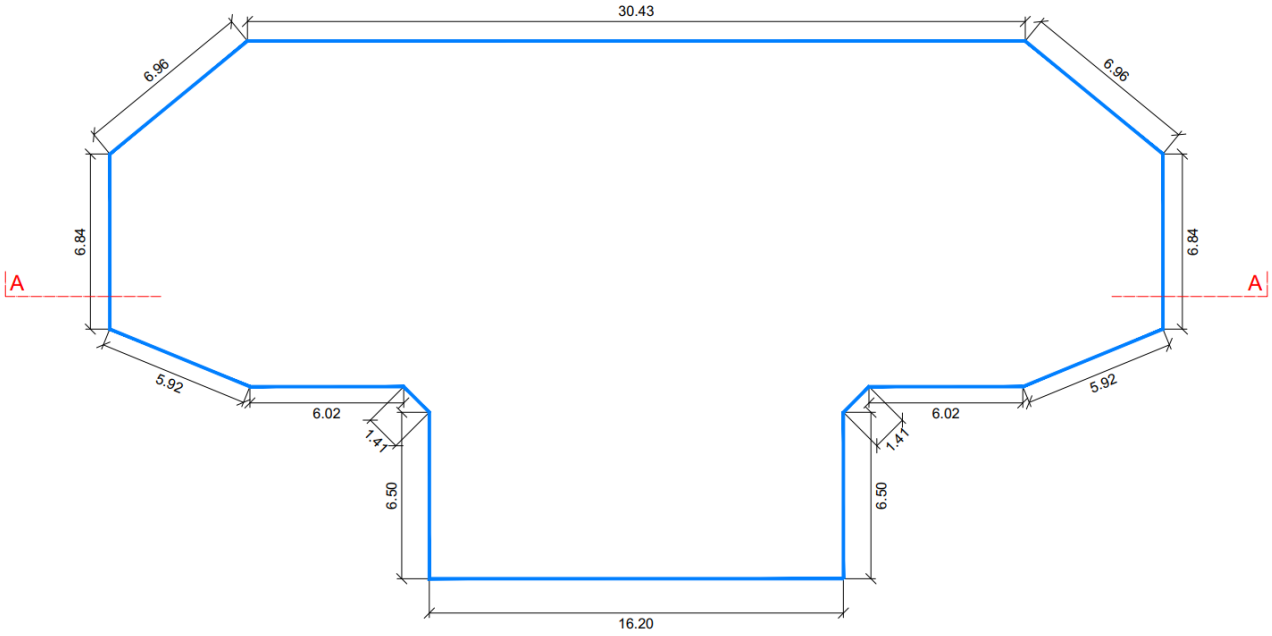

Source: LMCC (2021).

Due to the need for a high consumption of concrete for the construction of the structure, it was not possible to perform the casting of the entire structure in a single day. So, according to the concrete supplying company's availability and the construction planning, it was decided to divide the process into stages. Thus, it was chosen to start the study by dividing the casting into 5 layers 55 cm of thick each (L1, L2, L3, L4, and L5) and verifying the possibility of using this configuration according to the results obtained. In addition, there are a 0.10 m layer of regularization concrete and a 6.00 m layer of soil below the entire structure considered in the design. Figure 60 shows the 3D design of the structure in the b4cast software with the layout of the structure in 5 layers, and Figure 61 shows the AA cross-section.

Figure 60 – Raft foundation geometry defined in b4cast software

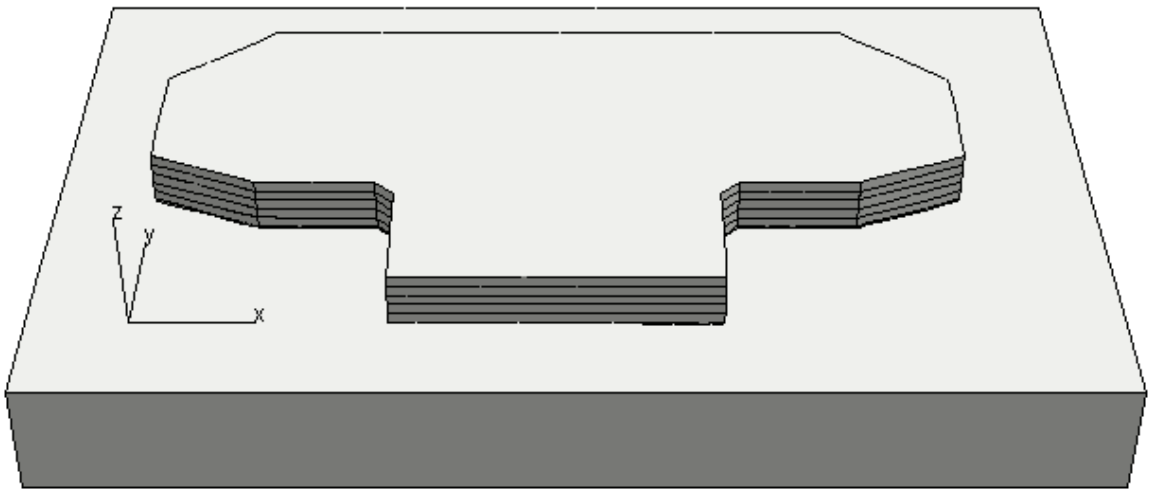

Source: Author (2022).

Figure 61 – Cross-section AA of the foundation with the initial proposal of division into 5 casting layers

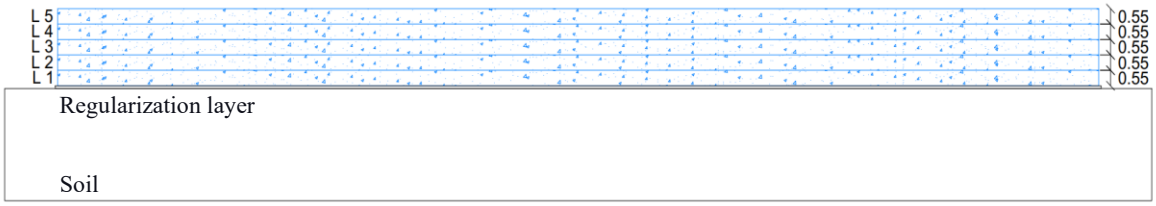

Source: Author (2022).

4.2.2. Material definition

For the computer simulations, it is important to determine the properties of the concrete and correctly characterize the materials that compose it. The thermal properties of the foundation materials in this case study were taken from the literature due to the absence of laboratory tests to obtain them. Table 14 shows the values of the concrete properties implemented in the b4cast software. It was necessary to define the properties of the soil layer underneath the entire structure. The thermal properties of the soil were obtained based on literature data and are described in Table 14.

For the casting process, two concrete mixes design with fck = 30MPa were used. At a vertical position from 0.00m to 0.55m height, mix T1 would be applied and at a vertical position from 0.55m to 2.75m, mix T2. Table 15 shows the main differences between the two mixtures (cement content and maximum coarse aggregate size). The cement type of the mixes is cement CP III (Blast-Furnace Portland Cement).

Another important point that needs to be implemented in thermal analyses of concrete structures is the rate of heat released during cement hydration. The heat of hydration curves of cement CP III used in the analyses were provided by the construction company and performed by the Associação Brasileira de Cimento Portland (ABCP) through the Langavant method, described in NBR 12006 (ABNT, 1990). The heat curve values implemented in the software are presented in Table 16. According to NBR 16697 (ABNT, 2018), the cement used was classified as low heat of hydration (LH).

Table 14 – Concrete and soil properties used in thermal analyses

Property	**Concrete Mix f_{ck} = 30 MPa**	**Soil**
Density	2350.00 kg/m³ (1)	1515.00 kg/m³ (5)
Heat Capacity	1.00 kJ/kg/°C (2)	0.80 kJ/kg/°C (5)
Thermal Conductivity	9.55 kJ/m/h/°C (3)	0.97 kJ/m/h/°C (5)
Coefficient of Thermal Expansion	10^{-5} /°C (4)	10^{-5} / °C (6)

Source:
(1) Construction Company of the building (2021); (2) Couto (2018); (3) Breugel (1998); (4) Mehta e Monteiro (2014); (5) Incropera *et al.* (2008); (6) Delage (2013).

Table 15 – Main differences between concrete mix design

Concrete Mix	**Cement Content**	**Maximum Coarse Aggregate Size**
T1	328 kg/m³	12.50 mm
T2	308 kg/m³	19.00 mm

Source: LMCC (2021).

Table 16 –Test results for determining the heat of hydration of cement

Time (h)	Results (J/g)
6	30
12	123
24	201
41	234
48	239
72	246
120	250
168	250

Source: ABCP (2021).

4.2.3. Boundary conditions definition

The next step for carrying out the thermal analyses was to apply the boundary conditions to the foundation block geometries, to improve the accuracy of the results.

Regarding the climatic conditions, the values for ambient temperature and wind speed were taken from forecasts provided by The Weather Channel (2021). According to the data obtained, the average temperatures in Fortaleza vary between 25 ºC and 32 ºC. And the wind speed in the city of the building site varies between 5.28 m/s and 9.17 m/s. The variation of these parameters was implemented in the software. The variation of these parameters over time, which was implemented in the software, is shown in Appendix B.

Finally, it was considered that, on the sides of the structure, there is masonry formwork composed of ceramic bricks (FIGURE 62), with an approximate thickness of 20 cm, which will be in contact with the concrete during the entire analysis process. In addition, it was considered the application of wet curing after the execution of each stage. It is emphasized that, for the analyses described in this chapter, heat exchange by radiation was not considered.

Figure 62 – Masonry formworks on the sides of the geometry

Source: Author (2022).

4.2.4. Mesh convergency study

FEM is a technique that involves the subdivision of a continuous object into a finite number of elements, which are connected at discrete points known as nodes. This approach enables detailed analysis of the behavior of structures and is widely used in modeling engineering problems. The type of analysis applied in this study is transient thermal that considers changes in temperature and boundary conditions over time (KIM, 2010). The tetrahedral elements were the ones used in the three-dimensional discretization of the analyzed structure in the b4cast software. As this software is specific for thermal analysis, there is no possibility of changing the type of element. According to Couto (2018), the use of tetrahedral elements proved suitable for this type of analysis.

The last step before starting the thermal analyses is to perform a mesh convergence study, which is to measure the relationship between the number of elements and the accuracy of the analyses (PATIL; JEYAKARTHIKEYAN, 2018). For the mesh convergence study of the structure under analysis in this chapter, it was chosen to vary the mesh size from 1.00 m to 0.40 m. Figure 63 shows the mesh refinement done for this study. The global maximum and minimum temperature data of the structure were analyzed in each test, and the results of the mesh convergence study are presented in Figure 64.

Figure 63 – Mesh refinement of raft

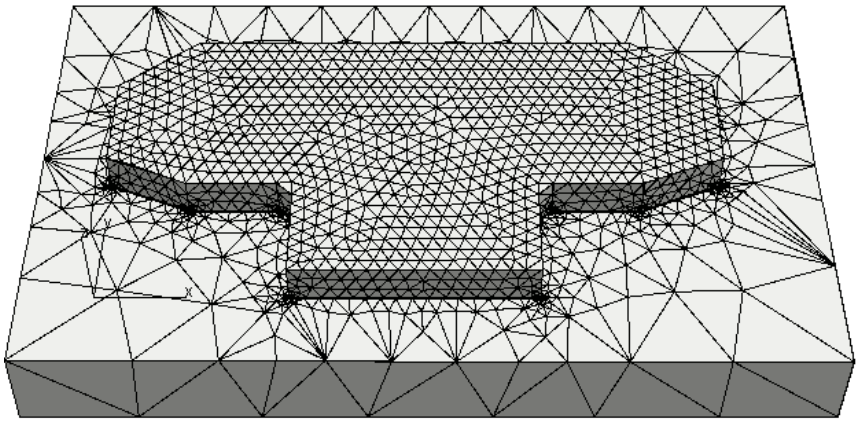

a) 1.00 m

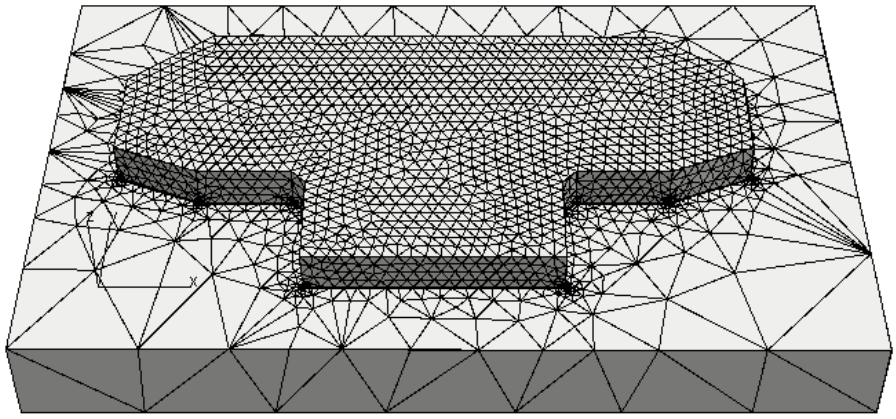

b) 0.80 m

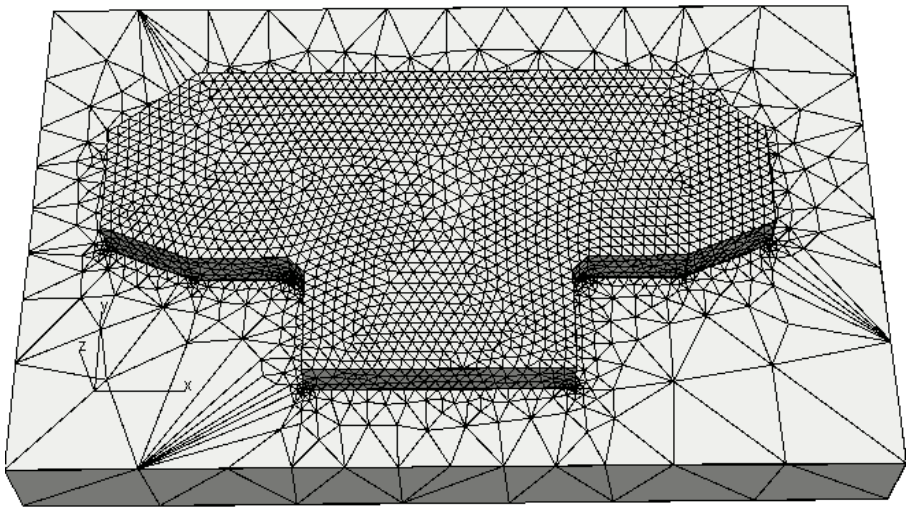

c) 0.70 m

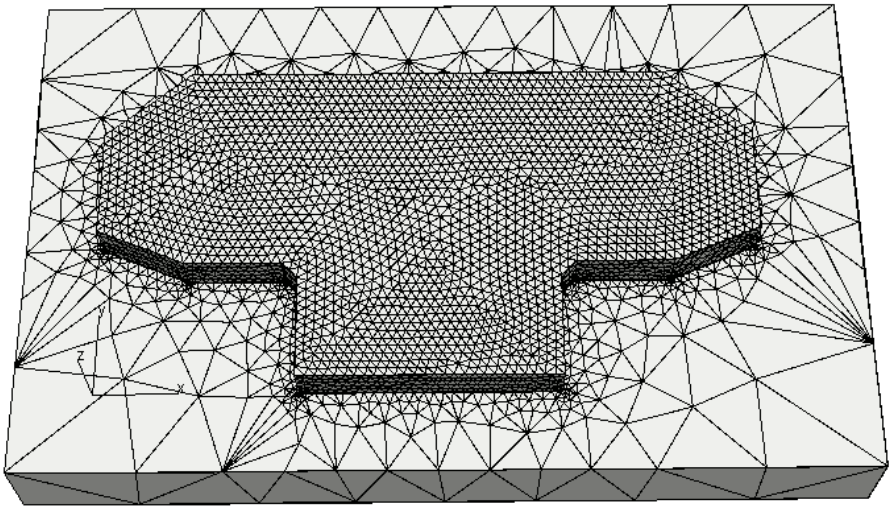

d) 0.60 m

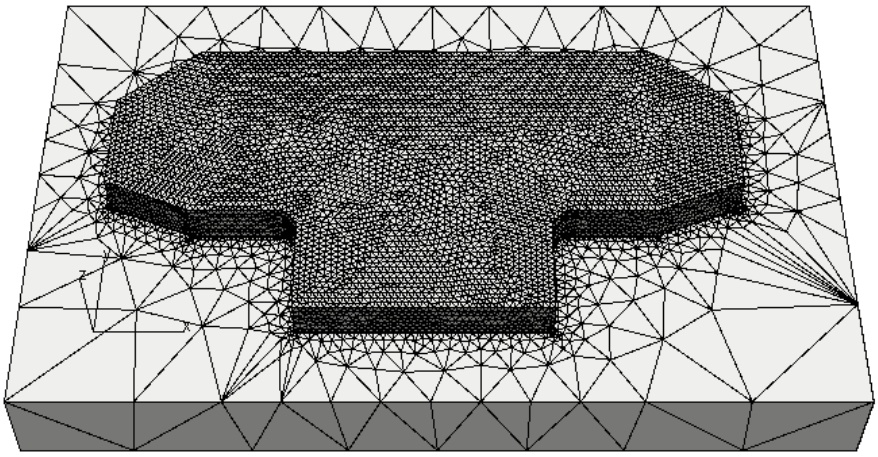

e) 0.40 m

Source: Author (2022).

Figure 64 – Mesh convergence study for the raft foundation

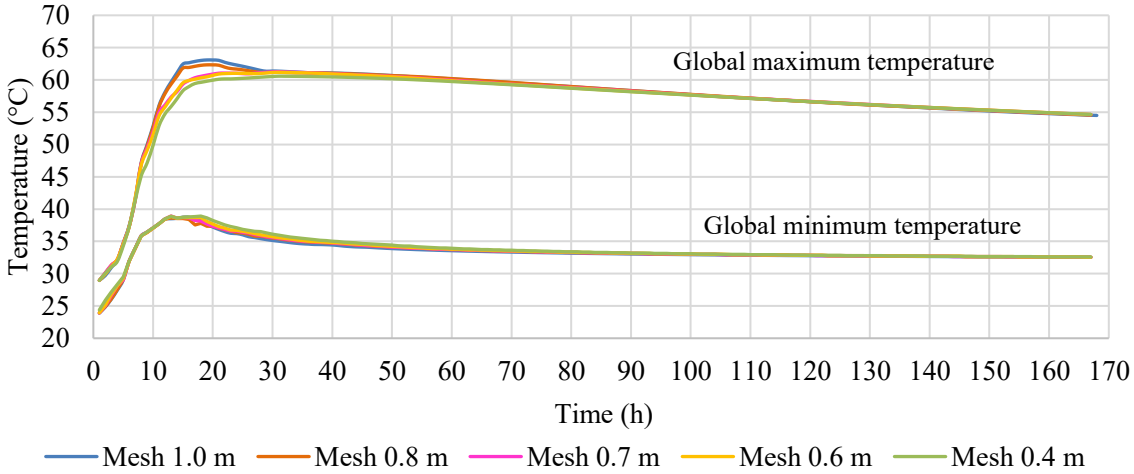

Source: Author (2022).

According to Figure 64, in the analysis of minimum temperatures, it was observed a small difference in the values of the 0.80 m mesh concerning the other meshes. As for the maximum temperatures, a discrepancy was observed between the values of maximum temperatures reached by the curves referring to the less refined meshes (1.00m and 0.80m) and the more refined meshes (0.70m, 0.60m, and 0.40m). Among the less refined meshes, there was little difference between the values. Due to this and the high computational effort required in the analysis with a mesh equal to 0.40m, it was chosen to perform the analyses of this chapter using the 0.60 m mesh.

4.3 Thermal analysis results

4.3.1. Definition of the number of stages, the time interval between each one and the temperature of concrete placing

As mentioned previously, according to the supply conditions and the construction planning, it was considered that the first study would be performed by dividing the structure into 5 concrete layers, each 0.55m thick. Thus, according to the results, the need to divide it into more layers was verified. The thermal analyses were performed with the main objective of defining the casting plan to be followed by the construction company.

Besides the number of steps, the time interval between the stages of casting and the placing temperature of the concrete are the main items that should be included in this plan, since it highlights, mainly, the concern about the rise in internal temperatures above the limit of 65 ºC (MEHTA; MONTEIRO, 2014).

To obtain these items, new computer simulations were performed, performing a parametric study, varying the placing temperature of the entire structure to 35 ºC, 30 ºC, and 25 ºC in the pursuit of the ideal temperature for the structure. The minimum temperature of 25 ºC was chosen due to the location of the site and, consequently, the difficulties of placing concrete at temperatures below this value. The maximum temperature considered (35°C) is close to the maximum environmental temperature considered for the location.

Regarding the choice of the ideal time interval for the placing of each step of the casting, it was chosen to vary the time in 14 h and 38 h (14 h + 24 h). It is worth noting that 14 hours is the average interval considered between the end of the casting of one step on one day and the beginning of the next step on the next day. Table 17 shows the summary of the new

simulations performed and the maximum temperatures reached by them. The highest temperatures were identified in layers L3 and L4, near the core of the structure.

Table 17 - Parameters used in the new simulations

Simulation	Time interval between each step (h)	Concrete placing temperature (ºC)	Maximum temperature (ºC)
S19	14	35	78.1
S20		30	75.6
S21		25	72.5
S22	38	35	71.6
S23		30	66.8
S24		25	62.5

Source: Author (2022).

Analyzing Table 17, it can be seen that the higher the placing temperature, the higher the values of maximum temperatures reached by the structure. In addition, the increase in the time interval between the casting steps from 14 h to 38 h contributed to a reduction in the maximum temperature values, since the increase of this interval provides a more intense cooling of the lower layers, thus reducing the influence of their thermal rise on the subsequent layers. It can be observed that only simulation S24 presented a maximum temperature below the 65 ºC limit. Thus, it is possible to conclude that the division of the casting process into 5 steps is feasible and that the minimum time interval between each step should be 38 hours. Therefore, the entire casting process would take 9 days. Table 18 compiles the casting guide for each stage. This methodology was approved by both the construction company and the concrete supplier.

Table 18 - Guide for casting steps of the raft foundation according to the time interval of 38 hours between the end of one step and the beginning of the next

Layer	**Height (m)**	**Pouring time (h)**	**Day of casting**
L1	0.55	0	1º
L2	0.55	38	3º
L3	0.55	76	5º
L4	0.55	114	7º
L5	0.55	152	9º

Source: Author (2022).

Concerning the ideal maximum launch temperature, according to Table 17, it can be seen that this temperature should be between 30 ºC and 25 ºC. Thus, for its definition, the values of the maximum temperatures reached by the structure in layer L3, which reached the highest internal temperatures, were plotted as a function of the placing temperatures of simulations S22, S23, and S24. Figure 65 shows the results.

Figure 65 – Predicted global maximum temperatures reached by the L3 layer of the foundation structure with the variation of the placing temperature in 35 ºC (S22), 30 ºC (S23) and 25 ºC (S24)

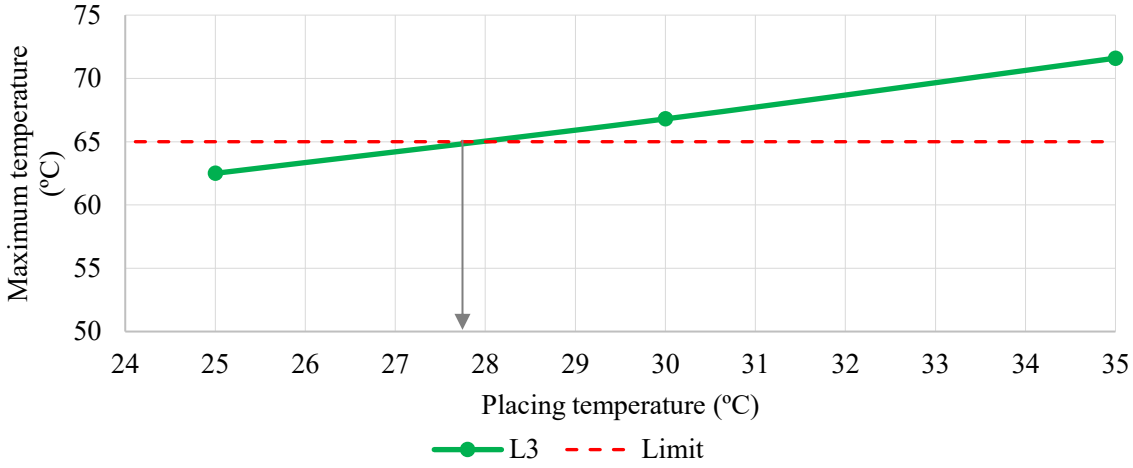

Source: Author (2022).

Considering the maximum limit of 65 ºC previously established for the maximum concrete temperatures, it can be seen in Figure 62 that the maximum ideal placing temperature for layer L3, located in the core of the structure, should be equal to 27 ºC. In the interest of safety, it was chosen to apply this placing temperature to the other layers. This temperature value would be reached by replacing part of the water in the mix design with ice.

Thus, a new simulation (S25) was carried out by applying 27 ºC as the placing temperature for all layers of the structure and 38 h as the time interval between the end of one casting step and the beginning of the next. Figure 66 presents the maximum temperatures reached by each layer of the structure in this simulation. In addition, a summary of simulations S19 to S25 is presented in Table 19, with emphasis on the chosen simulation (S25).

Figure 66 - Predicted maximum temperatures in layers L1, L2, L3, L4 and L5 of the raft foundation in simulation S25

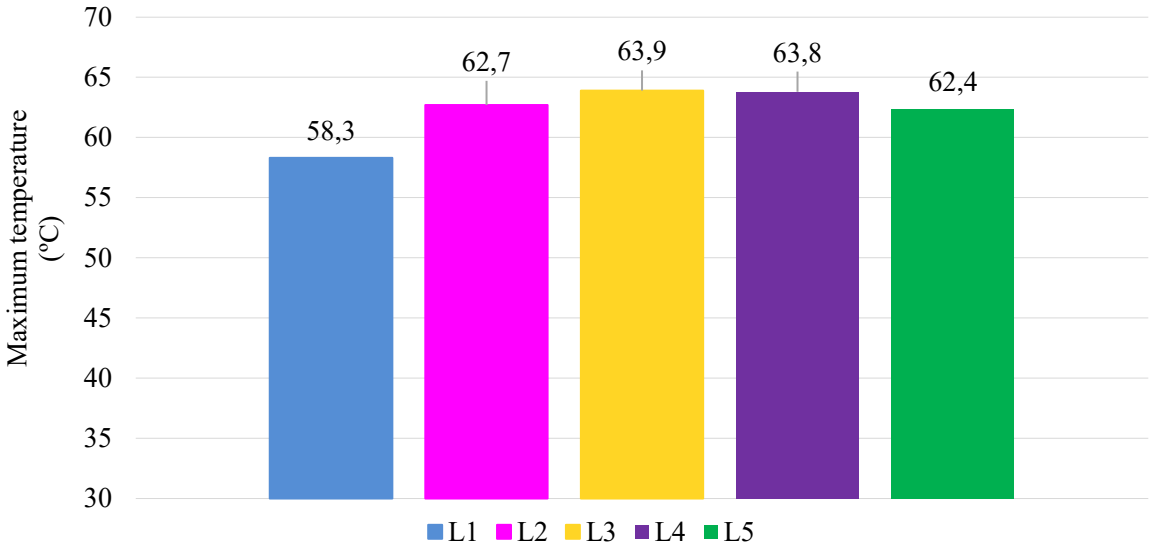

Source: Author (2022).

Table 19 - Summary of simulations S19 to S25 performed in this chapter

Simulation	Layer	Placing temperature (ºC)	Interval between the layers (h)	Predicted maximum temperatures (ºC)
S19	L1	35	14	69.0
	L2			76.3
	L3			77.8
	L4			78.1
	L5			72.6
S20	L1	30	14	66.2
	L2			73.6
	L3			75.1
	L4			75.6
	L5			68.0
S21	L1	25	14	63.2
	L2			71.0
	L3			72.3
	L4			72.5
	L5			63.7
S22	L1	35	38	65.7
	L2			70.3
	L3			71.6
	L4			71.3
	L5			69.8

Simulation	Layer	Placing temperature (ºC)	Interval between the layers (h)	Predicted maximum temperatures (ºC)
S23	L1	30	38	60.9
	L2			65.3
	L3			66.8
	L4			66.5
	L5			65.0
S24	L1	25	38	56.7
	L2			61.0
	L3			62.5
	L4			62.3
	L5			60.6
S25	L1	27	38	58.3
	L2			62.7
	L3			63.9
	L4			63.8
	L5			62.4

Source: Author (2022).

4.3.2. Definition of field monitoring points

Considering that simulation S25 was chosen to continue the study of the foundation block, Figure 67 shows the temperatures of each layer over time.

Figure 67 –Maximum temperatures reached by layers L1, L2, L3, L4 and L5 of the foundation block over time in simulation S25

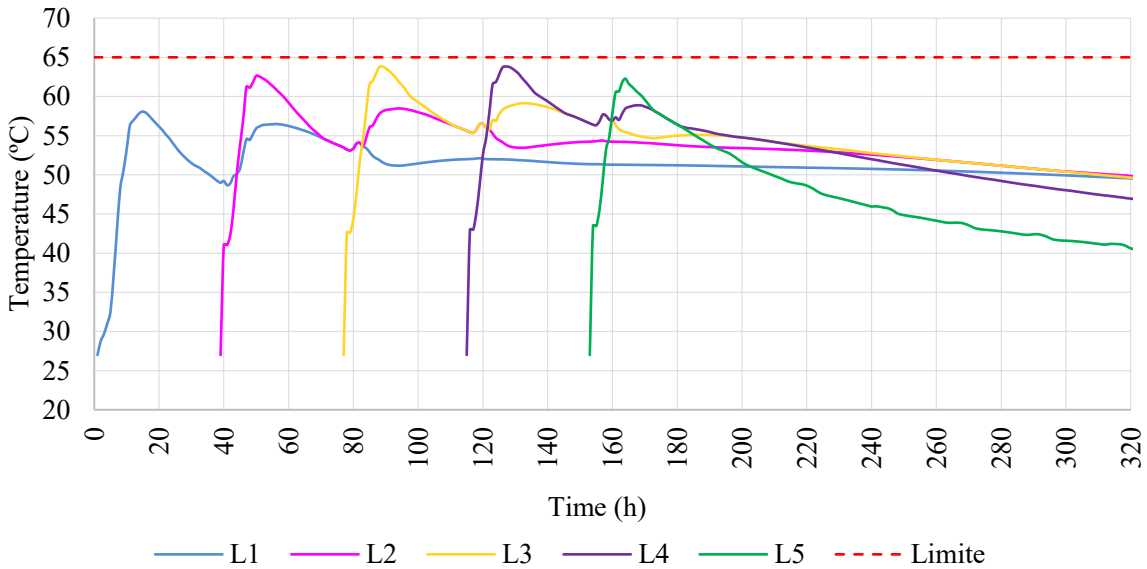

Source: Author (2022).

According to Figure 67, the placing of a layer influences the thermal behavior of the previous layer, which, during its cooling process, suffers another temperature peak when the new layer is placed. This is not seen in layer L5, because, after it, there is no other concrete layer. For this reason, and due to the proximity to the external environment, this layer has a faster cooling process.

The behavior observed in Figure 67 is also confirmed by looking at the isotherms of the structure. Figure 68a shows an example of its isotherms when the peak temperature of the L5 layer is reached. It can be seen that, despite the cooling of the other layers at this moment, the L4 layer, at points neighboring L5, and the L3 layer, in the core, have more difficulty in cooling. Figure 68b shows an example of its isotherms 168 h after the release of layer L5, with emphasis on the occurrence of higher temperatures at points near the geometric center of the structure and the ground, in addition to the cooling of the edges and layer L5.

Figure 68 – Example of isotherms at the foundation block core: (a) at the time of peak temperature of the L5 layer; (b) 168 h after the release of the L5 layer

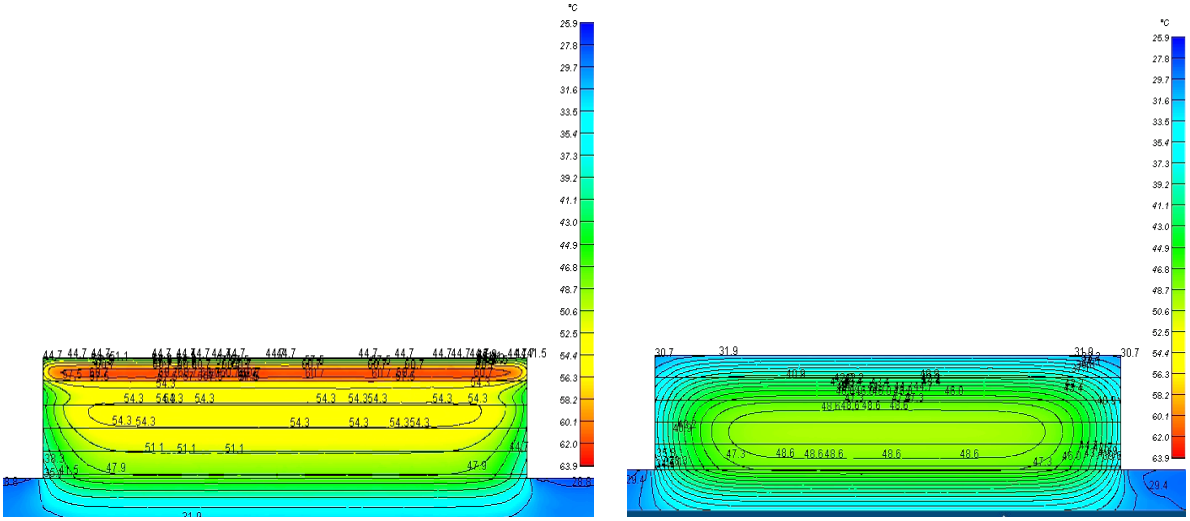

a) b)

Source: Author (2022).

In the sequence, 5 points (A, B, C, D, and E) were chosen to follow the temperatures over time in the simulations and the field. Figures 69, 70, and 71 show the location of each point on the structure. It was chosen to install points A and B in the center of all layers. Point B was installed very close to point A for safety since if there were failures in some of the thermocouples at point A, there would be a chance that point B was recording temperatures at

that location. Points C, D, and E were installed only in the center of layers L3 and L4 due to the greater possibility of reaching the maximum temperatures at these locations. In total, it was recommended to install 16 thermocouples inside the raft foundation. Table 20 shows the maximum temperatures reached by points A, B, C, D, and E in simulation S25.

Figure 69 –Location of the internal points chosen for monitoring the evolution of temperatures over time in the foundation

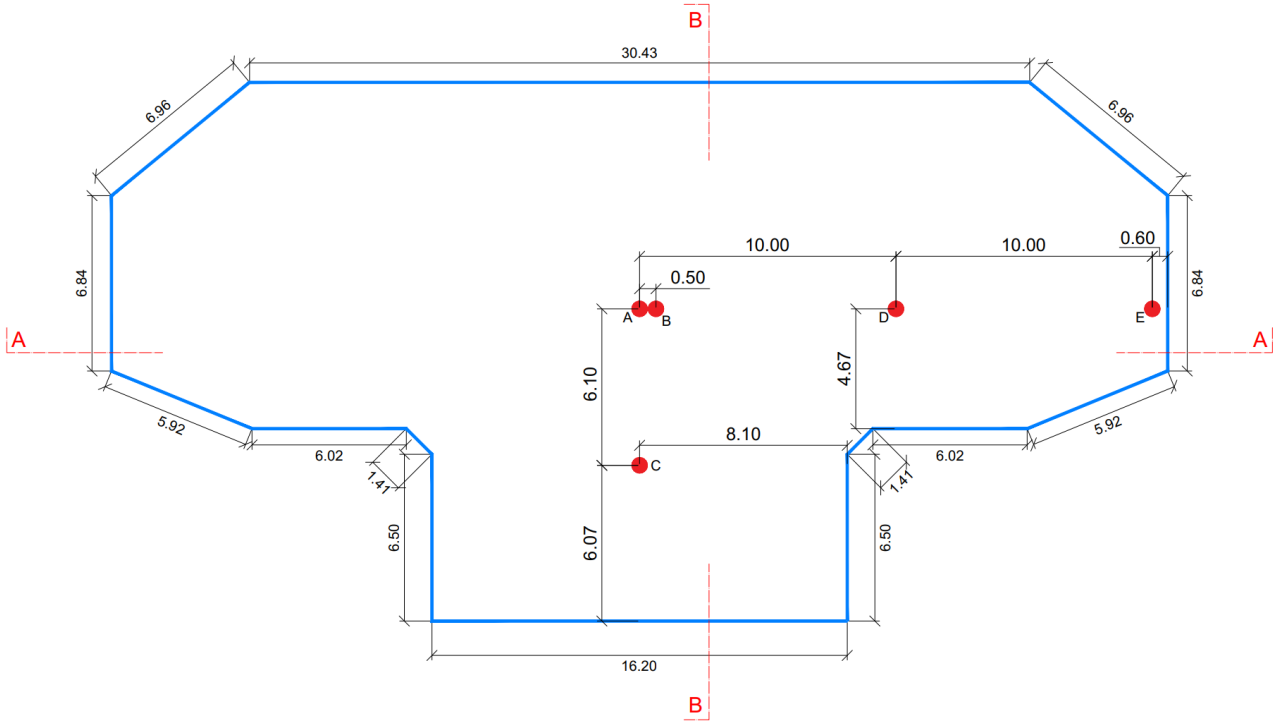

Source: Author (2022).

Figure 70 – Cross-section AA of the rafter with the location of points A, B, D, and E within the structure

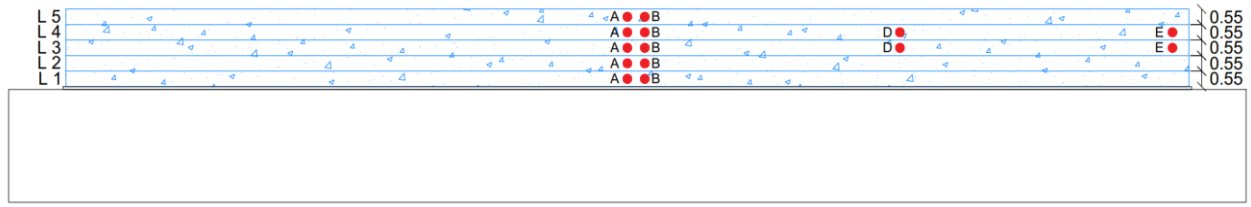

Source: Author (2022).

Figure 71 – Cross-section BB of the rafter with the location of points A, B, and C within the structure

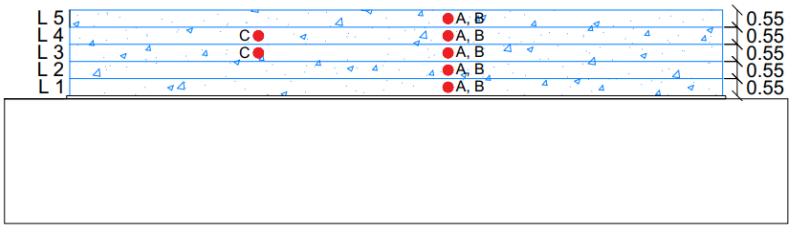

Source: Author (2022).

Table 20 – Maximum temperatures reached by points A, B, C, D and E in simulation S25

Layer	Point				
	A	B	C	D	E
L1	57.8 ºC	57.8 ºC	-	-	-
L2	62.5 ºC	62.5 ºC	-	-	-
L3	63.6 ºC	63.6 ºC	63.5 ºC	63.5 ºC	62.8 ºC
L4	63.7 ºC	63.7 ºC	63.7 ºC	63.7 ºC	62.9 ºC
L5	61.2 ºC	61.1 ºC	-	-	-

Source: Author (2022).

4.4 Follow-up of casting and monitoring of the structure in the field

The casting of the raft was performed between February 16 and 26, 2021. Table 21 shows the final concrete casting schedule applied. The interval between layers L2 and L3 was equal to 86 h due to the work interruption on the weekend. Thus, the casting duration was 11 days.

Table 21 – Schedule of the foundation casting

Layer	Date	Pouring time (h)	Day of casting
L1	16/02/2021	0	1º
L2	18/02/2021	38	3º
L3	22/02/2021	124	7º
L4	24/02/2021	162	9º
L5	26/02/2021	200	11º

Source: Author (2022).

The follow-up of the casting was monitored throughout the days. The quality control was done by a specialized company employed by the foundation construction company, which measured the placing temperatures of each truck mixer (FIGURE 72a), the highest of which was 27.90 ºC and the general average was approximately 25ºC. In addition, this control was performed through the consistency slump test (FIGURES 72b and 72c) and the molding of specimens for later compressive strength testing.

Figure 72 – Technological control of the concrete during the concrete placing steps

a) Measuring concrete placing temperature

b) Slump test

c) Slump test

Source: Author (2022).

The instrumentation of the structure for measuring the internal temperatures at points A, B, C, D, and E was done with the help of the construction company's technical team. The thermocouples (type K, with glass fiber insulation cable with a connector at one of its extremities, from Bagarel brand) were fixed to the steel reinforcements (FIGURE 73). The acquisition devices were positioned on top of the structure inside wooden boxes (FIGURE 74a). For the measurements, automatic devices (FIGURE 74b) and one manual acquisitor were used to check the integrity of the thermocouples after the casting (FIGURE 74c). The automatic acquisitors were kept on for up to 7 days after placement of each layer, with setup configured for hourly measurements. Both data acquisition devices used (manual and automatic) were from the brand Novus. The automatic devices (LogBox-AA) had

two input channels, being able to receive two thermocouples' input in each device. In addition, they are fully configurable devices using software that allows data collection, plotting, analysis and export. The manual equipment had only one channel.

Figure 73 – Installation of thermocouples on the raft foundation reinforcement

Source: Author (2022).

Figure 74 –Temperature acquisition devices used in the case study

a) Protection box b) Automatic device c) Manual device

Source: Author (2022).

The casting time of each layer was approximately 10 hours, requiring an average of 50 mixer trucks to fill each one. It is worth mentioning that, in the third step there was a problem in the concrete supply that caused the cancellation of this stage without the finishing of the L3 layer, placing only 40 mixer trucks. Because of this, there was the need to adapt the computational prediction model to verify the possibility of placing the missing part of layer L3 together with L4 and thus avoiding risks to the structure.

Therefore, a new simulation (S26) was developed to analyze this new casting configuration, which is shown in Figures 75, 76, and 77. The interruption of casting occurred in Region 2, where only 0.20 m of the L3 layer height was filled, leaving 0.35 m to be filled together with the L4 layer.

Figure 75 – Floor plan with the location of where the casting was interrupted in layer L3

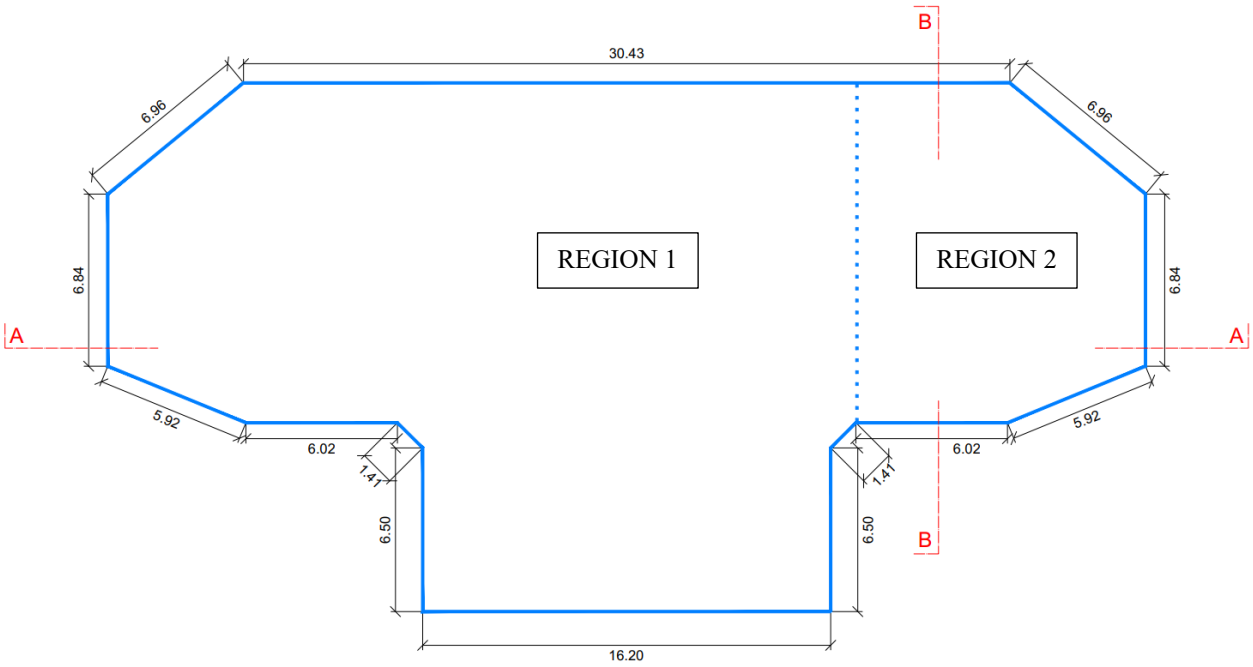

Source: Author (2022).

Figure 76 – Cross-section AA of the foundation with the new casting configuration implemented in simulation S26

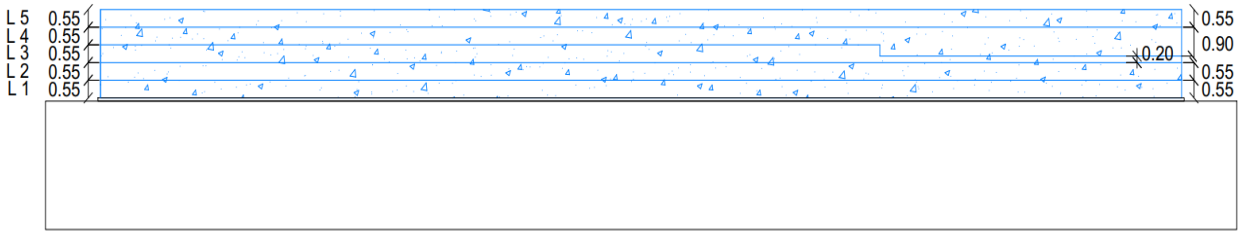

Source: Author (2022).

Figure 77 – Cross-section BB of the foundation with the new casting configuration implemented in simulation S26

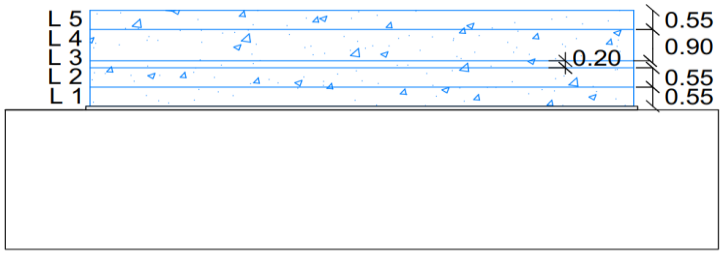

Source: Author (2022).

Furthermore, according to Table 21, the time interval between the end of the L2 layer casting and the beginning of the L3 layer increased by 48h, due to the weekend, being necessary to also implement this change in the computational model. Thus, simulation S26 was performed, and the maximum temperatures of points A, B, C, D, and E in this new configuration are presented in Table 22.

Table 22 – Maximum temperatures reached by points A, B, C, D, and E in simulation S26

Layer	**Point**				
	A	**B**	**C**	**D**	**E**
L1	57.7 ºC	57.7 ºC	-	-	-
L2	62.5 ºC	62.5 ºC	-	-	-
L3	61.7 ºC	61.7 ºC	61.7 ºC	58.1 ºC	56.56 ºC
L4	63.1 ºC	63.2 ºC	63.0 ºC	64.5 ºC	63.8 ºC
L5	61.2 ºC	61.1 ºC	-	-	-

Source: Author (2022).

According to Table 22, the feasibility of placing the remaining volume of concrete from layer L3 together with layer L4 can be seen, since there was no temperature of the structure above the safety limit of 65 ºC at any of the points, especially at points D and E, where the part with the highest thickness (0.90 m) is located. With these results, the construction company proceeded with the casting, thus finalizing the construction of the raft. The monitoring of the temperatures in the last L5 layer was carried out until March 3, 2021.

According to the experience in the field, it is important to highlight the care that should be taken during the casting of massive concrete foundations. Besides the development of previous studies to define the casting plan, the installation of thermocouples should be done with extreme caution due to the fragility of this equipment, which should be fixed to avoid rupture during the placing of concrete. The temperature acquisition devices must be protected from exposure to sunlight and humidity to avoid damage and improper operation. The placing temperature must be controlled in each concrete mixer truck because if the value exceeds the established limit, corrections must be applied. Finally, we emphasize the importance of monitoring the casting of concrete, because unexpected situations can occur, and it may be necessary to conduct new studies to support decision-making at critical moments during this process.

4.5 Results of comparison between computational results and field monitoring data

To finalize the case study described in this chapter, it was decided to perform a comparison between the field monitoring data extracted from the temperature acquisition devices and the results of the S26 simulation, described in the previous item. The comparisons were made to verify the reliability of the thermal predictions and identify points for improvement in this type of analysis. The results for points A, B, C, D, and E, where the thermocouples were installed, are presented in Figures 78, 79, 80, 81, and 82, respectively. It is noteworthy that some thermocouples were damaged during the monitoring process, and the data from them were discarded, among them, it is possible to mention: the thermocouple installed at point A in layer L5 and thermocouples installed at point B in layers L1 and L4. In layers L3 and L5, the recording of temperatures was interrupted before 180 h at point B.

When plotting the curves, it was noticed that, in all cases, the monitoring data showed lower temperatures than the simulation data throughout the analysis time, which can be

justified by the fact that some concrete batches were cast with temperatures below the maximum limit of 27ºC and because of the weather conditions during the casting days, which were cloudy and with little sunlight, which may have prevented further heating of the structure. This shows that the climate forecasts used may not have correctly represented the reality of the casting days. Moreover, as mentioned in the previous chapter, the fact that the thermal properties, such as specific heat, were taken from the literature may be another reason for this divergence, because the values implemented in the software may not have characterized well the foundation materials. Thus, although the computational results were favorable to safety, i.e., higher than the field data, it is important to perform tests to obtain the material properties and/or preliminary studies with prototypes to adjust the prediction models before the casting of the structures.

Another point of divergence observed was concerning the beginning of structure heating, which was slower and presented lower peaks in the results measured in the field. This may have happened due to the influence of the admixtures used in the concrete mix design, as retarders of the setting time. The influence of the admixtures was not considered in the test performed to obtain the heat of hydration curve implemented in the b4cast software. According to Zhang *et al.* (2018) and Antoniazzi *et al.* (2021), the increase in the content of some additives in concrete may contribute to these results.

Despite this, a similarity in the trend between the curves of the measured and simulated results was noticed. Thus, it was decided to plot a new curve moving the S26 simulation results in the X direction to approximate the heating initiation time with the time of the field data curve. With this, it was confirmed that, despite the differences described above, the similarity in the behavior of the computational and field results is confirmed for practically the entire analysis period at all points.

Figure 78 – Comparison between the field monitoring data from raft foundation and the S26 computer simulation results obtained in b4cast for point A at layers L1 (a), L2 (b), L3 (c) e L4 (d)

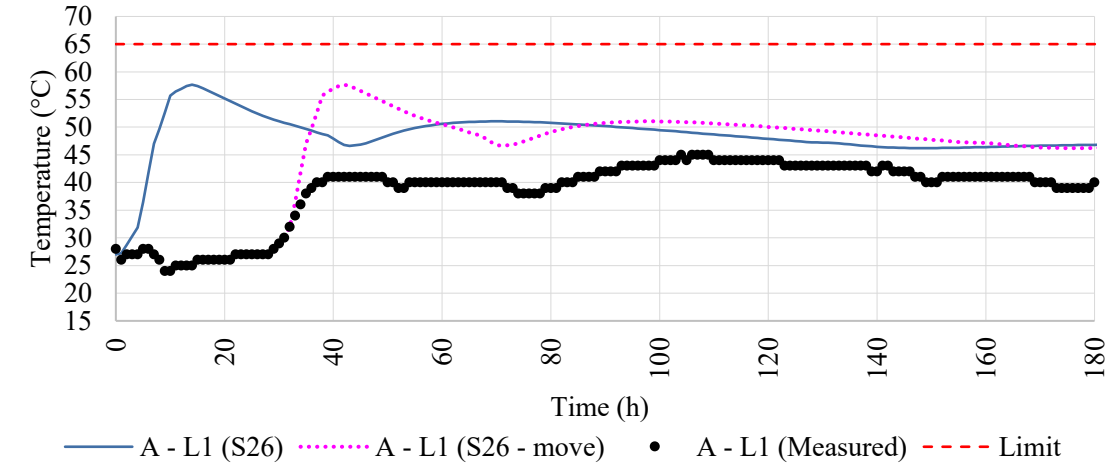

a) Layer L1

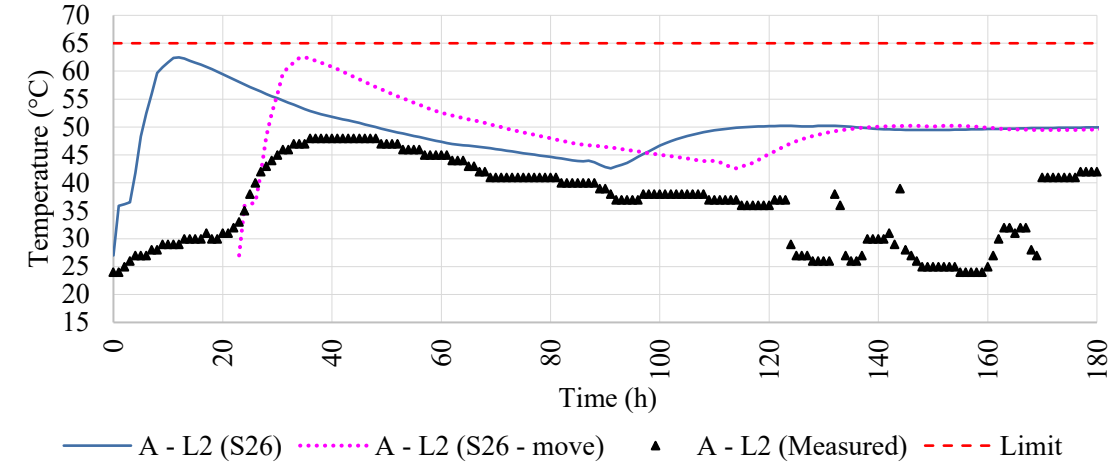

b) Layer L2

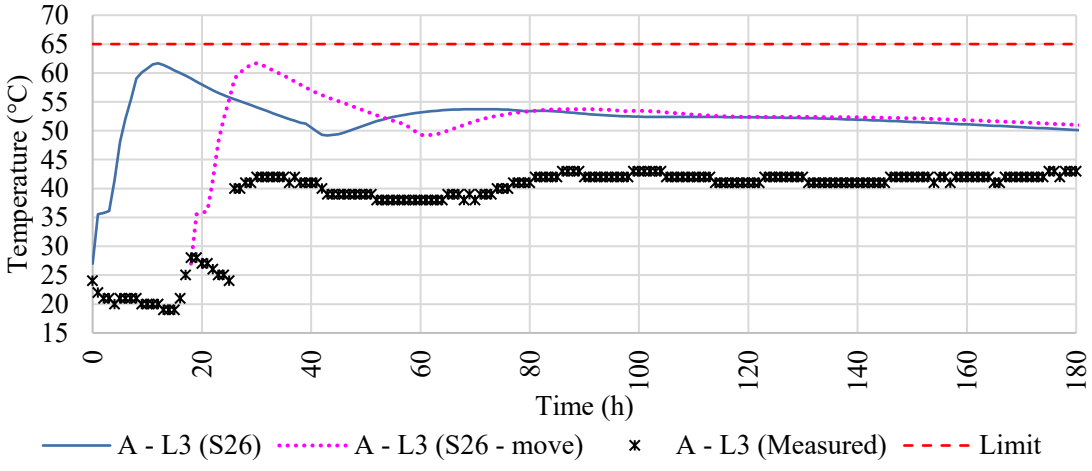

c) Layer L3

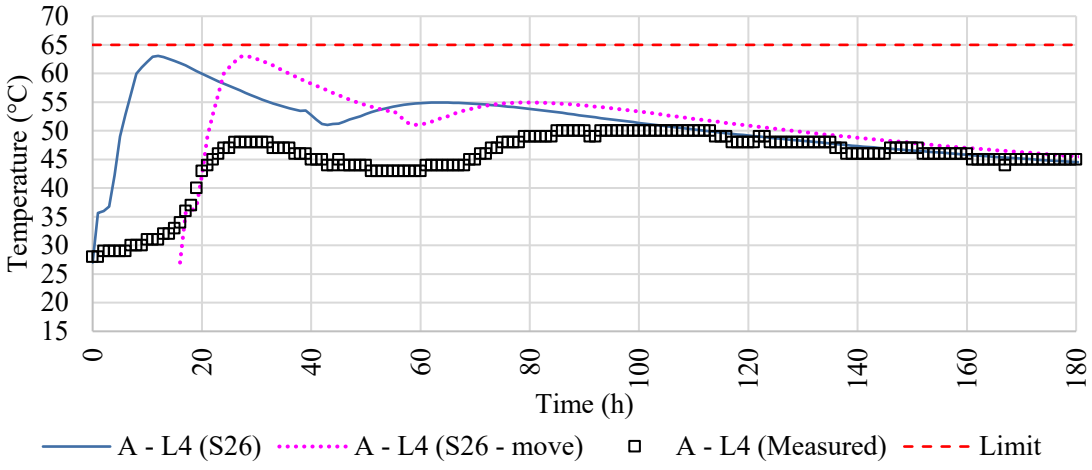

d) Layer L4

Source: Author (2022).

Figure 79 – Comparison between the field monitoring data from raft foundation and the S26 computer simulation results obtained in b4cast for point B at layers L2 (a), L3 (b) e L5 (c)

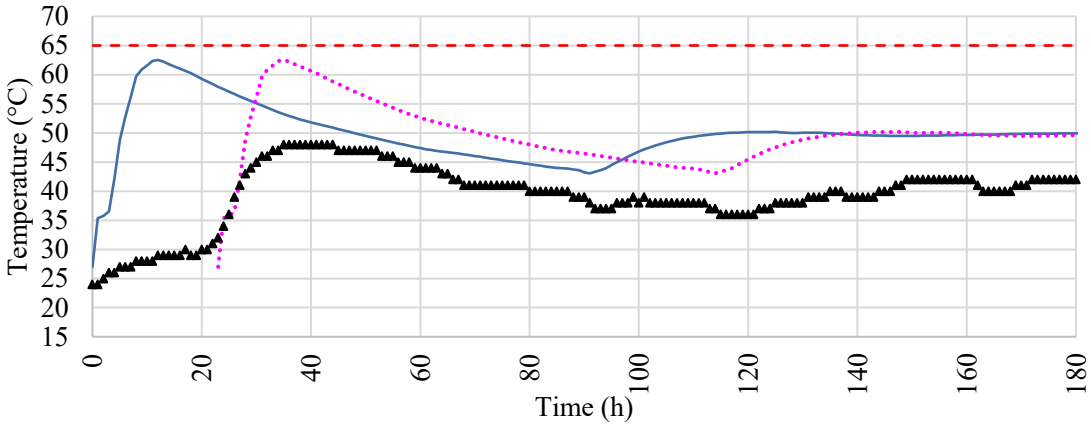

a) Layer L2

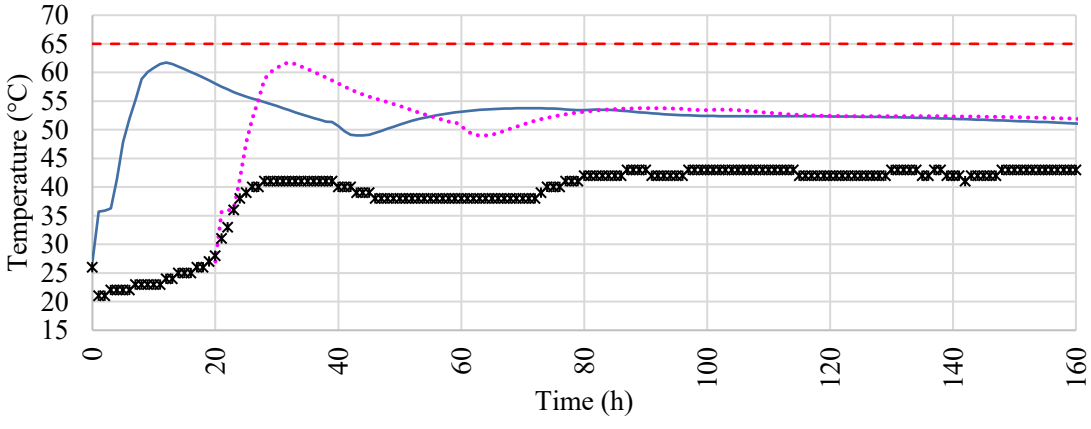

b) Layer L3

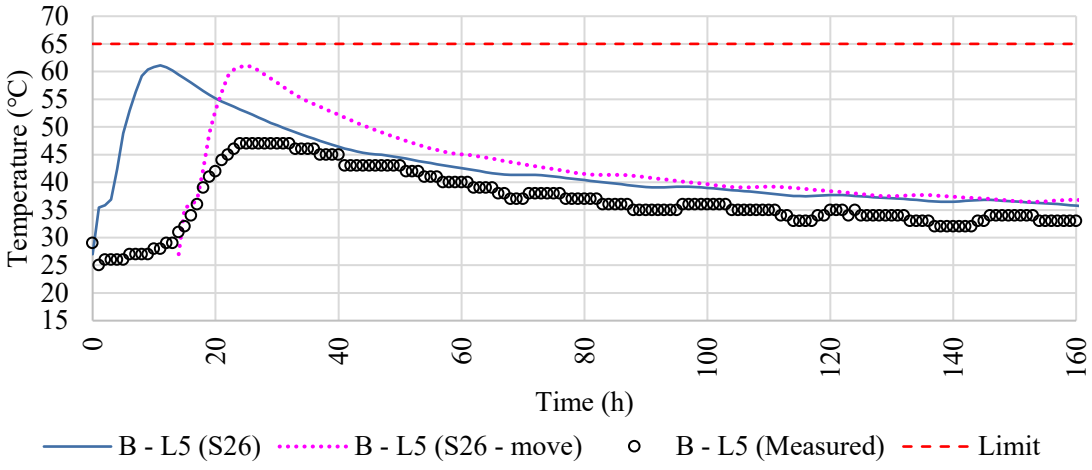

c) Layer L5

Source: Author (2022).

Figure 80 – Comparison between the field monitoring data from raft foundation and the S26 computer simulation results obtained in b4cast for point C at layers L3 (a) e L4 (b)

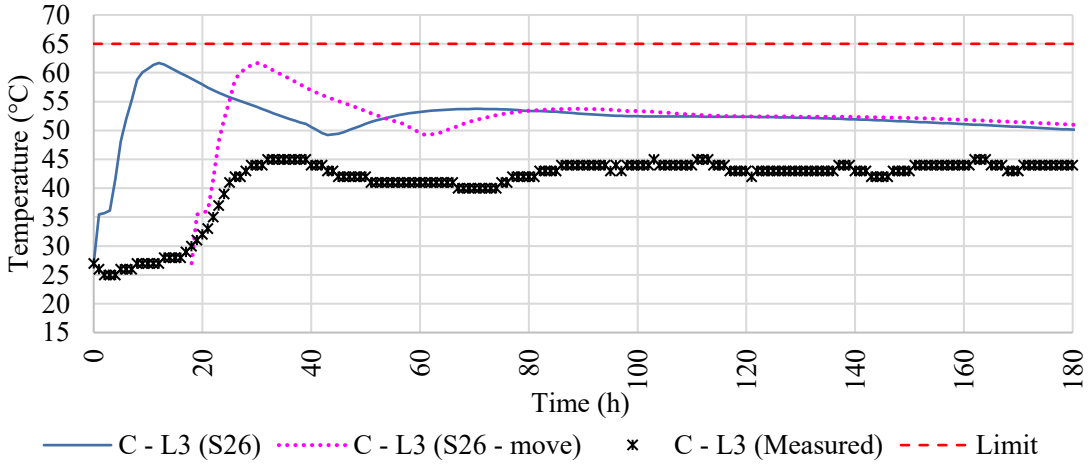

a) Layer L3

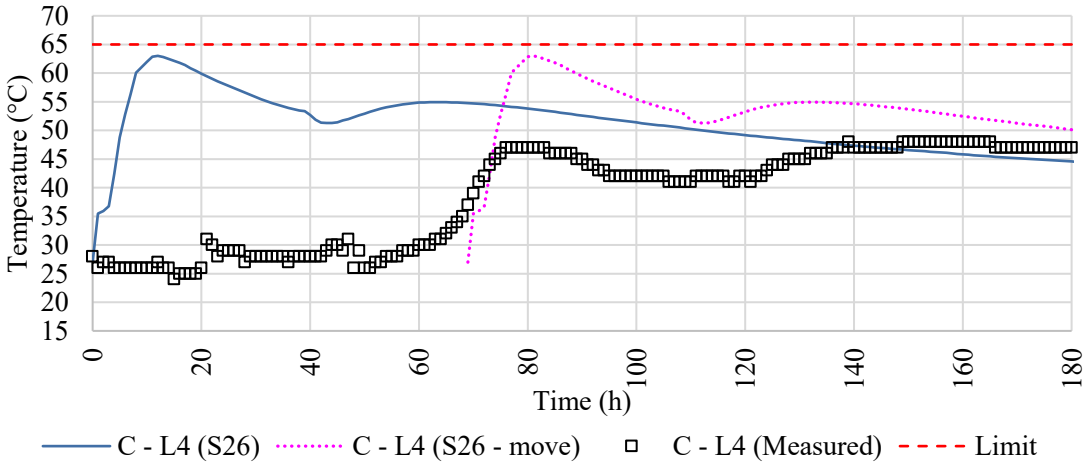

b) Layer L4

Source: Author (2022).

Figure 81 – Comparison between the field monitoring data from raft foundation and the S26 computer simulation results obtained in b4cast for point D at layers L3 (a) e L4 (b)

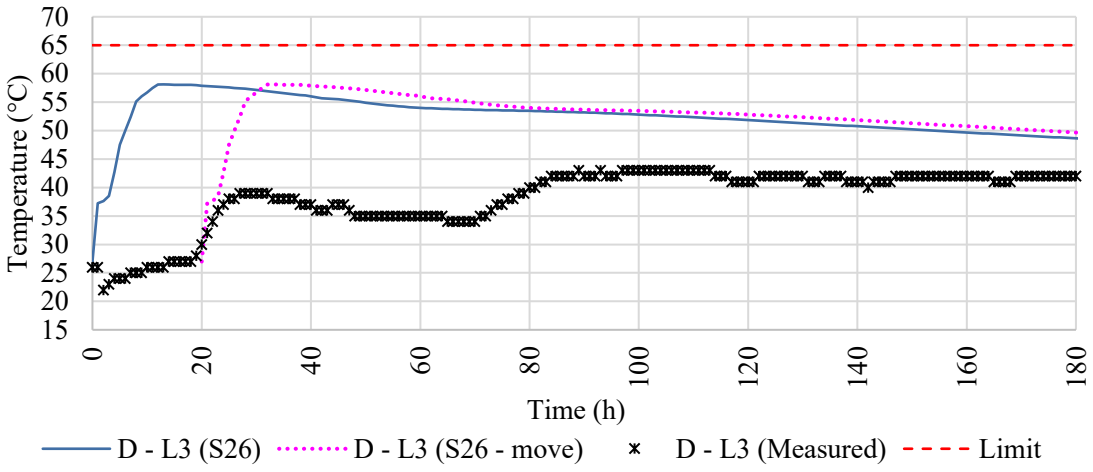

a) Layer L3

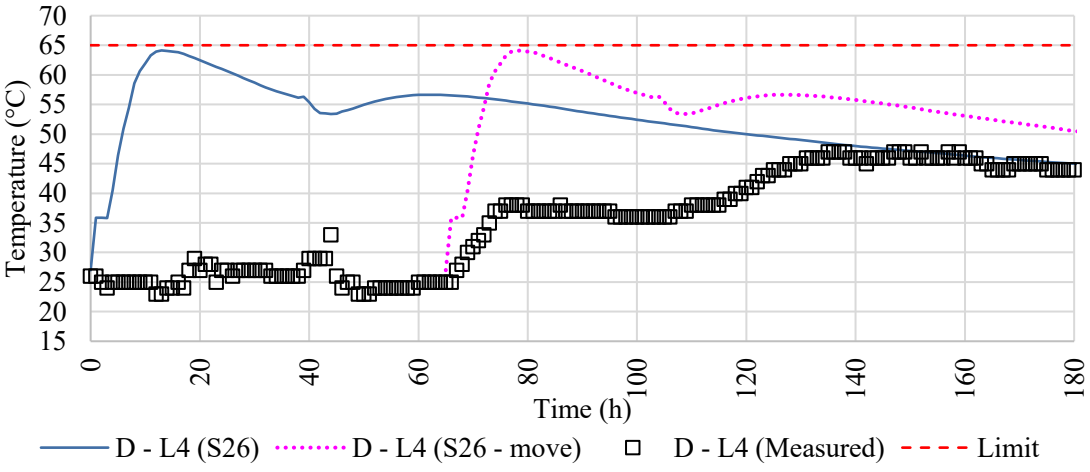

b) Layer L4

Source: Author (2022).

Figure 82 – Comparison between the field monitoring data from raft foundation and the S26 computer simulation results obtained in b4cast for point E at layers L3 (a) e L4 (b)

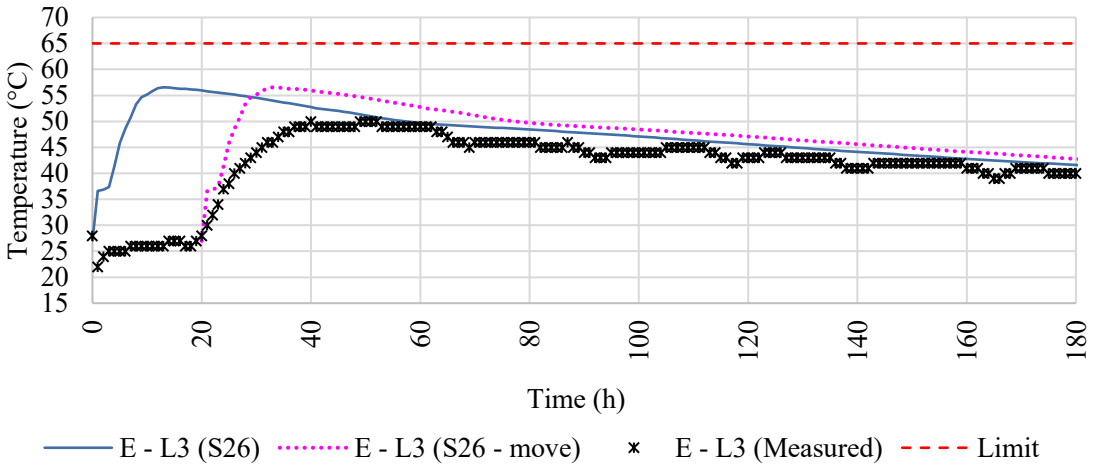

a) Layer L3

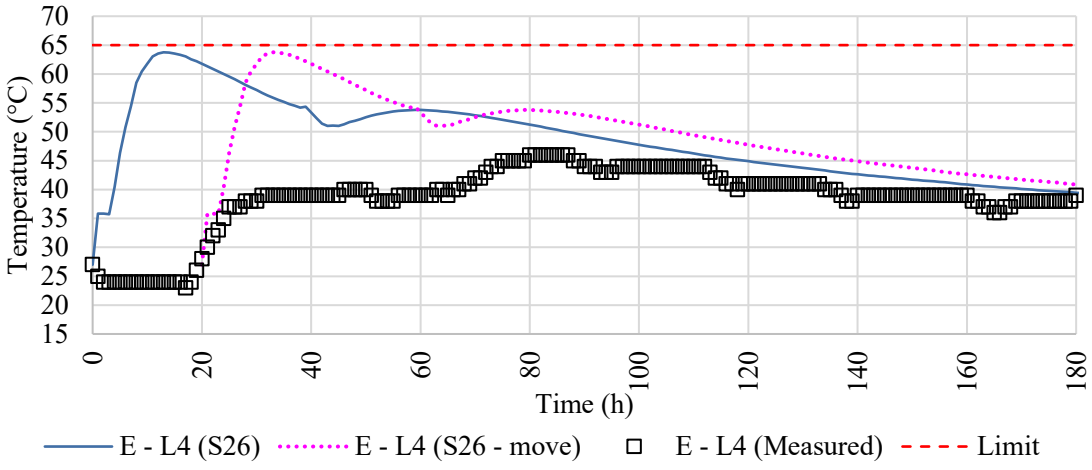

b) Layer L4

Source: Author (2022).

Finally, a study was conducted comparing the differences between the maximum temperatures of the data measured in the field and the S26 simulation, performed according to the implemented casting process. Table 23 presents the results.

Table 23 –Differences between maximum temperatures reached in simulation S26 and in field monitoring (Simulation S26 – Field Monitoring)

Layer	**Point**				
	A	**B**	**C**	**D**	**E**
L1	12.67 ºC	-	-	-	-
L2	14.47 ºC	14.52 ºC	-	-	-
L3	18.68 ºC	18.73 ºC	16.69 ºC	15.12 ºC	6.56 ºC
L4	13.08 ºC	-	15.01 ºC	17.13 ºC	17.76 ºC
L5	-	14.12 ºC	-	-	-

Source: Author (2022).

According to Table 23, it is possible to see that, for points A, B, and C, the highest differences were found in layer L3. Moreover, regarding this layer, according to the field monitoring data presented in Figures 78 to 82, it can also be seen that this layer was one of those with the lowest temperature rise over time, against what was expected for it, which is located in the core of the structure, where a greater possibility of internal heating is expected. The lower heating of this layer occurred because of the longer time interval (86h) between the casting of layer L2 and layer L3, i.e., when layer L3 was cast, L2 was already cooler, thus

generating little impact on the internal heating of layer L3. Regarding the major differences found between field measurement data and computer simulation results, especially for this layer, the use of literature parameters (such as material properties) and climate predictions in the simulations did not perfectly represent the reality experienced in the field.

Regarding points D and E, the largest differences were found in layer L4. This was expected because points D and E are inserted in the part where there was an interruption of the casting and, thus, layer L4, at these locations, has the biggest thickness (0.90 m) and presented the highest heating. As the computational results were higher than those measured in the field at all points throughout the analysis time, the biggest differences identified between these data would be exactly at the points with the highest heating.

4.6 Final comments

This chapter focused on conducting a case study, with the development of thermal behavior predictions in a finite element software for the definition of the casting methodology to be applied in a mass concrete foundation of a high-rise building. In addition, the application of this methodology and the instrumentation and monitoring of the internal temperatures of this structure were followed up. The comparison between data from field measurements and computer simulations was fundamental to analyzing the reliability of the predictive model used. The main conclusions regarding the results obtained were:

- to define the casting plan, it is essential to align it with the planning of the structure's construction company and, especially, with the concrete supply company to avoid losses and delays during the process;
- the increase in the time interval between the placing of each casting stage reduces the thermal rise experienced by the structure since when a layer is placed, the previous one is already undergoing a cooling process, which increases over time;
- attention is drawn to the influence caused by the casting of each new layer on the previously placed layers, which, even in the cooling process, showed temperature peaks at the time of the casting of the adjacent layers.
- the importance of following up on the casting and monitoring of the structure is emphasized due to the occurrence of unexpected events that may require the adaptation of prediction models to evaluate the probability of risks to the structure and, thus, facilitate decision-

making during critical periods in the casting;

- the reliability of the prediction model used was confirmed since the field results presented internal temperatures lower than the computational results. Despite this being in the benefit of safety, a large difference was observed especially between the results of maximum temperatures, whose simulations results exceeded by almost 19 °C the maximum temperature obtained in the field at certain points;
- there was a divergence between the time to reach maximum temperatures in the field data and the simulation, highlighting the need to consider the influence of the admixtures used in the mix design on the results of the cement hydration heat.
- these divergences between the values of the maximum temperatures demonstrate the need to use input parameters that effectively characterize the materials and the boundary conditions that will be applied in the field.
- in the absence of tests to obtain these parameters, it is recommended to develop prototypes using the same materials and applying the same boundary conditions to bring the computational models closer to the real situation that will be experienced during the casting process;
- among the main challenges and care during the study of thermal behavior and subsequent monitoring of mass concrete structures, it is worth mentioning the execution of tests to characterize the thermal properties of materials and the monitoring of climatic conditions at the site of the structure's construction, the care taken during the installation of thermocouples due to the fragility of this equipment and, especially, during casting so as not to break them, the protection of temperature monitors to avoid damage during readings and the monitoring and tracking of casting to assist in adapting the computer models when necessary during the process.

Based on the case study and field experience, a casting plan was developed with the presentation of a checklist to assist in the process of predicting the thermal behavior of mass concrete structures and a template with the main results to guide the casting process. This document is presented in Appendix C.

5 FINAL CONSIDERATIONS AND SUGGESTION FOR FUTURE RESEARCH

This research had as main objective to contribute to the evaluation of the predicted and the measured thermal behavior of mass concrete foundations. For this, the research included the analysis of thermal predictions in two different computational tools (one more widespread in consulting activities for thermal analysis of concrete and the other more restricted to Academia) and the development of parametric studies to approximate the simulations to the field measured results. It also described the development of a casting plan and monitoring strategy of a mass concrete structure with the follow-up of its application in the field.

The suggested process allowed for a better understanding of the thermal behavior of mass concrete structures, especially regarding the influence of some fundamental parameters to this type of study and the care and challenges found from the forecast development to the monitoring of the internal temperatures of these structural elements.

5.1 Summary of conclusions

Chapter 2 focused on achieving specific objective 1 of this work by developing thermal analyses of a wind turbine concrete foundation in two software packages: Ansys and b4cast. The main difference between the results obtained by them was concerning the time of reaching the maximum internal temperatures of the structure. In Ansys, the temperature peaks occurred near the end of the analysis, showing a more divergent relation to the measurements made in the field. About the maximum temperature values, b4cast presented higher values in almost all the analyses performed, being closer to the maximum values found in the field. The highest differences between the temperature values reached by the two software were at points closer to the outside, showing a divergence between the heat exchange of the structure and the environment, which deserves to be investigated.

Although the results were superior in b4cast, a convergence in the definition of the ideal placing temperatures for the structure and in the curves trend of the thermal behavior of the structure over time was observed between the two software. Finally, it is highlighted that the parameters used in the computational models developed in this chapter did not accurately characterize the real structure. This occurs because the maximum temperature values obtained in the computational predictions, one of the main requirements to avoid the emergence of DEF, were lower than the values reached by the structure in the field.

Thus, a new study was done, described in Chapter 3, analyzing the same foundation structure to evaluate the influence of certain parameters on thermal behavior and looking for an approximation between the computational models developed and the measurement data. This Chapter focused on achieving the specific objective 2 of this work. The variation in the thermal properties of concrete can generate differences in the results of the internal temperatures reached by the structure. Of the two properties studied, thermal conductivity coefficient and specific heat, the variation of the latter generated a significant influence on the results. This caused an approximation of the predictive model with the field monitoring data, especially concerning the maximum temperatures reached.

The study of the division of the casting in layers showed a difference of less than 1 ºC in the results. This small difference was due to the short interval applied between the placement of the layers. Although this influence was not considered so significant in this case, it is important to emphasize the importance of implementing this configuration so that the simulation is as close as possible to the reality of the construction site. The last part of this Chapter analyzed the variation of climatic conditions (environment temperature and wind speed) over time. It did not show a significant influence on the simulated results due to the low range of variation of the implemented data, emphasizing the importance of studying other factors, such as heat exchange by radiation.

Chapter 4 focused on the achievement of specific objective 3 by performing a case study on a high-rise building foundation. It is important to highlight the importance of the alignment between the construction company and the concrete supply company to better define and control the casting plan of a mass concrete structure. It was proven that the temperature rise of the structure reduces as the time interval applied between the placing of each concrete layer increases. Furthermore, it is emphasized the influence caused by the placement of a new layer in the increase of the internal temperatures of previously placed layers. The importance of following up on the casting process and monitoring the structure in the field was proven due to the occurrence of unpredictable situations that can change the thermal behavior predicted.

The main challenges and care during the study of thermal behavior and subsequent monitoring of mass concrete structures observed were the tests to obtain all the properties, the care in the installation of thermocouples and during casting to avoid the breakage of these types of equipment, and the care with the data acquisitors to avoid damage and, consequently, reading errors.

Regarding the reliability of computer models developed for high-rise building foundations, the results of the temperature predictions were higher than the results of the field

monitoring, showing that the computational model developed with some improvements identified in the previous chapters was in favor of safety. Although this is something positive, the differences identified between simulated and field measured data could be minimized with the use of more realistic material properties (that should be measured for the investigated material) and boundary conditions, thus contributing to a possible reduction of costs related to the concrete casting process (with the use of lower ice content in the mix design, for example) and to increase the reliability of the predictive models.

In general, the oscillations in internal temperatures identified in field measurements were not observed in the simulations performed, due to the small amplitude identified in the implemented climate parameters and to not considering heat exchange by radiation in the computational analyses.

Finally, in the raft foundation analysis, a divergence was observed concerning the time to reach the maximum temperatures that may have been caused by the influence of admixtures in the mix design, which was not considered in the test to obtain the cement heat curve.

5.2 Future research suggestions

This work was also useful to identify the need for the development of new complementary studies to improve the understanding of the thermal behavior of mass concrete structures. Then, suggestions are given next for future research.

As a result of the Covid-19 pandemic, some activities initially under the planned scope of this work were not carried out, including the development of laboratory tests to obtain material properties. Thus, a new case study is recommended, applying the actual data of the material properties that will be used in the construction of the structure, as well as the correct boundary conditions.

Furthermore, it is recommended to do another case study applying a previous optimization of the prediction models developed from the building of smaller-scale prototypes with the same materials and boundary conditions that will be applied in the construction of the actual structure. The prototypes should be monitored, and the data obtained compared with the preliminary simulations, further validating the models in a more controlled environment. Then, if the need is verified, the computer models can be adapted to present greater reliability in their results.

The heat exchange between the structure and the environment by radiation (cyclic solar radiation occurs in the investigated foundations) was not considered in the analyses performed. Thus, further studies are recommended to evaluate the influence of this condition on the thermal behavior of mass concrete structures.

A research on the boundary conditions is suggested to address this late peak of temperature obtained in Ansys.

Finally, as divergences were verified in the time to reach the maximum temperatures between the field measured data and the computer simulations, a study is recommended regarding the influence of the types and contents of additives that can be used in the concrete mixes on the thermal behavior of these structures.

REFERENCES

ABEEÓLICA – ASSOCIAÇÃO BRASILEIRA DE ENERGIA EÓLICA. Energia Eólica**:** os bons ventos do brasil. **Infovento 25.** Brasil, 18 mar. 2022. Disponível em: https://abeeolica.org.br/wp-content/uploads/2022/04/2022_03_InfoVento25.pdf. Acesso em: 15 ago. 2022.

ABEEÓLICA – ASSOCIAÇÃO BRASILEIRA DE ENERGIA EÓLICA. Energia Eólica**:** os bons ventos do brasil. **Infovento 27.** Brasil, 12 set. 2022. Disponível em: https://abeeolica.org.br/wp-content/uploads/2022/09/2022_09_InfoVento27.pdf. Acesso em: 31 out. 2022.

ABNT – ASSOCIAÇÃO BRASILEIRA DE NORMAS TÉCNICAS. **NBR 12817:** Concreto endurecido — Determinação do calor específico — Método de ensaio. Rio de Janeiro, 2012.

ABNT – ASSOCIAÇÃO BRASILEIRA DE NORMAS TÉCNICAS. **NBR 12818**: Concreto — Determinação da difusividade térmica — Método de ensaio. Rio de Janeiro, 2012.

ABNT – ASSOCIAÇÃO BRASILEIRA DE NORMAS TÉCNICAS. **NBR 12820:** Concreto endurecido — Determinação da condutividade térmica — Método de ensaio. Rio de Janeiro, 2012.

ABNT – ASSOCIAÇÃO BRASILEIRA DE NORMAS TÉCNICAS. **NBR 5738:** Concreto — Procedimento para moldagem e cura de corpos de prova. Rio de Janeiro, 2016.

ABNT – ASSOCIAÇÃO BRASILEIRA DE NORMAS TÉCNICAS. **NBR 16697:** Cimento Portland - Requisitos. Rio de Janeiro, 2018.

ABNT – ASSOCIAÇÃO BRASILEIRA DE NORMAS TÉCNICAS. **NBR 12006:** Cimento - Determinação do calor de hidratação pelo método de garrafa de Langavant - Método de ensaio. Rio de Janeiro, 1990.

ACI – AMERICAN CONCRETE INSTITUTE. **ACI 207.1R:** Guide to Mass Concrete. ACI Committee 207, p. 1-30, Farmington Hills, MI, 2006.

ACI – AMERICAN CONCRETE INSTITUTE. **ACI 207.2R:** Report on Thermal and Volume Change Effects on Cracking of Mass Concrete. ACI Committee 207, p. 1-32, Farmington Hills, MI, 2007.

ACI – AMERICAN CONCRETE INSTITUTE. **ACI 301:** Specifications for Structural Concrete. ACI Committee 301, p. 1-81, Farmington Hills, MI, 2010.

ASTM – AMERICAN SOCIETY FOR TESTING AND MATERIALS. **ASTM C150:** Standard Specification for Portland Cement. West Conshohocken, Pennsylvania, 2012.

ASTM – AMERICAN SOCIETY FOR TESTING AND MATERIALS. **ASTM C1702**: Standard Test Method for Measurement of Heat of Hydration of Hydraulic Cementitious Materials Using Isothermal Conduction Calorimetry. Philadelphia, 2017.

AMIN, M. N.; KIM, J.; LEE, Y.; KIM, J. Simulation of the thermal stress in mass concrete using a thermal stress measuring device. **Cement and Concrete Research**, Oxford, v. 9, n. 3, p. 154-164, mar. 2009. Elsevier BV. DOI: http://dx.doi.org/10.1016/j.cemconres.2008.12.008. Disponível em: https://www.sciencedirect.com/science/article/pii/S0008884608002378?via%3Dihub. Acesso em: 31 ago 2019.

ANISKIN, N.; NGUYEN, T. C. Influence factors on the temperature field in a mass concrete. **E3S Web of Conferences**, vol. 97, 2019. DOI: https://doi.org/10.1051/e3sconf/20199705021. Disponível em: https://www.e3s-conferences.org/articles/e3sconf/pdf/2019/23/e3sconf_form2018_05021.pdf. Acesso em: 20 jan 2022.

ANISKIN, N.; NGUYEN, T. C. Evaluation of thermal cracks in mass concrete structures during construction. Iop Conference Series: **Materials Science and Engineering**, [S.L.], v. 869, p. 072028, 10 jul. 2020. IOP Publishing. DOI: http://dx.doi.org/10.1088/1757-899x/869/7/072028. Disponível em: https://iopscience.iop.org/article/10.1088/1757-899X/869/7/072028/meta. Acesso em: 15 jun 2021.

ANTONIAZZI, J. P.; MOHAMAD, G.; CASALI, J. M. Influence of cement type, air-entrained admixture and hydration stabilizing admixture on mortars' setting time. **Revista Ibracon de Estruturas e Materiais**, [S.L.], v. 14, n. 1, p. 1-11, 2021. FapUNIFESP (SciELO). DOI: http://dx.doi.org/10.1590/s1983-41952021000100014. Disponível em: https://www.scielo.br/j/riem/a/jBzN5zvwvTVkvRxgTSrSjGB/#:~:text=Ready%20mix%20mortar%20is%20a,greater%20workability%20to%20the%20mixture. Acesso em: 20 mar 2022.

AZENHA, M. A. D. **Numerical simulation of the structural behaviour of concrete since its early ages**. 2009. 379 f. Tese (Doutorado) - Faculdade de Engenharia, Universidade do Porto, Porto, 2009. Cap. 8. Disponível em: https://repositorio-aberto.up.pt/ . Acesso em: 25 jun 2021.

AZENHA, M.; KANAVARIS, F.; SCHLICKE, D.; JE˛DRZEJEWSKA, A.; BENBOUDJEMA, F.; HONORIO, T.; S˘MILAUER, V.; SERRA, C.; FORTH, J.; RIDING, K.; KHADKA, B.; SOUSA, C.; BRIFFAUT, M.; LACARRIÈRE, L.; KOENDERS, E.; KANSTAD, T.; KLAUSEN, A.; TORRENTI, J. M.; FAIRBAIRN, E. M. R. Recommendations of RILEM TC 287-CCS: Thermo-Chemo-Mechanical Modelling of Massive Concrete Structures towards Cracking Risk Assessment. **Materials and Structures**, vol. 54, no 4, agosto de 2021, p. 135. DOI: https://doi.org/10.1617/s11527-021-01732-8. Disponível em: https://link.springer.com/article/10.1617/s11527-021-01732-8. Acesso em: 15 ago 2022.

B4CAST. (Versão 7.08) [Software]. Allerød, Denmark: ConTech Analysis ApS. 2022.

BAMFORTH, P. B. **Early-age thermal crack control in concrete**. London: Ciria Guide C660, 2007. 113 p. (978-8-86107-660-2).

BEAUDOIN, J.; ODLER, I. Hydration, Setting and Hardening of Portland Cement. **Lea's Chemistry of Cement and Concrete**, [s.l.], p. 157-250, 2019. Elsevier. DOI: http://dx.doi.org/10.1016/b978-0-08-100773-0.00005-8. Acesso em: 28 nov 2020.

BOBKO, C. P.; EDWARDS, A. J.; SERACINO, R.; ZIA, P. Thermal Cracking of Mass Concrete Bridge Footings in Coastal Environments. **Journal Of Performance of Constructed Facilities**, [s.l.], v. 29, n. 6, dez. 2015. American Society of Civil Engineers (ASCE). DOI: http://dx.doi.org/10.1061/(asce)cf.1943-5509.0000664. Disponível em: https://ascelibrary.org/doi/10.1061/%28ASCE%29CF.1943-5509.0000664. Acesso em: 31 ago 2019.

BOFANG, Z. Introduction. **Thermal Stresses And Temperature Control Of Mass Concrete**, [s.l.], p. 1-10, 2014. Elsevier. DOI: http://dx.doi.org/10.1016/b978-0-12-407723-2.00001-4. Disponível em: https://www.sciencedirect.com/science/article/abs/pii/B9780124077232000014?via%3Dihub. Acesso em: 21 set 2019.

BOURCHY, A.; BARNES, L.; BESSETTE, L.; TORRENTI, J. M. Effect of the Cement Composition on the Temperature and Strength Rising at Early Age. **High Tech Concrete: Where Technology and Engineering Meet**, organizado por D.A. Hordijk e M. Luković, Springer International Publishing, 2018, p. 100–08. DOI: https://doi.org/10.1007/978-3-319-59471-2_13. Disponível em: https://www.researchgate.net/publication/322168224_Effect_of_the_Cement_Composition_on_the_Temperature_and_Strength_Rising_at_Early_Age. Acesso em: 10 jan 2020.

BRAZILIAN GOVERNMENT. **Energia eólica registra primeiro recorde de geração instantânea de 2022**. 2022. Disponível em: https://www.gov.br/pt-br/noticias/energia-minerais-e-combustiveis/2022/08/energia-eolica-registra-primeiro-recorde-de-geracao-instantanea-de-2022. Acesso em: 01 ago 2022.

BREUGEL, K. Prediction of temperature development in hardening concrete. In: Prevention of thermal cracking in concrete at early ages. Report 15, R. Springenschmid, E & FN SPON, 1998. Disponível em: https://www.taylorfrancis.com/chapters/mono/10.1201/9781482271812-11/prediction-temperature-development-hardening-concrete-springenschmid. Acesso em: 10 jan 2020.

CABRAL, A. E. B.; MACHADO, A. M. L.; BABADOPULOS, L. F. A. L. Aspectos de análise termomecânica e de rigidez de concretos para torres eólicas. **CONCRETO & Construções**, vol. XLVIII, no. 98, p. 47–57, 2020. DOI: https://doi.org/10.4322/1809-7197.2020.98.0004. Disponível em: https://ibracon.org.br/site_revista/concreto_construcoes/pdfs/edicao98/4_aspecto_analise.pdf. Acesso em: 01 nov 2020.

CAPASSO, M. M.; PEQUENO, R. A falência seletiva do Plano Diretor de Fortaleza. **Cadernos Metrópole**, [S.L.], v. 23, n. 51, p. 763-786, ago. 2021. FapUNIFESP

(SciELO). DOI: http://dx.doi.org/10.1590/2236-9996.2021-5114. Disponível em: https://www.scielo.br/j/cm/a/zTPXFZXzDpT35nfnJGKw5ss/. Acesso em: 15 mar 2022.

CARINO, N. J.; LEW, H. S.. The Maturity Method: from theory to application. **Structures 2001**, [s.l.], 18 maio 2001. American Society of Civil Engineers (ASCE). DOI: http://dx.doi.org/10.1061/40558(2001)17. Disponível em: https://ascelibrary.org/doi/abs/10.1061/40558%282001%2917. Acesso em: 15 mar 2022.

CHOKTAWEEKARN, P.; TANGTERMSIRIKUL, S. Effect of aggregate type, casting, thickness and curing condition on restrained strain of mass concrete. **Songklanakarin Journal of Science & Technology**, v. 32, n. 4, 2010. Disponível em: https://www.researchgate.net/publication/286890160_Effect_of_aggregate_type_casting_thickness_and_curing_condition_on_restrained_strain_of_mass_concrete. Acesso em: 03 fev 2019.

COELHO, N. A. **Um estudo numérico do efeito térmico em concreto massa**. 2012. Dissertação (Mestrado em Estruturas e Construção Civil) – Faculdade de Tecnologia, Universidade de Brasília. Brasília, 2012. Disponível em: http://repositorio.unb.br/jspui/handle/10482/11251. Acesso em: 28 nov 2020.

COELHO, N. A.; PEDROSO, L. J.; RÊGO, J. H. .S.; NEPOMUCENO, A. A. Use of ANSYS for Thermal Analysis in Mass Concrete. **Journal of Civil Engineering and Architecture**, [s.l.], v. 8, n. 7, p. 860-868, 28 jul. 2014. David Publishing Company. DOI: http://dx.doi.org/10.17265/1934-7359/2014.07.007. Disponível em: https://portais.univasf.edu.br/nupecc/menu-lateral/artigos/mef-1/use-of-ansys-for-thermal-analysis-in-mass-concrete.pdf. Acesso em: 03 fev 2019.

COELHO, N. A. **Métodos Analíticos e Numéricos para o Estudo dos Efeitos Termomecânicos no Concreto Massa Orientados às Barragens de Gravidade**. 275p. Tese (Doutorado em Estruturas e Construção civil) - Departamento de Engenharia Civil e Ambiental da Faculdade de Tecnologia da Universidade de Brasília – UnB. Brasília, 2016. Disponível em: http://icts.unb.br/jspui/handle/10482/22990. Acesso em: 05 mai 2020.

COLLEPARDI, M. A state-of-the-art review on delayed ettringite attack on concrete. **Cement and Concrete Composites**, [s.l.], v. 25, n. 4-5, p. 401-407, maio 2003. Elsevier BV. DOI: http://dx.doi.org/10.1016/s0958-9465(02)00080-x. Disponível em: https://www.sciencedirect.com/science/article/pii/S095894650200080X. Acesso em: 23 jul 2020.

COUTO, D. A. **Considerações sobre a temperatura em elementos de fundação em concreto de grandes dimensões**. 2018. 145 f. Dissertação (Mestrado) − Curso de Faculdade de Engenharia Civil, Arquitetura e Urbanismo, Universidade Estadual de Campinas, Campinas, 2018. Disponível em: https://www.phd.eng.br/wp-content/uploads/2018/11/18.10.01-Disserta%C3%A7%C3%A3o_DOUGLAS-COUTO_REVISADO-Final-Arial-R02.pdf. Acesso em: 02 set 2019.

COUNCIL ON TALL BUILDINGS AND URBAN HABITAT (org.). **Brazil**. Estados Unidos da América, 2022. Disponível em: https://www.skyscrapercenter.com/country/brazil. Acesso em: 30 ago. 2022.

DELAGE, P. On the thermal impact on the excavation damaged zone around deep radioactive waste disposal. **Journal Of Rock Mechanics And Geotechnical Engineering**, [S.L.], v. 5, n. 3, p. 179-190, jun. 2013. Elsevier BV. DOI: http://dx.doi.org/10.1016/j.jrmge.2013.04.002. Disponível em: https://www.sciencedirect.com/science/article/pii/S1674775513000346. Acesso em: 05 mar 2020.

EMBORG, M.; BERNANDER, S. Assessment of Risk of Thermal Cracking in Hardening Concrete. **Journal of Structural Engineering**, [s.l.], v. 120, n. 10, p. 2893-2912, out. 1994. American Society of Civil Engineers (ASCE). DOI: http://dx.doi.org/10.1061/(asce)0733-9445(1994)120:10(2893). Disponível em: https://ascelibrary.org/doi/10.1061/%28ASCE%290733-9445%281994%29120%3A10%282893%29. Acesso em: 01 nov 2020.

FORSBERG, C. H. Introduction to heat transfer. **Heat Transfer Principles and Applications**, [s.l.], p. 1-21, 2021a. Elsevier. DOI: http://dx.doi.org/10.1016/b978-0-12-802296-2.00001-9.

FORSBERG, C. H. Numerical methods (steady and unsteady). **Heat Transfer Principles and Applications**, [s.l.], p. 163-210, 2021b. Elsevier. http://dx.doi.org/10.1016/b978-0-12-802296-2.00005-6. Disponível em: https://www.sciencedirect.com/book/9780128022962/heat-transfer-principles-and-applications. Acesso em: 10 jan 2022.

FUNAHASHI JUNIOR, E. I.; KUPERMAN, S. C.; VICENTE, G. R.; FORNI, E. S.; LIMA, E. C. Simulação de tensões térmicas da sala de radioterapia do Hospital das Clínicas de Ribeirão Preto-SP. **Anais do 52º Congresso Brasileiro do Concreto.** Fortaleza, out. 2010. Disponível em: https://www.desek.com.br/_files/ugd/c893e0_f4ac604ed03045f59d9455384dae4d0b.pdf. Acesso em: 05 set 2022.

FUNAHASHI JUNIOR, E. I.; GAMBALE, P. G. Controle da temperatura do concreto massa de elevada resistência. **Anais do 5° Congresso Brasileiro de Patologia das Construções.** Gramado, ago. 2022. Disponível em: https://www.desek.com.br/_files/ugd/8537ca_e4e46072b86449a3980e1a960b21dd52.pdf. Acesso em: 05 set 2022.

GAMBALE, P. G. **Estudo do calor de hidratação do concreto massa e contribuição ao cálculo térmico e à previsão de fissuras de retração**. 2017. 132 f. Dissertação (Mestrado) - Curso de Mestrado em Engenharia Civil, Programa de Pós-Graduação em Geotecnia, Estruturas e Construção Civil, Universidade Federal de Goiás, Goiânia, 2017. Disponível em: https://repositorio.bc.ufg.br/tede/items/a88b4df9-5f20-415f-af18-f3783b46087e. Acesso em: 23 jul 2020.

GONÇALVES, L. F. **Avaliação de propriedades térmicas do concreto com cinza volante em fundação de aerogeradores**. 2018. 85 f. Dissertação (Mestrado) - Curso de Mestrado em Engenharia Civil: Construção Civil, Departamento de Engenharia Estrutural e Construção Civil, Universidade Federal do Ceará, Fortaleza, 2018. Disponível em: https://repositorio.ufc.br/handle/riufc/37964. Acesso em: 02 set 2019.

GWEC – GLOBAL WIND ENERGY CONCIL. **Global Wind Report 2022**. Belgium, 2022. Disponível em: https://gwec.net/global-wind-report-2022/. Acesso em: 20 out 2022.

HA, J.; JUNG, Y.; CHO, Y. Thermal crack control in mass concrete structure using an automated curing system. **Automation in Construction**, [s.l.], v. 45, p. 16-24, set. 2014. Elsevier BV. DOI: http://dx.doi.org/10.1016/j.autcon.2014.04.014. Disponível em: https://www.sciencedirect.com/science/article/pii/S0926580514001095. Acesso em: 01 nov 2020.

HASPARYK, N. P.; KUPERMAN, S. C.; TORRES, J. R. Combined attack from AAR and DEF in the foundation blocks of a building. **15Th International Conference On Alkali-Aggregate Reaction.** São Paulo, jul. 2016. Disponível em: https://icaarconcrete.org/wp-content/uploads/2020/11/15ICAAR-HasparykNP-3.pdf. Acesso em: 02 set 2019.

HONORIO, T.; BARY, B.; BENBOUDJEMA, F. Thermal properties of cement-based materials: Multiscale estimations at early-age. **Cement and Concrete Composites**, [s. l.], n. 87, p. 205-2019, 2018. DOI: https://doi.org/10.1016/j.cemconcomp.2018.01.003. Disponível em: https://www.sciencedirect.com/science/article/pii/S0958946516305200. Acesso em: 19 fev 2021.

HUANG, Yonghui; LIU, Guoxing; HUANG, Shiping; RAO, Rui; HU, Changfu. Experimental and finite element investigations on the temperature field of a massive bridge pier caused by the hydration heat of concrete. **Construction And Building Materials**, [s.l.], v. 192, p. 240-252, dez. 2018. Elsevier BV. DOI: http://dx.doi.org/10.1016/j.conbuildmat.2018.10.128. Disponível em: https://www.sciencedirect.com/science/article/pii/S0950061818325182. Acesso em: 28 nov 2020.

INCROPERA, F. P.; DeWITT, D. P.; BERGMAN, T. L.; LAVINE, A. S. **Fundamentos da transferência de calor e de Massa**. 6ª ed. Tradução e Revisão de Eduardo M. Queiroz e Fernando Luiz P. Pessoa. Ed. LTC. Rio de Janeiro, 2008.

JU, Y.; LEI, H. Actual Temperature Evolution of Thick Raft Concrete Foundations and Cracking Risk Analysis. **Advances In Materials Science And Engineering**, [s.l.], v. 2019, p. 1-11, 21 jan. 2019. Hindawi Limited. DOI: http://dx.doi.org/10.1155/2019/7029671. Disponível em: https://www.researchgate.net/publication/330538319_Actual_Temperature_Evolution_of_Thick_Raft_Concrete_Foundations_and_Cracking_Risk_Analysis. Acesso em: 18 fev 2021.

KIM, S. G. Effect of heat generation from cement hydration on mass concrete placement. 125 p. Master Thesis. **Civil Engineering (Geothecnical Engineering)**, Master of Science. Iowa

State University, Ames, 2010. Disponível em: https://dr.lib.iastate.edu/entities/publication/dcbe959c-5524-4767-83ff-f5fdb2478174. Acesso em: 03 fev 2019.

KIM, K.; JEON, S.; KIM, J.; YANG, S. An experimental study on thermal conductivity of concrete. **Cement and Concrete Research**, [s.l.], v. 33, n. 3, p. 363-371, mar. 2003. Elsevier BV. DOI: http://dx.doi.org/10.1016/s0008-8846(02)00965-1. Disponível em: https://www.sciencedirect.com/science/article/pii/S0008884602009651. Acesso em: 02 mai 2020.

LACARRIÈRE, L.; KNOPPIK, A.; SILVA, W. R. l.; HONORIO, T.; MILAUER, V.; ASAMOTO, S.; FAIRBAIRN, E. M. R. Hydration and Heat Development. **Thermal Cracking of Massive Concrete Structures**, [s.l.], p. 13-46, 24 maio 2018. Springer International Publishing. DOI: http://dx.doi.org/10.1007/978-3-319-76617-1_2. Disponível em: https://link.springer.com/book/10.1007/978-3-319-76617-1. Acesso em: 19 fev 2021.

LAGUNDŽIJA, S.; THIAM, M. **Temperature reduction during concrete hydration in massive structures**. 2017. 132 p. Dissertação (Mestrado) - Vetenskap Och Konst, Estolcomo, Suécia, 2017. Disponível em: https://kth.divaportal.org/smash/get/diva2:1116691/FULLTEXT01.pdf. Acesso em: 10 mai 2021.

LAROSCHE, C.J. Types and causes of cracking in concrete structures. **Failure, Distress and Repair of Concrete Structures**, [s.l.], p. 57-83, 2009. Elsevier. DOI: http://dx.doi.org/10.1533/9781845697037.1.57. Disponível em: https://www.sciencedirect.com/science/article/abs/pii/B9781845694081500038. Acesso em: 15 jan 2022.

LEVENSPIEL, O. **Engineering flow and heat exchange**. 3. ed. Corvallis: Springer, 2014. 409 p. (978-1-4899-7454-9).

LMCC – LABORATÓRIO DE MATERIAIS DE CONSTRUÇÃO CIVIL. **Dosagem de concreto para Parque Eólico**: relatório técnico. Universidade Federal do Ceará. Fortaleza, 2019.

LMCC – LABORATÓRIO DE MATERIAIS DE CONSTRUÇÃO CIVIL. **Estudo térmico da concretagem do radier do Acqualina Condomínio**: relatório técnico. Universidade Federal do Ceará. Fortaleza, 2021.

MEHTA, P. K.; MONTEIRO, P. J. M. **Concreto: Estrutura, Propriedades e Materiais.** 2a ed. São Paulo: IBRACON, 2014.

NGUYEN, T.; TANG, V.; HUYNH, T. An Early-age Evaluation of Thermal Cracking Index of Heavy Concrete Applying for Airport Pavement. **Periodica Polytechnica Civil Engineering**, [s.l.], 2 mar. 2020. Periodica Polytechnica Budapest University of Technology and Economics. DOI: http://dx.doi.org/10.3311/ppci.13731. Disponível em: https://pp.bme.hu/ci/article/view/13731. Acesso em: 06 jul 2021.

NGUYEN, T. C.; BUI, A. K.; HOANG, Q. L. Thermal Cracks in Concrete Structure—The Basic Issues to Be Understood. **Lecture Notes In Civil Engineering**, [S.L.], p. 229-240, 2021. Springer Singapore. DOI: http://dx.doi.org/10.1007/978-981-16-0945-9_19. Disponível em: https://www.researchgate.net/publication/352289697_Thermal_Cracks_in_Concrete_Structure-The_Basic_Issues_to_Be_Understood. Acesso em: 23 mar 2022.

PATIL, H.; JEYAKARTHIKEYAN, P V. Mesh convergence study and estimation of discretization error of hub in clutch disc with integration of ANSYS. **Iop Conference Series**: Materials Science and Engineering, [s.l.], v. 402, p. 012065, 1 out. 2018. IOP Publishing. DOI: http://dx.doi.org/10.1088/1757-899x/402/1/012065. Disponível em: https://iopscience.iop.org/article/10.1088/1757-899X/402/1/012065. Acesso em: 29 out 2021.

PAULON, V. A. **Estudo Técnico - O fenômeno térmico no concreto.** Associação Brasileira de Cimento Portland (ABCP), São Paulo, jun. 1987, 48p. Disponível em: https://abcp.org.br/wp-content/uploads/2016/01/ET-85.pdf. Acesso em: 03 fev 2019.

PERRY, M.; FUSIEK, G.; NIEWCZAS, P.; RUBERT, T.; MCALORUM, J. Wireless Concrete Strength Monitoring of Wind Turbine Foundations. **Sensors**, [s.l.], v. 17, n. 12, p.2928-2950, 16 dez. 2017. MDPI AG. DOI: http://dx.doi.org/10.3390/s17122928. Disponível em: https://www.mdpi.com/1424-8220/17/12/2928. Acesso em: 19 fev 2021.

POULOS, H. G.. Tall building foundations: design methods and applications. **Innovative Infrastructure Solutions**, [S.L.], v. 1, n. 1, 13 jun. 2016. Springer Science and Business Media LLC. DOI: http://dx.doi.org/10.1007/s41062-016-0010-2. Disponível em: https://link.springer.com/article/10.1007/s41062-016-0010-2. Acesso em: 28 nov 2020.

RIDING, K. A. **Early Age Concrete Thermal Stress Measurement and Modeling**. 2007. 610 p. Tese (Doutorado), University Of Texas At Austin, Austin, 2007. Disponível em: https://repositories.lib.utexas.edu/items/724dc5cd-6251-4152-bda3-9391a60af151. Acesso em: 18 fev 2021.

ROSO, M.; OLIVEIRA, T. D. de; BEUTER, N. C. Por que verticalizar? Um estudo sobre o processo de verticalização nas cidades. **Research, Society And Development**, [S.L.], v. 10, n. 17, p. 1-10, 30 dez. 2021. Research, Society and Development. DOI: http://dx.doi.org/10.33448/rsd-v10i17.24737. Disponível em: https://rsdjournal.org/index.php/rsd/article/download/24737/21559/291413. Acesso em: 27 set 2022.

SABNIS, A.; PRANESH, M R. Sustainability Development Index (SDI) for high-rise buildings with concept of figure of merit. **International Journal of Research In Engineering And Technology.** Bangalore, India, 2016. Disponível em: https://www.researchgate.net/profile/Ajit-Sabnis/publication/310124226_SUSTAINABILITY_DEVELOPMENT_INDEX_SDI_FOR_HIGHRISE_BUILDINGS_WITH_CONCEPT_OF_FIGURE_OF_MERIT/links/5829462608

aecfd7b8c43b2f/SUSTAINABILITY-DEVELOPMENT-INDEX-SDI-FOR-HIGHRISE-BUILDINGS-WITH-CONCEPT-OF-FIGURE-OF-MERIT.pdf. Acesso em: 20 fev 2019.

SHAFIGH, P.; ASADI, I.; MAHYUDDIN, N. B. Concrete as a thermal mass material for building applications - A review. **Journal of Building Engineering**, [s.l.], v. 19, p. 14-25, set. 2018. Elsevier BV. DOI: http://dx.doi.org/10.1016/j.jobe.2018.04.021. Disponível em: https://www.sciencedirect.com/science/article/pii/S2352710218301992. Acesso em: 10 mai 2021.

SILVA, M. D. **Tipificação de fundações de torres eólicas em parques industriais, para diversos tipos de solos.** 136 p. Dissertação (Mestrado em Engenharia Civil) - Instituto Superior de Engenharia de Lisboa. Lisboa, 2014. Disponível em: https://repositorio.ipl.pt/handle/10400.21/4286. Acesso em: 15 jan 2022.

SFIKAS, I. P.; INGHAM, J.; BABER, J. Using finite-element analysis to assess the thermal behaviour of concrete structures**.** 2017. **The Concrete Society UK** (www.concrete.org.uk). Disponível em: https://www.researchgate.net/publication/313661324_Using_finite-element_analysis_to_assess_the_thermal_behaviour_of_concrete_structures. Acesso em: 11 maio 2020.

SFIKAS, I. P.; INGHAM, J.; BABER, J. Simulating thermal behaviour of concrete by FEA: state-of-the-art review. : state-of-the-art review. **Proceedings of the Institution of Civil Engineers - Construction Materials**, [s.l.], v. 171, n. 2, p. 59-71, abr. 2018. Thomas Telford Ltd.. DOI: http://dx.doi.org/10.1680/jcoma.15.00052. Disponível em: https://www.icevirtuallibrary.com/doi/full/10.1680/jcoma.15.00052. Acesso em: 28 nov 2020.

SMOLANA, A.; KLEMCZAK, B.; AZENHA, M.; SCHLICKE, D. Thermo-Mechanical Analysis of Mass Concrete Foundation Slabs at Early Age—Essential Aspects and Experiences from the FE Modelling. **Materials**, [S.L.], v. 15, n. 5, p. 1815, 28 fev. 2022. MDPI AG. DOI: http://dx.doi.org/10.3390/ma15051815. Disponível em: https://www.mdpi.com/1996-1944/15/5/1815. Acesso em: 10 set 2022.

TAHERSIMA, M.; TIKALSKY, P. Finite element modeling of hydration heat in a concrete slab-on-grade floor with limestone blended cement. **Construction And Building Materials**, [s.l.], v. 154, p. 44-50, nov. 2017. Elsevier BV. DOI: http://dx.doi.org/10.1016/j.conbuildmat.2017.07.176. Disponível em: https://www.sciencedirect.com/science/article/pii/S0950061817315180. Acesso em: 23 mar 2022.

TAYLOR, H. F. W.; FAMY, C; SCRIVENER, K. L. Delayed ettringite formation. **Cement and Concrete Research**, [s.l.], v. 31, n. 5, p. 683-693, maio 2001. Elsevier BV. DOI: http://dx.doi.org/10.1016/s0008-8846(01)00466-5. Disponível em: https://www.sciencedirect.com/science/article/pii/S0008884601004665. Acesso em: 02 mai 2020.

TANG, S.; HUANG, D.; HE, Z. A review of autogenous shrinkage models of concrete. **Journal Of Building Engineering**, [S.L.], v. 44, p. 103412, dez. 2021. Elsevier

BV. DOI: http://dx.doi.org/10.1016/j.jobe.2021.103412. Disponível em: https://www.sciencedirect.com/science/article/pii/S. Acesso em: 27 set 2022.

TEXAS DOT – TEXAS DEPARTMENT OF TRANSPORTATION. Item 420 - Concrete Substructures, 2014. Disponível em: https://ftp.txdot.gov/pub/txdot-info/cmd/cserve/specs/2014/standard/s420.pdf. Acesso em: 20 out 2020.

VIRGINIA DOT – VIRGINIA DEPARTMENT OF TRANSPORTATION. Road and Bridge Specifications, 2016. Disponível em: https://www.vdot.virginia.gov/media/vdotvirginiagov/doing-business/technical-guidance-and-support/technical-guidance-documents/construction/migrated-acc/VDOT_2016_RB_Specs_acc071522.pdf. Acesso em: 20 out 2020.

WU, S.; HUANG, D.; LIN, F.; ZHAO, H.; WANG, P. Estimation of cracking risk of concrete at early age based on thermal stress analysis. **Journal of Thermal Analysis and Calorimetry**, v. 105, n. 1, p. 171-186, 2011. DOI: https://doi.org/10.1007/s10973-011-1512-y. Disponível em: https://link.springer.com/article/10.1007/s10973-011-1512-y. Acesso em: 06 jul 2021.

THE WEATHER CHANNEL (org.). Disponível em: https://weather.com/. Acesso em: 30 ago. 2021.

WWEA - World Wind Energy Association. World Wind Energy Report 2009. In: **9th World Wind Energy Conference & Exhibition Large-scale Integration of Wind Power**. Istanbul, Turkey, 2010. Disponível em: http://large.stanford.edu/courses/2010/ph240/sleiter2/docs/worldwindenergyreport2009_s.pdf. Acesso em: 03 fev 2019.

ZHAO, Y.; LI, G.; FAN, C.; PANG, W.; WANG, Y. Effect of Thermal Parameters on Hydration Heat Temperature and Thermal Stress of Mass Concrete. **Advances In Materials Science And Engineering**, [S.L.], v. 2021, p. 1-16, 2 mar. 2021. Hindawi Limited. DOI: http://dx.doi.org/10.1155/2021/5541181. Disponível em: https://onlinelibrary.wiley.com/doi/10.1155/2021/5541181. Acesso em: 15 jan 2022.

APPENDIX

APPENDIX A - ENVIRONMENTAL TEMPERATURE AND WIND SPEED DATA IN THE CONSTRUCTION CITY OF THE WIND FARM OF FOUNDATION ANALYZED

The city data used in the simulations were obtained from the Weather website (2021), which shows the variation in hourly of temperatures and wind speeds.

Hour	Temperature (ºC)	Wind Speed (m/s)
6:00	28	5.56
7:00	29	6.94
8:00	30	7.78
9:00	31	8.61
10:00	32	8.89
11:00	32	9.17
12:00	32	9.17
13:00	32	9.72
14:00	32	9.44
15:00	31	9.17
16:00	30	8.33
17:00	29	7.50
18:00	28	6.67
19:00	28	6.11
20:00	28	5.83
21:00	28	5.83
22:00	28	6.11
23:00	28	6.11
0:00	28	6.39
1:00	28	6.39
2:00	28	6.11
3:00	28	6.11
4:00	28	5.83
5:00	28	5.83
6:00	28	5.56
7:00	29	6.94
8:00	30	7.78
9:00	31	8.61
10:00	32	8.89
11:00	32	9.17
12:00	32	9.17
13:00	32	9.17
14:00	32	8.89
15:00	31	8.61
16:00	31	8.06

17:00	30	7.22
18:00	29	6.39
19:00	28	5.83
20:00	28	5.83
21:00	28	5.83
22:00	28	6.11
23:00	28	6.11
0:00	28	6.11
1:00	28	6.11
2:00	28	6.11
3:00	28	5.83
4:00	28	5.83
5:00	28	5.83
6:00	28	5.56
7:00	29	6.67
8:00	30	7.78
9:00	31	8.33
10:00	32	8.61
11:00	32	8.89
12:00	32	8.89
13:00	32	9.17
14:00	32	8.89
15:00	31	8.61
16:00	31	8.06
17:00	30	7.22
18:00	29	6.39
19:00	28	5.83
20:00	28	5.83
21:00	28	5.83
22:00	28	6.11
23:00	28	6.11
0:00	28	6.11
1:00	28	6.11
2:00	28	6.11
3:00	28	5.83
4:00	28	5.83
5:00	28	5.83
6:00	28	5.56
7:00	29	6.94
8:00	30	7.78
9:00	31	8.61
10:00	32	8.89
11:00	32	9.17
12:00	32	9.17
13:00	32	9.72
14:00	32	9.44

15:00	31	9.17
16:00	30	8.33
17:00	29	7.50
18:00	28	6.67
19:00	28	6.11
20:00	28	5.83
21:00	28	5.83
22:00	28	6.11
23:00	28	6.11
0:00	28	6.39
1:00	28	6.39
2:00	28	6.11
3:00	28	6.11
4:00	28	5.83
5:00	28	5.83
6:00	28	5.56
7:00	29	6.94
8:00	30	7.78
9:00	31	8.61
10:00	32	8.89
11:00	32	9.17
12:00	32	9.17
13:00	32	9.17
14:00	32	8.89
15:00	31	8.61
16:00	31	8.06
17:00	30	7.22
18:00	29	6.39
19:00	28	5.83
20:00	28	5.83
21:00	28	5.83
22:00	28	6.11
23:00	28	6.11
0:00	28	6.11
1:00	28	6.11
2:00	28	6.11
3:00	28	5.83
4:00	28	5.83
5:00	28	5.83
6:00	28	5.56
7:00	29	6.67
8:00	30	7.78
9:00	31	8.33
10:00	32	8.61
11:00	32	8.89
12:00	32	8.89

13:00	32	9.17
14:00	32	8.89
15:00	31	8.61
16:00	31	8.06
17:00	30	7.22
18:00	29	6.39
19:00	28	5.83
20:00	28	5.83
21:00	28	5.83
22:00	28	6.11
23:00	28	6.11
0:00	28	6.11
1:00	28	6.11
2:00	28	6.11
3:00	28	5.83
4:00	28	5.83
5:00	28	5.83
6:00	28	5.56
7:00	29	6.94
8:00	30	7.78
9:00	31	8.61
10:00	32	8.89
11:00	32	9.17
12:00	32	9.17
13:00	32	9.72
14:00	32	9.44
15:00	31	9.17
16:00	30	8.33
17:00	29	7.50
18:00	28	6.67
19:00	28	6.11
20:00	28	5.83
21:00	28	5.83
22:00	28	6.11
23:00	28	6.11
0:00	28	6.39
1:00	28	6.39
2:00	28	6.11
3:00	28	6.11
4:00	28	5.83
5:00	28	5.83
6:00	28	5.56

APPENDIX B - ENVIRONMENTAL TEMPERATURE AND WIND SPEED DATA IN FORTALEZA, THE CITY OF CONSTRUCTION OF THE ACQUALINA BUILDING

The city data used in the simulations were obtained from the Weather website (2021), which shows the variation in hourly of temperatures and wind speeds.

Hour	Temperature (ºC)	Wind Speed (m/s)
27	0	6.11
28	1	7.5
30	2	8.61
31	3	8.89
32	4	9.17
32	5	8.89
32	6	8.61
31	7	8.33
30	8	8.06
29	9	7.22
28	10	6.94
27	11	6.39
27	12	6.11
27	13	6.11
27	14	6.39
27	15	6.39
27	16	6.94
27	17	7.5
27	18	7.5
27	19	7.5
26	20	7.5
26	21	6.94
26	22	6.39
25	23	5.83
26	24	6.11
28	25	7.5
29	26	8.61
30	27	8.89
31	28	9.17
32	29	8.89
32	30	8.61
31	31	8.33
29	32	8.06
29	33	7.22
28	34	6.94
27	35	6.11

27	36	5.83
27	37	5.56
27	38	5.56
27	39	5.83
27	40	6.11
27	41	6.39
27	42	6.67
27	43	6.67
27	44	6.67
26	45	6.39
26	46	5.83
26	47	5.28
27	48	5.56
28	49	6.94
30	50	8.33
31	51	8.89
32	52	9.17
32	53	9.17
32	54	8.89
31	55	8.33
30	56	8.06
29	57	7.22
28	58	6.67
27	59	6.39
27	60	6.11
27	61	6.11
27	62	6.39
27	63	6.39
27	64	6.94
27	65	7.5
27	66	7.5
27	67	7.5
27	68	7.5
26	69	6.94
26	70	6.39
26	71	5.83
27	72	6.11
28	73	7.5
30	74	8.61
31	75	8.89
32	76	9.17
32	77	8.89
32	78	8.61
31	79	8.33
30	80	8.06
29	81	7.22

28	82	6.94
27	83	6.39
27	84	6.11
27	85	6.11
27	86	6.39
27	87	6.39
27	88	6.94
27	89	7.5
27	90	7.5
27	91	7.5
26	92	7.5
26	93	6.94
26	94	6.39
25	95	5.83
26	96	6.11
28	97	7.5
29	98	8.61
30	99	8.89
31	100	9.17
32	101	8.89
32	102	8.61
31	103	8.33
29	104	8.06
29	105	7.22
28	106	6.94
27	107	6.11
27	108	5.83
27	109	5.56
27	110	5.56
27	111	5.83
27	112	6.11
27	113	6.39
27	114	6.67
27	115	6.67
27	116	6.67
26	117	6.39
26	118	5.83
26	119	5.28
27	120	5.56
28	121	6.94
30	122	8.33
31	123	8.89
32	124	9.17
32	125	9.17
32	126	8.89
31	127	8.33

30	128	8.06
29	129	7.22
28	130	6.67
27	131	6.39
27	132	6.11
27	133	6.11
27	134	6.39
27	135	6.39
27	136	6.94
27	137	7.5
27	138	7.5
27	139	7.5
27	140	7.5
26	141	6.94
26	142	6.39
26	143	5.83
27	144	6.11
28	145	7.5
30	146	8.61
31	147	8.89
32	148	9.17
32	149	8.89
32	150	8.61
31	151	8.33
30	152	8.06
29	153	7.22
28	154	6.94
27	155	6.39
27	156	6.11
27	157	6.11
27	158	6.39
27	159	6.39
27	160	6.94
27	161	7.5
27	162	7.5
27	163	7.5
26	164	7.5
26	165	6.94
26	166	6.39
25	167	5.83
26	168	6.11

APPENDIX C - CASTING PLAN TEMPLATE FOR MASS CONCRETE STRUCTURES

1) PRELIMINARY INFORMATION FOR THE DEVELOPMENT OF THE THERMAL ANALYSIS	
Checklist of information provided by the construction company	**Description**
○ Concrete mix design	○ Type of materials ○ Content
○ Thermo-physical properties of concrete	○ Density ○ Thermal conductivity ○ Specific heat ○ Coefficient of Thermal Expansion ○ Other
○ Cement heat of hydration curve	Has the influence of additives been considered? ○ Yes ○ No
○ Structure design	○ Floor plan ○ Sections
○ Site climate information	○ Environment temperature ○ Wind speed ○ Humidity ○ Solar radiation ○ Other
○ Boundary conditions	○ Type and thickness of the formwork ○ Estimated time for formwork removal ○ Type of concrete curing ○ Estimated curing time ○ Substrates in contact with the structure and (example: rock or soil below the concrete structure, other concrete structures, etc) ○ Properties and dimensions of theses substrates ○ Thickness of the concrete regularization layer
○ Additional Information	

2) RESULTS OF THE THERMAL ANALYSIS (CASTING PLAN)	
• Number of casting layers	
• Thickness of each layer	
• Layer casting interval	
• Curing time applied	
• Formwork removal time applied	
• Placing temperature of each layer	
• Content and temperature of the water in the concrete mix design	
• Ice content in the concrete mix design	
3) CASTING PLAN DESIGN	
• Insert the casting plan design, showing floor plan and cross-sections of the layers.	
4) MONITORING OF INTERNAL TEMPERATURES	
• Number of monitoring points	
• Monitoring Time	

5) INSTRUMENTATION DESIGN OF THE STRUCTURE

- Insert monitoring plan design, showing floor plan and cross-section of the structure with the precise location of all the chosen points.

NOTES:

- In the absence of information about the materials and site properties, this information will be taken from literature and weather forecasts, thus reducing the reliability of the results.
- The occurrence of any unexpected situation that modifies the application of the casting plan must be informed.